AD-763 450

ENERGY/ENERGY RATE METER FOR ENERGY MANAGEMENT IN FLIGHT

D. C. Sederstrom, et al

Honeywell, Incorporated

Prepared for:

Office of Naval Research

February 1973

ENERGY/ENERGY RATE METER FOR ENERGY MANAGEMENT IN FLIGHT

(Final Report)

D. C. Sederstrom
N.R. Zagelsky
R. C. McLane

Honeywell Inc.

February 1973

Contract: N00014-72-C-0324
NR 213-054

Sponsored by
Office of Naval Research, Code 461
Arlington, Virginia 22217

Security Classification

DOCUMENT CONTROL DATA - R & D

Security classification of title, body of abstract and indexing annotation must be entered when the overall report is classified)

1 ORIGINATING ACTIVITY (Corporate author) Honeywell Inc., Systems and Research Division 2700 Ridgway Parkway Minneapolis, Minnesota 55413	2a. REPORT SECURITY CLASSIFICATION Unclassified 2b. GROUP

3 REPORT TITLE

ENERGY/ENERGY RATE METER FOR ENERGY MANAGEMENT IN FLIGHT

4 DESCRIPTIVE NOTES (Type of report and inclusive dates)
Final Report

5 AUTHOR(S) (First name, middle initial, last name)
D. C. Sederstrom
N. R. Zagalsky
R. C. McLane

6 REPORT DATE February 1973	7a. TOTAL NO. OF PAGES ~~99~~ 110	7b. NO. OF REFS 6
8a. CONTRACT OR GRANT NO. N00014-72-C-0194 b PROJECT NO NR213-094/10-19-71 c 461 d	9a. ORIGINATOR'S REPORT NUMBER(S) F2039-FR 9b. OTHER REPORT NO(S) (Any other numbers that may be assigned this report)	

10 DISTRIBUTION STATEMENT
This document has been approved for public release and sale; its distribution is unlimited.

11 SUPPLEMENTARY NOTES Reproduction in whole or in part is permitted for any purpose of the United States Government	12 SPONSORING MILITARY ACTIVITY Office of Naval Research, Code 461 Department of the Navy Arlington, Virginia 22217

13 ABSTRACT

A 14-month program is described which culminated in fabrication and limited flight tests of a cockpit meter instrumentation system displaying aircraft specific energy and energy rate (specific excess power). Detailed account is given of the analysis and design processes, including man-in-the-loop hybrid simulation and display, through which the meter and its uses were developed. Preliminary flight test results are also cited.

DD FORM 1 NOV 68 1473 REPLACES DD FORM 1473, 1 JAN 68, WHICH IS OBSOLETE FOR ARMY USE.

Security Classification

Security Classification

14 KEY WORDS	LINK A		LINK B		LINK C	
	ROLE	WT	ROLE	WT	ROLE	WT
Energy						
Energy meter						
Energy/energy rate meter						
E meter						
Display						

FOREWORD

This final report is submitted in fulfillment of Office of Naval Research Contract N00014-72-C-0194, contract authority NR 213-094/10-19-72 (Code 461). Mr. G. Flohil of the Naval Applications and Analysis Division, Aeronautics Programs, was the scientific officer. The work was performed by Honeywell from 1 January 1972 to 12 February 1973. Mr. N.R. Zagalsky served as program manager; Mr. D.C. Sederstrom was principal investigator, assisted by Mr. R.C. McLane. The design and fabrication of the energy meters was directed by Mr. O.F. Rice. His team included Messrs. E. Wuori, R. Johnson, W. Dougherty, and D. Montbriand.

The work was performed at Honeywell's Systems and Research Center, and Government and Aeronautical Products Division, Aircraft Instruments and Microwave Systems Section, Minneapolis, Minnesota. Flight tests were conducted by the Naval Air Test Center, Flight Test Division, Patuxent River, Maryland. The cooperation of Lt. Dave Walker, USN and Captain Terry Bryan, USMC, and Messrs. Mike Branch, Sam Porter, and their flight test support personnel is gratefully acknowledged.

ABSTRACT

A 14-month program is described which culminated in fabrication and limited flight tests of a cockpit meter instrumentation system displaying aircraft specific energy and energy rate (specific excess power). Detailed account is given of the analysis and design processes, including man-in-the-loop hybrid simulation and display, through which the meter and its uses were developed. Preliminary flight test results are also cited.

NOMENCLATURE

Symbols used in the text define their use as they pertain to the requirements of this program. Inasmuch as practical, effort was made to conform to standard AIAA (American Institute of Aeronautics and Astronautics) terminology.

E	aircraft specific energy	ft
$\dot{E}$	energy rate (specific excess power)	ft/sec
V	true airspeed (also TAS)	ft/sec
h	altitude	ft
α	angle of attack	rad
a_n	normal acceleration	ft/sec^2
a_ℓ	longitudinal acceleration	ft/sec^2
g	gravitational constant	ft/sec^2
C_L	lift coefficient	
C_{L_α}	lift coefficient as a function of angle of attack	per rad
C_D	drag coefficient	
M	Mach number	
C_1, C_2, C_3	drag equation coefficient	
W	aircraft weight	lb
q	dynamic pressure	lb/ft^2
KCAS	knots calibrated airspeed	knots
γ	ratio of specific heats flight path angle	rad
L	lift force	lb
D	drag force	lb
F_n	aircraft net thrust	lb
p	static pressure	lb/ft^2

TABLE OF CONTENTS

		Page
SECTION I	INTRODUCTION	1
SECTION II	CONCLUSIONS AND RECOMMENDATIONS	3
	Conclusions	3
	Recommendations	4
SECTION III	BACKGROUND AND SUMMARY	6
	Background	6
	Summary	6
SECTION IV	THEORY OF OPERATION AND USES OF THE ENERGY METER	12
	Introduction	12
	Applications - Energy Scale	15
	Schedule Following	15
	Energy Maneuverability (Turning Efficiency)	17
	Flight Envelopes	18
	Applications - Energy Rate Scale	19
	Performance Monitoring	19
	Performance Calibration	19
	Establishing Flight Conditions	20
	Throttle Setting Aid	20
SECTION V	ANALYSIS AND SIMULATION	22
	Introduction	22
	Performance	22
	Aircraft Model	22
	Optimal Flight Paths	24
	Sensitivity Studies	29
	Simulation	38
	Description of the Simulator Facility	38
	Man-in-the-Loop Studies	40
	Pilot Evaluations	54
SECTION VI	METER DESIGN	57
	Introduction	57
	Mechanization Approach	57
	Interface Definition	59
	Determination of Flight Path Acceleration Scaling	59
	Energy Rate Null Adjustment Knob for Pilots	61

TABLE OF CONTENTS -- CONCLUDED

		Page
SECTION VII	FLIGHT TEST	62
	Introduction	62
	Proposed Energy Meter Flight Test Plan	62
	Flight Test Results	64
	Pilot Debriefing Document	68
SECTION VIII	REFERENCES	70
APPENDIX A	ENERGY/ENERGY RATE INDICATOR AIRCRAFT WIRING INFORMATION	71
APPENDIX B	PILOT'S DEBRIEFING DOCUMENT	77
APPENDIX C	ENERGY METER PROGRAM FOR NASA FLIGHT RESEARCH CENTER	89
APPENDIX D	ENERGY METER PROGRAM FOR USAF	92
APPENDIX E	ENERGY METER CHARACTERISTICS	99

LIST OF ILLUSTRATIONS

Figure		Page
1	Energy/Energy Rate Meter JG1077AA-01	7
2	Instantaneous Performance Capability	9
3	Program Summary	10
4	Energy/Energy Rate Contours	13
5	Energy/Energy Rate Meter	14
6	Instantaneous Performance Capability	15
7	Implementing Optimal Flight Paths	16
8	Maneuverability with the E Mete.	17
9	Instantaneous Performance Capability	18
10	Energy/Energy Rate Meter	19
11	Energy/Energy Rate Meter with Peripheral Scales to Aid Throttle Setting for Optimal Flight Paths	21
12	Drag Polar	23
13	Drag Thrust	23
14	Total Fuel Flow	23
15	Excess Power Contours, Slatted Aircraft	25
16	Slatted versus Unslatted Drag Polars	26
17	Excess Power Contours, Unslatted Aircraft	27
18	Minimum Time Energy Climbs	28
19	Slatted F-4E Excess Power Contours -- Hot Day	30
20	Slatted F-4E Excess Power Contours -- Cold Day	30
21	Slatted F-4E Excess Power Contours -- Intermediate Hot Day	31
22	Slatted F-4E Excess Power Contours -- Intermediate Cold Day	31

LIST OF ILLUSTRATIONS -- CONCLUDED

Figure		Page
23	Non-standard Day Minimum Time Energy Climb Paths	32
24	Calibrated Airspeed Overlay for Energy Meter	33
25	Approximate Corrections to Constant Calibrated Airspeed Climb	34
26	Minimum Time Energy Climb as a Function of Weight	36
27	Minimum Time Energy Climb Drag Sensitivity	36
28	Climb Comparison	37
29	Man-in-the-Loop Simulation	38
30	Simulation Flow Chart	39
31	Energy Management Display	41
32	Peak Energy Rate Determination	45
33	Graphical Determination of Minimum Time Energy Climb Path	45
34	Minimum Time Climb Path -- Slatted F-4J	46
35	Energy Contours in Subsonic Region	47
36	Altitude Coincidence at Energy/Energy Rate Tangency	47
37	Military Thrust Climbs -- Slatted F-4J	49
38	Minimum Fuel Climb Calibration Curves -- Slatted F-4J with Military Thrust Drag Increment	50
39	Minimum Fuel Climb Calibration Curves -- Slatted F-4J without Military Thrust Drag Increment	50
40	Comparison of Minimum Fuel Climbs	53
41	Man-in-the-Loop Energy Rate Command Following -- Energy Meter Overlay	55
42	Subassemblies, Energy/Energy Rate Meter JG1077AA-01	60
43	Energy Meter Readings versus Computed Values for Steady Points No. 7 and 8	67

LIST OF TABLES

Table		Page
I	Slatted Aircraft Performance Comparison	26
II	Unslatted Aircraft Performance Comparison	26
III	Effect of Temperature on Calibrated Airspeed	33
IV	Time to Climb versus Display Comparison	43
V	Partial Throttle Command	52
VI	Pilot Recorded Data for 22 Steady Points	65

SECTION I
INTRODUCTION

Nearly two decades ago, Rutowski (Ref. 1) wrote: "Because of the possibility of ready interchanges of kinetic and potential energy by means of a dive or zoom, the concept of specific energy has tactical significance. It would seem more important for an interceptor to have a specific energy capability greater than that of its bombing adversary than to have simply an altitude or speed advantage. Even in the case of other than tactical aircraft (research vehicles, for example), the concept of specific energy is useful in that it permits rapid estimation of the maximum speed in a dive or the maximum altitude in a zoom." The objective of the program reported herein was to determine, by means of simulation and flight test, the feasibility and utility of a cockpit meter which displays the aircraft's specific energy and energy rate. A man-in-the-loop simulation was modified to incorporate the necessary energy and energy rate computations, to simulate the F-4J test aircraft, and to provide a flexible tool for development of the meter display format. The simulation was also used to investigate utilization procedures and as a system integration aid in checking out the completed meter. With the aid of the simulation, the meter was evaluated both in simulated and hardware form by Naval Air Test Center (NATC) test pilots. After limited environmental and flightworthiness tests, the first unit was delivered to the Patuxent River Naval Air Test Center on 1 August 1972.

The assigned priority of the meter flight test in the slatted F-4J test vehicle and periodic downtime of the aircraft have combined to limit somewhat severely the amount of flight test data generated in the program. Consequently, the results, though positive, are not complete. Conclusions and recommendations made on the basis of results to date are presented in Section II. The program background and summary are given in Section III.

The theory of meter operation, together with a discussion of its potential uses, is contained in Section IV. This section is written with the idea of being suitable for pilot indoctrination.

In Section V, aircraft performance analysis and computer work leading to the design, fabrication, and checkout of the meter are described. A principal tool in this development was a man-in-the-loop hybrid simulation.

A discussion of the meter design is given in Section VI, and Section VII contains flight test results. Considerably more data will be available in the near future.

The appendixes include aircraft wiring information, a pilot debriefing form, and descriptions of energy meter programs undertaken at the direction of ONR in support of separate NASA and USAF flight research programs. The reduced-scale drawings included as a part of Appendixes A, C, and D are intended to indicate only the nature of the data supplied to the Government during the course of this contract. The mechanical and electrical characteristics of the meter are given in Appendix E.

SECTION II
CONCLUSIONS AND RECOMMENDATIONS

CONCLUSIONS

The following conclusions and recommendations are based on analyses and simulation studies conducted in this study, and on the limited flight testing accomplished to date.

- Flight tests have established the energy/energy rate indicator accuracies to be ±360 ft and ±5 ft/sec, respectively. This is well within the design goals.

- The addition of an energy rate null adjust knob facilitates compensation by the pilot for accelerometer or angle-of-attack sensor calibration errors. This feature was included on the USAF energy meters.

- The energy rate indication provides a means for bridging the gap between energy maneuverability theory and operational implementation of that theory. Namely, the pilot can, with the meter, learn to implement turning maneuvers which optimize the tradeoff between turning rate and energy rate loss.

- The energy indicator facilitates the implementation of optimal mach-altitude climb schedules. The less experienced the pilot, the greater is his benefit from use of the meter. It thus has potential as a training aid.

- Simulation experiments with the meter established that the following performance improvements result from implementation of optimal flight paths:

  - A 21 percent time saving (60 sec) in the minimum time climb of a 40,000-lb F-4J aircraft when compared with a subsonic climb from 29,500 to 40,000 ft, followed by an acceleration to mach 1.85.

  - Compared with a military throttle minimum fuel climb, an optimal partial afterburner climb results in a 9 percent saving in fuel (125 lb) and a 45 percent saving in time (187 sec).

- The energy/energy rate meter provides the necessary cues for simultaneous manual stick and throttle control as required above.

- Man-in-the-loop simulations have verified the meter's utility as an aircraft calibration device. Specific excess power contours developed with the meter provide an economical means for periodic performance evaluations of the aircraft/engine system.

RECOMMENDATIONS

Recommendations as a result of this study are as follows:

- The meter should be tested as a training aid.
- The meter should be provided in those aircraft assigned to tactics development. Quantification of maneuvers provides a firmer basis for the generation of tactics.
- To provide the pilot with a heads-up capability, the energy/energy rate information should ultimately be provided on a heads-up or helmet-mounted display. Such implementation precludes the use of precomputed template overlays and instead requires computer storage and generation of the overlay information. The meter, with its template overlays, provides a cost-effective way to introduce energy management to the instrument panel of aircraft not currently equipped with computer-driven displays.
- Display concepts being developed for a more sophisticated computer-driven system should be flight evaluated in an energy meter equipped aircraft. The versatility allowed by the use of template overlays tailored to characteristics of any type aircraft and to nonstandard atmosphere profiles provides a cost-effective method for in-flight evaluation for progressing toward new display concepts.
- Further study of the use of the meter for decoupling the pilot's elevator and throttle control strategies is warranted. This application would facilitate implementation of variable throttle climbouts, as well as establishing steady-state flight conditions (speed-power points).
- The meter should be an aid to flight test programs where the test aircraft's performance may not match the published data. An aircraft calibration with the meter would provide an economical means of defining the test aircraft's performance in comparison to nominal.
- Additional "free" flights with the energy meter should be scheduled to allow highly skilled and imaginative pilots to explore its potential on their own.

- The unique geometry of each aerial combat situation has not yet been taken into account in energy maneuverability theory. A study should be undertaken to define how to best integrate energy maneuverability information and own aircraft/target geometry. The study should consider the Helmet-Mounted Sight/Display as one means for such integration.

SECTION III
BACKGROUND AND SUMMARY

BACKGROUND

Energy management is directed at attaining aircraft performance improvements through judicious application of the aircraft's limited kinetic, potential, and chemical energy resources. The significant benefits to be gained from selection of the correct flight path or schedule have been demonstrated in flight tests dating back more than a decade (Ref. 2). However, aircraft adherence to optimal flight paths is not being regularly achieved at the operational level. While some research has been directed at the development of future on-board computer-based aircraft energy management systems, little has been done to provide today's pilot with an interim aid. This program was directed at realizing such an aid by providing the pilot with those flight parameters he could easily translate into the appropriate flight path or tactic.

The ability of high-performance aircraft to interchange altitude (potential energy) and airspeed (kinetic energy) through high-speed dives and zooms has led to the use of specific energy and specific energy rate as important indicators of flight status. Since these parameters have long been used (Refs. 3, 4) as a theoretical basis for definition and evaluation of optimal flight paths and tactics, it was expected that their display would provide the desired interim aid, and thus serve to bridge the gap between energy management theory and operational implementation of the tactics resulting from that theory.

SUMMARY

This program culminated in the fabrication and flight test of the energy/energy rate meter* shown in Figure 1. During the course of the contract, two meters were supplied to the Navy for their evaluation at the Patuxent River Naval Air Test Center. The program's objective was to determine the feasibility and utility of such a cockpit display. Additionally, under modifications to this contract, two (each) such meters were fabricated and delivered to the NASA Flight Research Center, Edwards AFB, and to USAF ADC/ASD/ADWC for use in their respective flight research programs.

*This cockpit meter display of specific energy and energy rate (specific excess power) is often abbreviated to energy meter and E meter in this report.

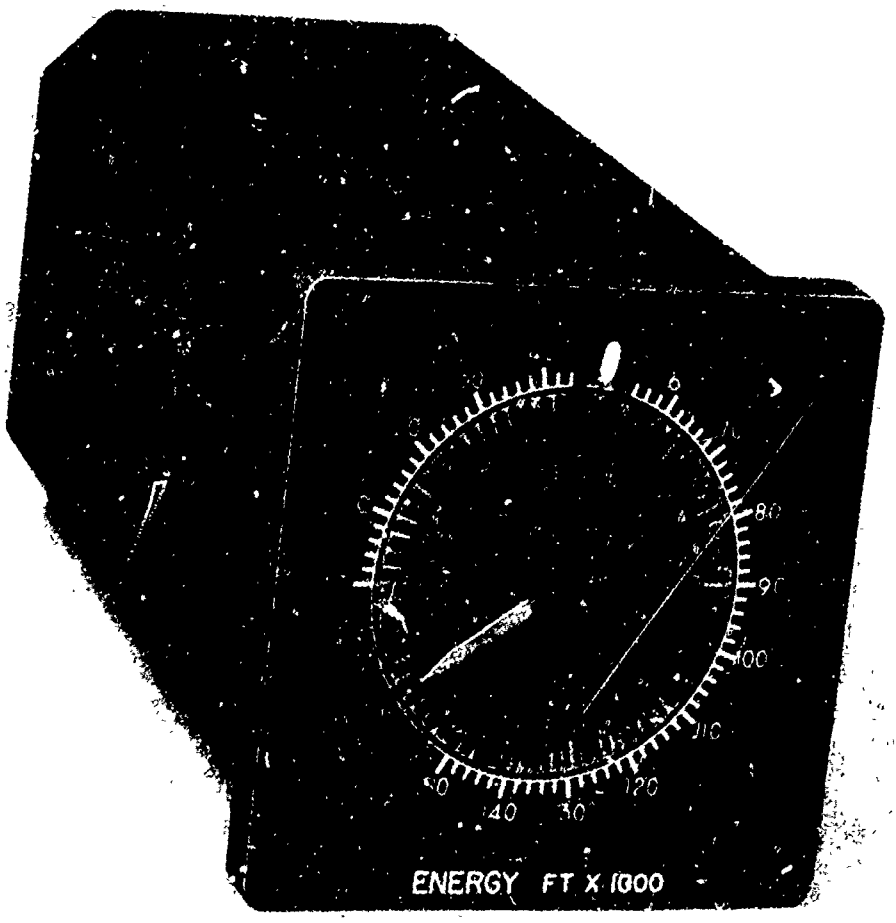

Figure 1. Energy/Energy Rate Meter JG1077AA-01

The utility of the display is based on the ability of high-performance aircraft to interchange altitude (potential energy) and airspeed (kinetic energy) through high-speed dives and zooms. This permits a single flight state (specific energy) description for the aircraft motion. Specific energy, E, is defined as the sum of potential and kinetic energies per unit weight, as given by

$$E = h + V^2/2g$$

where

h is altitude

V is velocity

g is the gravitational constant

The specific energy and its rate of change, specific energy rate, are flight variables which are readily associated in a one-to-one fashion with optimal flight paths or tactics. With this reduced order model of the aircraft motion, the velocity (or altitude) is not considered a state of the aircraft, but a control parameter. That is, assume that airspeed and altitude interchanges can be made in times which are negligible in comparison with times required for other phases of an energy-managed flight. Within this context, such performance limits as maximum altitude or maximum airspeed become control limits which are dependent on the aircraft's current flight state (its energy). Optimal flight paths for transitioning between different flight states become feedback control laws [i.e., the control (V or h) is specified as a function of the state (E)].

Many of the meter applications are based on such correlation of performance limits or tactics with energy level. For example, the maximum speed attainable in a constant-energy dive, or the maximum altitude attainable in a zoom, is given by the intersection of the aircraft's current energy level with the placard or buffet onset limits. Thus, the aircraft's instantaneous flight limits can be correlated with energy level.

As indicated in Figure 2, the energy/energy rate meter can provide a graphic display of this correlation. The limit speed and altitude at each energy level are shown on a peripheral scale. The energy indicator points not only to the current energy level, but also to the flight limits associated with that energy level. Knowledge of these limits allows the pilot to select the appropriate tactic for achieving a specified high-altitude or high-speed flight state. If that state exceeds his current limit, he knows that he must implement an energy-gaining maneuver. Otherwise, a simple zoom or dive maneuver is adequate.

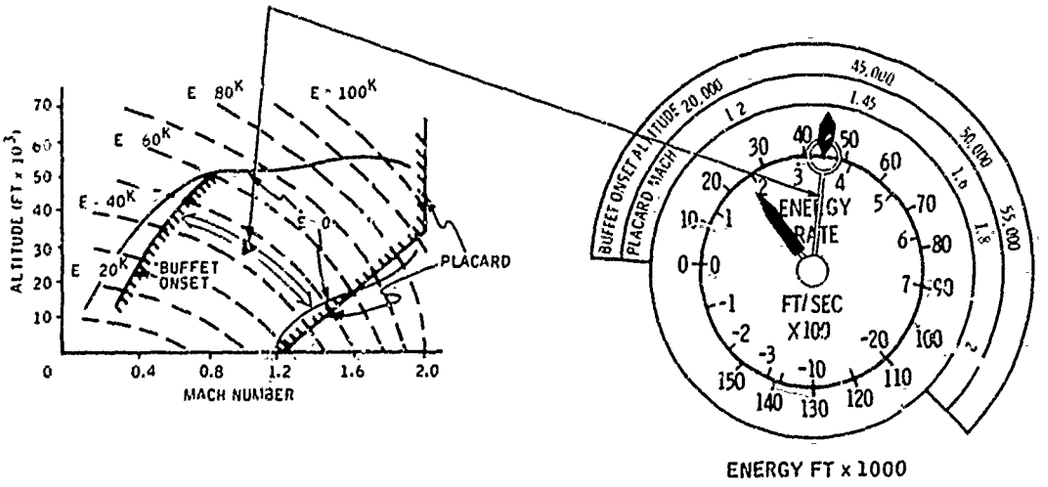

Figure 2. Instantaneous Performance Capability

Applications of the meter suggested by this program are:

- Minimum time or minimum fuel climb schedule following
- Maneuverability technique development for minimum loss of energy in turns
- Flight envelope boundaries for one and multiple-g flight
- Aircraft performance monitoring against vehicle standard values
- Aircraft performance calibration
- Setting up flight conditions quickly and accurately
- Throttle setting aid for fuel-time tradeoffs

The progression of the study, design, and fabrication efforts are delineated in Figure 3. To meet the desired flight test schedule, the meter design cycle had to start before all of the meter characteristics were defined. The formulation of the mechanization equations for energy and energy rate had been established by the preceding company-sponsored studies. Only the dynamic ranges of scale factors had to be determined through analysis and simulation of thrust and drag data for the test aircraft. Signal

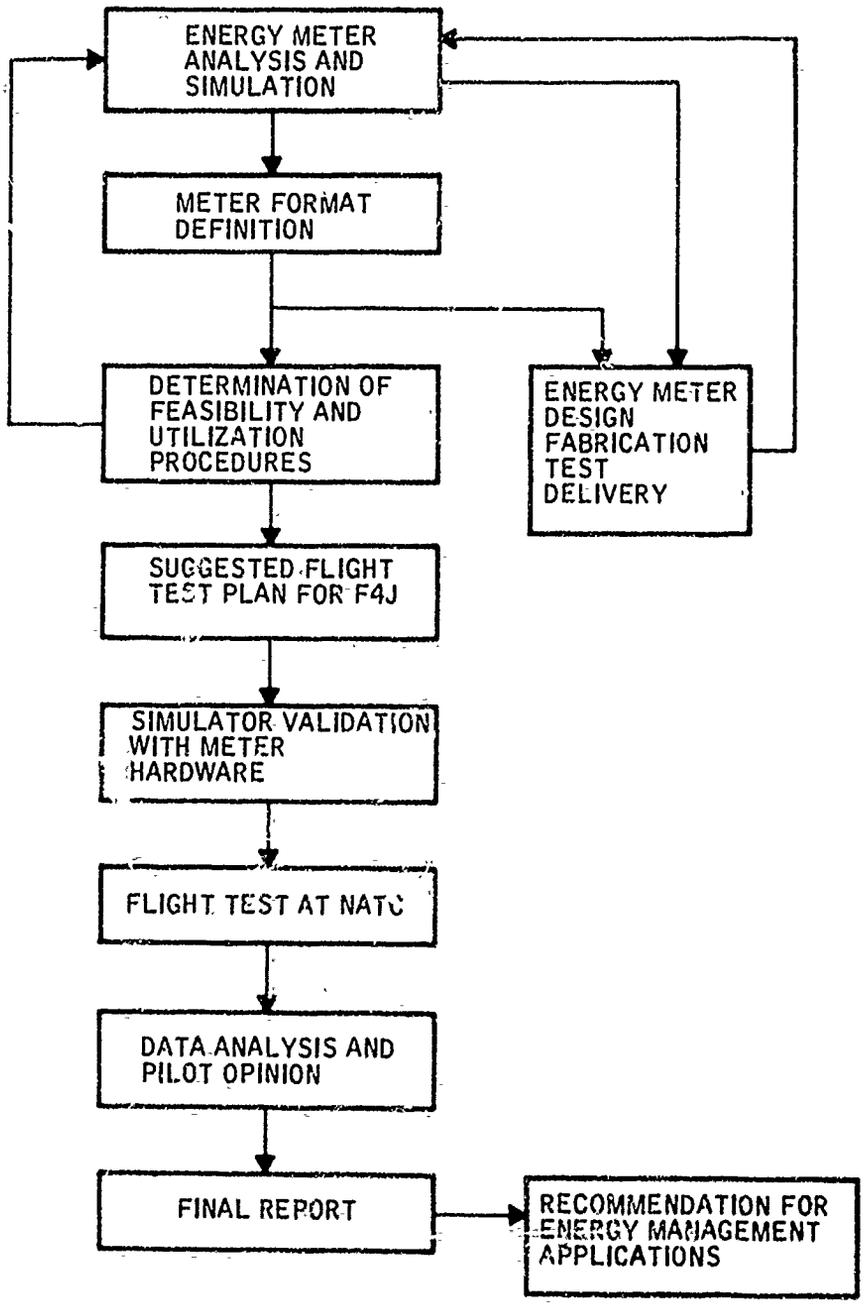

Figure 3. Program Summary

sources were identified from the instrumentation of the specific F-4J aircraft (Serial number 153088) at NATC. This defined the interface requirements for the energy meter. Investigation of both thick and thin film circuit technology indicated cost and time savings for this program in the thick film method. This approach, including the use of function generation for resolving angle-of-attack information in calculating flight path acceleration in the energy rate equation, permitted a single package for the entire computing and display mechanization. In addition to determination of meter design requirements, the hybrid computer simulation was employed in evaluation of the use of optimum climb schedules, and use of the energy meter in simulated aircraft calibration by determination of excess power contours.

Following fabrication of the first meter, simulation flight evaluation was accomplished by tying it into a hybrid computer-driven cockpit display. Two NATC pilots scheduled for the flight test program participated in this shakedown. They also contributed to modifications of the suggested flight test plan. Following delivery of the meter to NATC, numerous aircraft mechanical repairs, engine parts shortages, and maintenance schedule delays, plus additional priority project demands on the aircraft severely curtailed the flight tests. These delays essentially reduced the scope of the tests to establishing repeatability and calibration accuracy of the meter indications. This has been successfully accomplished. It is anticipated that a second phase of flight testing will evaluate potential benefits to the pilot from use of the meter.

Under modifications to this contract, equipment was fabricated for energy meter flight test research programs with NASA Flight Research Center and USAF ADC/ASD/ADWC.

SECTION IV

THEORY OF OPERATION AND USES OF THE ENERGY METER

INTRODUCTION

Energy management has been defined as the efficient use of the total resources (potential, kinetic and chemical energy) of an aircraft in accomplishing the space-time requirements of the mission. As used in the term energy meter, the word energy applies directly to the first two of these resources, potential and kinetic energies. An aircraft that is airborne has potential energy by virtue of its having altitude; in fact, the aircraft's altitude multiplied by its weight is its potential energy. Kinetic energy, the energy of motion, is equal to the work (work and energy are interchangeable terms) required to take a body from rest to its present speed. The total energy is the sum of these two. In the energy meter, the quantity that is computed and displayed is specific total energy, the total energy per unit weight. Although it is often referred to as specific energy, it is herein referred to simply as energy, denoted as E, and defined mathematically by

$$\text{Energy} = \text{altitude} + (\text{true airspeed})^2 / 2x \text{ acceleration of gravity}$$

or

$$E = h + \frac{V^2}{2g}$$

The rate of change of this energy, the energy rate ($\dot{E}$), may be written several ways. One way relates aircraft net thrust, F_n, drag, D, true airspeed, V, and aircraft weight, W, as follows:

$$\dot{E} = \frac{(F_n - D)\, V}{W}$$

Note that, since D includes a g-dependent induced drag term, energy rate is a function of normal acceleration. The details of this relationship are discussed in Section VI.

Some understanding of energy rate is essential to an appreciation of the subject under consideration. Figure 4 is an altitude-mach number plot with constant energy lines (dashed), which apply for any aircraft, and constant energy rate lines representative of full afterburner operation of a supersonic fighter.

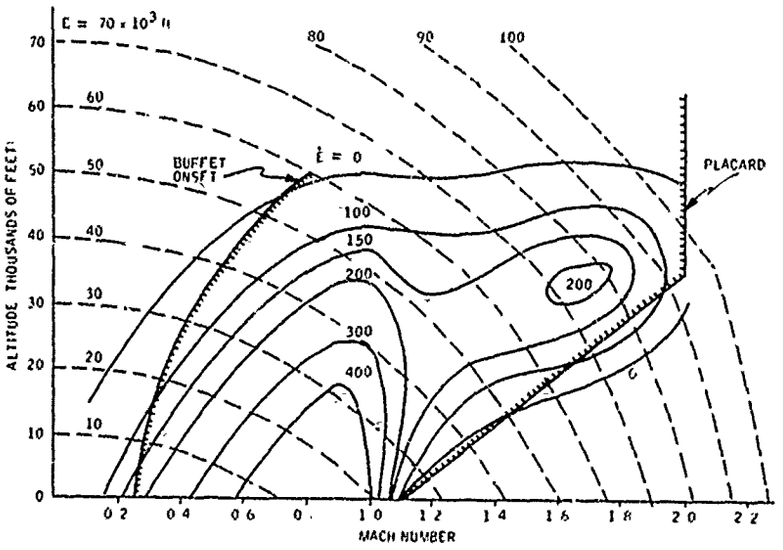

Figure 4. Energy/Energy Rate Contours

The latter are often called (specific) excess power contours and apply, as shown, to 1-g flight. The outermost of these contours, zero energy rate, is the familiar flight envelope when bounded on the right by the placard limit and on the left by buffet onset.

Within this envelope the numbers refer to the aircraft's ability to climb or accelerate. For example, along the contour marked 300, the aircraft can climb at 300 ft/sec or accelerate at 300 times g divided by true airspeed in ft/sec (or roughly 300 divided by one-twentieth of the true airspeed in knots).

The energy/energy rate meter, related in Figure 5 to the above contours, has been developed as an aid for the pilot in managing his potential and kinetic energy resources. The energy indicator designates the specific energy of the aircraft, while the energy rate indicator displays the rate at which the aircraft is transitioning between energy levels.

An important factor in the discussion of energy management concepts is the capability of modern high-performance aircraft to interchange altitude and airspeed quickly. Often it is assumed to occur in zero time; for the slatted F-4J a figure of 500 ft/sec altitude rate along a constant energy line is more representative. With this idea of the ability to traverse a constant energy line rapidly, one can discuss the equivalence of energy level and flight state.

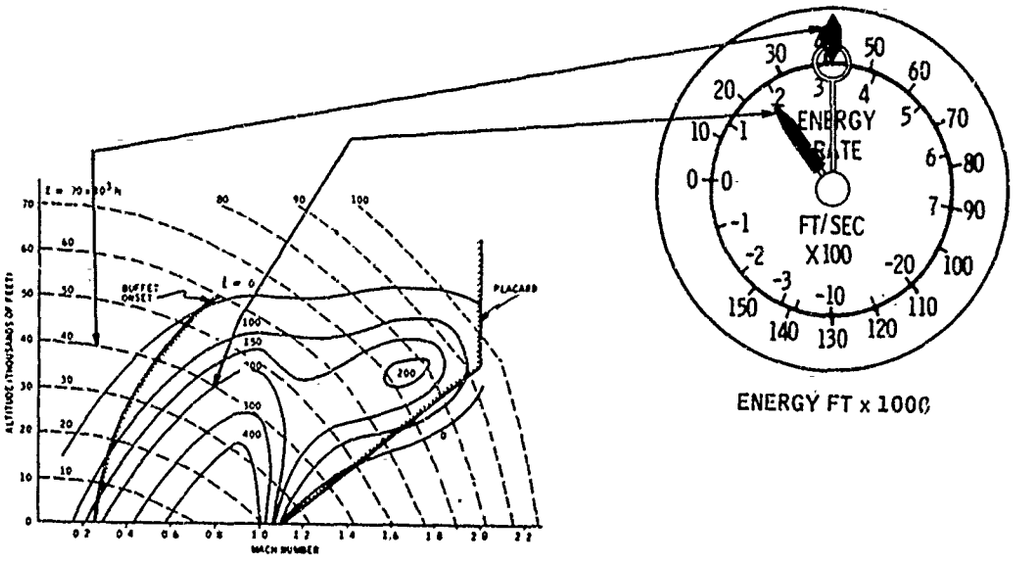

Figure 5. Energy/Energy Rate Meter

For example, consider mach 1.2 at 15,000 ft altitude as being essentially the same flight state as Mach 0.6 at 35,000 ft altitude, because they occur at the same energy level, 40,000 ft (Figure 5). This further allows the use of a simplified set of equations of motion, the Energy State Approximation.

With these simplified equations, the velocity (or the altitude) is not considered a state of the aircraft, but a control parameter. That is, assume that the elevator commands airspeed-altitude exchanges fast enough to be considered "instantaneous." Within this context, such performance limits as maximum altitude or maximum airspeed become control limits which are dependent on the aircraft's current flight state (its energy). Optimal flight paths for transitioning between different flight states become feedback control laws [i.e., the control (V or h) is specified as a function of the state (E)].

Many meter applications are based on such correlation of performance limits or tactics with energy level. For example, the maximum speed attainable in a constant energy dive, or the maximum altitude attainable in a zoom, is given by the intersection of the aircraft's current energy level with the placard or buffet onset limits. Thus, the aircraft's instantaneous flight limits can be correlated with energy level.

As indicated in Figure 6, the energy/energy rate meter can provide a graphic display of this correlation. The limit speed and altitude at each energy level are shown on a peripheral scale. The energy indicator points not only to the current energy level, but also to the flight limits associated with that energy level. Knowledge of these limits allows the pilot to select the appropriate tactic for achieving a specified high-altitude or high-speed flight state. If that state exceeds his current limit, he knows that he must implement an energy-gaining maneuver; otherwise, a simple zoom or dive maneuver is adequate.

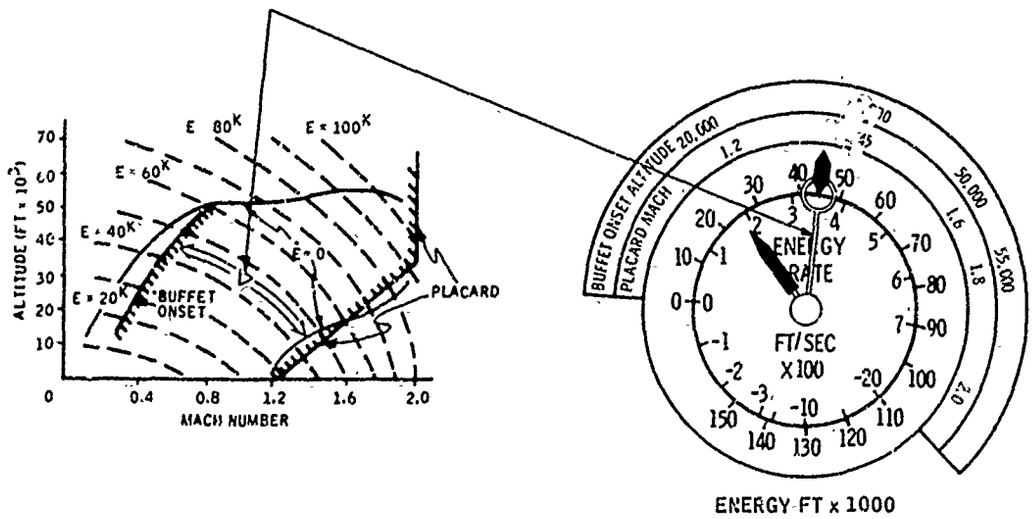

Figure 6. Instantaneous Performance Capability

With this introduction, those applications of the meter associated most directly with the energy scale will be presented. These include schedule following, energy maneuverability, and multiple-g flight envelopes.

APPLICATIONS - ENERGY SCALE

Schedule Following

Whatever the rationale for choosing a climb (or descent) schedule, that schedule can be presented conventionally (altitude versus mach number or altitude versus airspeed), or it can be presented in the form of mach number (or altitude or velocity) versus energy. The latter form, with energy as the independent variable, has the advantage of just one, unequivocal dependent

variable to be controlled with the one control input available, the elevator. In this example, the objective is considered to be to gain energy in minimum time. With slight modification, the argument would apply equally to a minimum fuel climb.

Figure 7 illustrates the problem. The pilot wants to initiate a climb from the point indicated. An h-M schedule requires guessing the point at which he should optimally intercept the schedule; with an energy meter overlay, he can read the command mach number directly. In this case it is 1.4. He can reach this point in a constant energy dive; however, since time saving is the objective, he will maintain full thrust, and this type of dive is impossible under those circumstances. The following rule of thumb has been developed for this application:

- Note the command mach number (1.4 in this example)
- Dive at -10 to -15 deg pitch altitude
- Begin the pullout at 2 g when M = 1.5 (0.1 higher than above)
- Ease off the stick backpressure as command and actual mach number converge

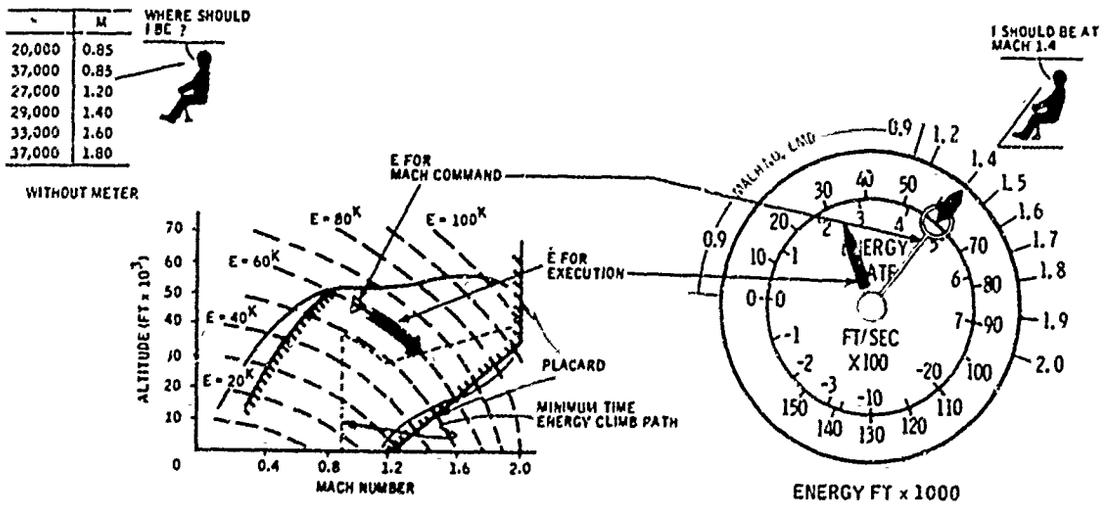

Figure 7. Implementing Optimal Flight Paths

Energy Maneuverability (Turning Efficiency)

Energy Maneuverability Theory is directed at optimizing the tradeoff between energy rate and turn rate. This tradeoff exists because the aircraft's energy rate decreases with the increased level of induced drag associated with high turn rates. Boyd, et al. (Ref. 3) have shown that constrained energy-minimum time turns can be accomplished by diving or zooming toward the "Maximum Maneuver Corridor" while initiating the turn. This corridor is a region of mach-altitude space where energy rate is a maximum for any specified turn rate. Figure 8 illustrates the use of the E meter to facilitate such maneuvers. The center of the Maneuver Corridor is correlated with energy and indicated on a meter overlay as shown. The maneuver is performed as follows:

- When the aircraft is in the position shown, the pilot rolls the aircraft into a diving turn with a fixed dive angle, maintaining zero energy rate with the elevator.
- When half of the turn has been completed, a climbing turn is begun, and the maneuver is completed at the desired final flight condition.
- If the initial condition is on the other side of the maneuver corridor, a similar procedure is followed, with dive and climb interchanged in the above steps.

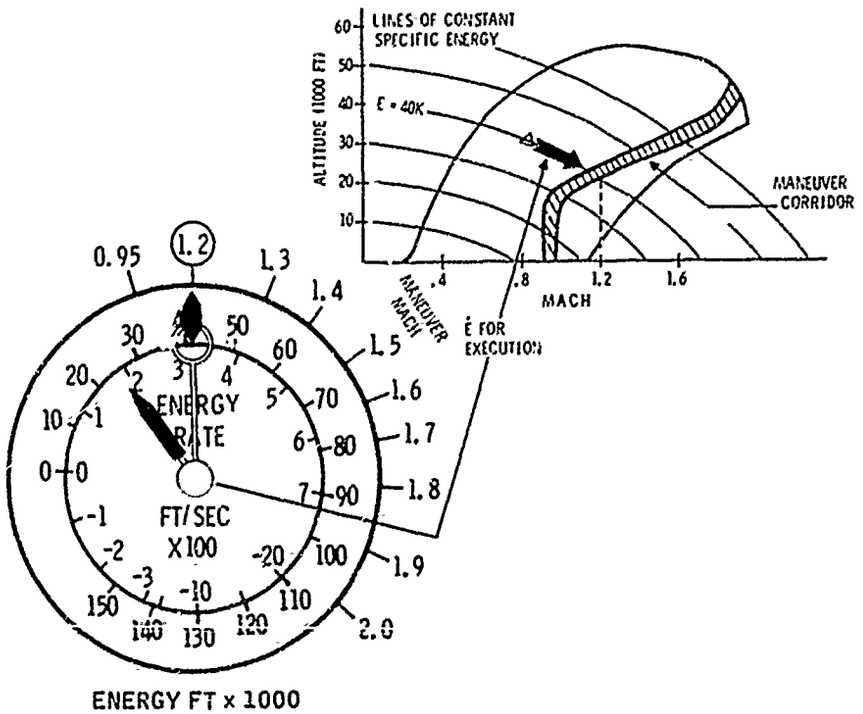

Figure 8. Maneuverability with the E Meter

Generally, some negative energy rate level would be tolerable, and the first step could be so modified. Note that the above procedure results in a varying "g" level as the corridor is approached. The application, as discussed here, is suggested for training only since in actual flight operations the pilot would not want his attention to be directed at a head down display.

Flight Envelopes

The E meter overlay can be used to show a pilot the placard limit mach number and the buffet onset altitude corresponding to a given energy level; i.e., the 1-g flight envelope, as discussed in the introduction to this section. In addition, the same type of information for multiple-g flight could be displayed on an overlay. Figure 9 shows a 5-g envelope sketched inside the familiar 1-g envelope. Five-g flight could not be sustained at the point indicated; a negative energy rate would exist. As an alternative, an overlay could provide the mach number for maximum $\dot{E}$ (smallest negative $\dot{E}$ outside the envelope).

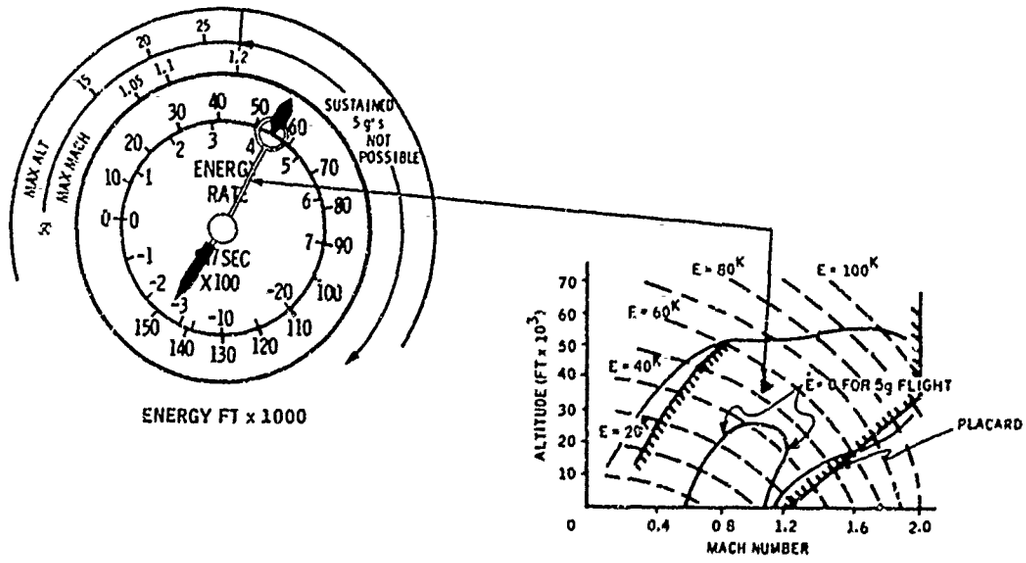

Figure 9. Instantaneous Performance Capability

APPLICATIONS - ENERGY RATE SCALE

The foregoing applications clearly have not been related exclusively to energy. However, energy was the principal item of concern. Similarly, in the following applications, energy rate is the primary, but not the exclusive, element. Currently envisioned applications include performance monitoring, performance calibration, flight condition setup, and throttle setting aid. Energy rate display also provides a means for moderating pullups associated with schedule following.

Performance Monitoring

Energy rate, or excess power, is a standard measure of aircraft performance. If the pilot has an understanding of expected performance at a given point in the flight envelope, he can readily check the aircraft's current status against the standard. This is illustrated in Figure 10.

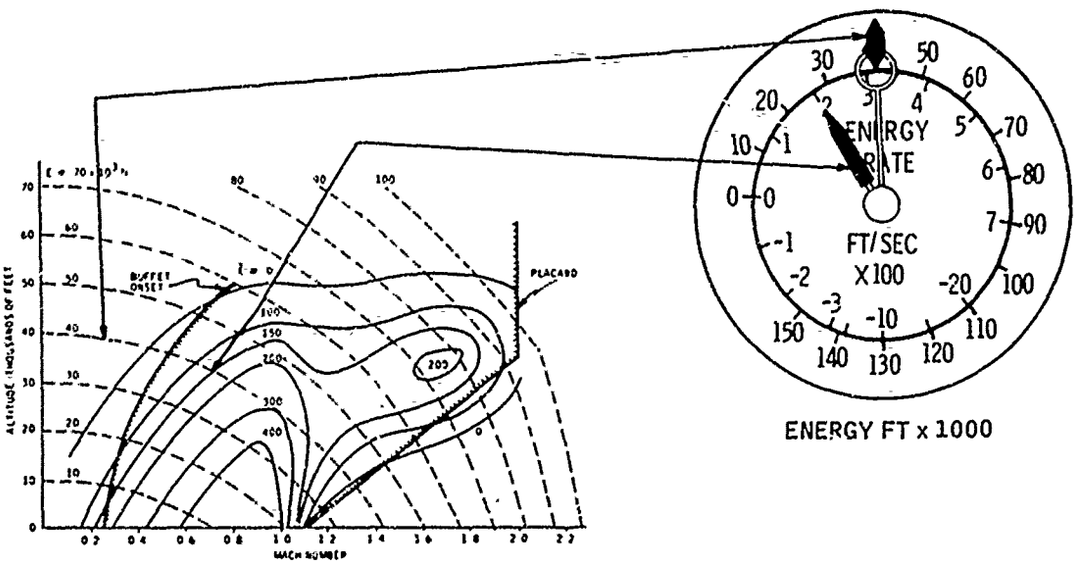

Figure 10. Energy/Energy Rate Meter

Performance Calibration

If a status check indicates degraded performance, the E meter can be used to establish the actual excess power contours. Short of this, to save time and fuel, a calibration of a restricted region of the flight envelope can

be undertaken. For example, the objective may be to determine the minimum time energy climb path. For a predetermined energy range, the pilot flies a series of level acceleration runs, noting energy rate at selected energy levels. By a method described in Section V of this report, the data can be processed to provide the desired path. A similar technique can be used to generate the minimum fuel climb, but this requires simultaneous recording of fuel flow.

Establishing Flight Conditions

In-flight research, steady-state flight conditions, or speed-power points are often required. The establishment of these points, which sometimes takes from 45 seconds to two minutes, can be facilitated by an E meter using the energy rate null point. Because input signals to the meter may have null biases causing nonzero $\dot{E}$ readings in steady flight, a null adjust knob was incorporated later.

Throttle Setting Aid

The use of variable throttle climbouts results in significant fuel-time tradeoffs. In a short simulation experiment, it was determined that energy rate could be used to set up a given throttle schedule in a climb. Figure 11 demonstrates how peripheral scales may be used with the energy-energy rate meter to aid the pilot in flying optimal flight paths. The pilot uses the control stick and the throttle to set up (and maintain) the optimal mach and throttle conditions required at the instantaneous energy level (as indicated on the meter). The control stick is used to command mach; the stick is modulated to cause the mach number to coincide with the command mach number on the peripheral scale opposite the energy needle of the meter. The throttle is used to command energy rate; the throttle is modulated to cause the energy rate to correspond to the value of command energy rate (throttle setting parameter). This is read on the second peripheral scale, referenced to the energy needle of the meter.

This discussion covers the principal potential uses envisioned for the meter. It is hoped that additional uses will become evident as more flight testing is accomplished.

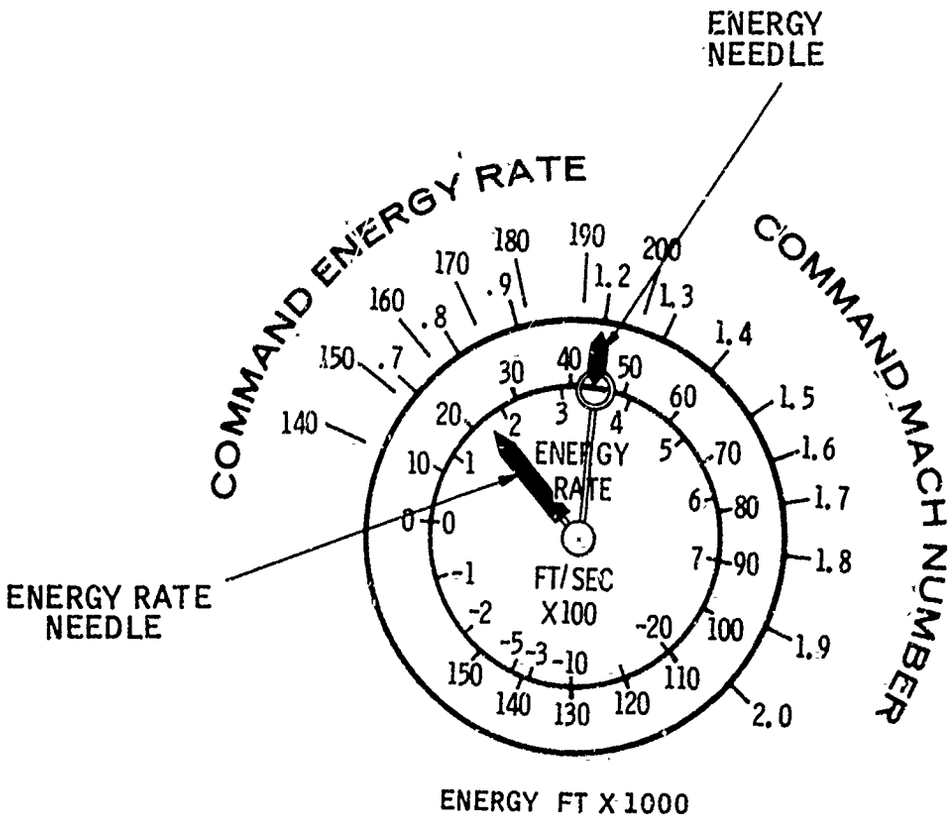

Figure 11. Energy/Energy Rate Meter with Peripheral Scales to Aid Throttle Setting for Optimal Flight Paths

SECTION V
ANALYSIS AND SIMULATION

INTRODUCTION

The aircraft assigned by the Naval Air Test Center to serve as a test bed for the energy/energy rate meter was an F-4J in which fixed slats were being installed (Serial number 153088). Thrust, drag, and fuel flow data were received from McDonnell Douglas Corporation (Ref. 5). These data were reduced to polynomial form for incorporation in Honeywell Computer Network time-share programs in which optimal climb paths and excess power contours could be generated. These provided an early indication of aircraft capabilities; e.g., the specific energy and specific energy rate or excess power ranges which should be incorporated in the meter. Later, they also made possible a check of the computations, data, and observed performance in the hybrid man-in-the-loop simulation.

This section describes design analysis and simulations. These are arranged under two main headings, performance and simulation. The aircraft model is first discussed. Performance computations based on digital simulations follow; these include development of excess power contours and optimal climb paths, comparison of nominal performance with optimal, and several sensitivity studies. Under the simulation heading a description of the hybrid simulation is given, followed by a series of man-in-the-loop studies; the section concludes with a discussion of pilot evaluations.

PERFORMANCE

Aircraft Model

Data used in the simulation of the aircraft were received from McDonnell Aircraft Company. They apply specifically to an F-4E with fixed maneuver slats and were reported to represent adequately an F-4J with the same slats. Because of the proprietary nature of the data, they are not reproduced in this report. However, Figures 12, 13, and 14 show the form in which they appeared.

Drag polars were included for both slatted and unslatted aircraft. Thrust and fuel flow curves were given for normal, military, and afterburner power settings.

Each of these curves was fitted with a polynomial for use in performance computations, sensitivity studies, and the man-in-the-loop simulation. The

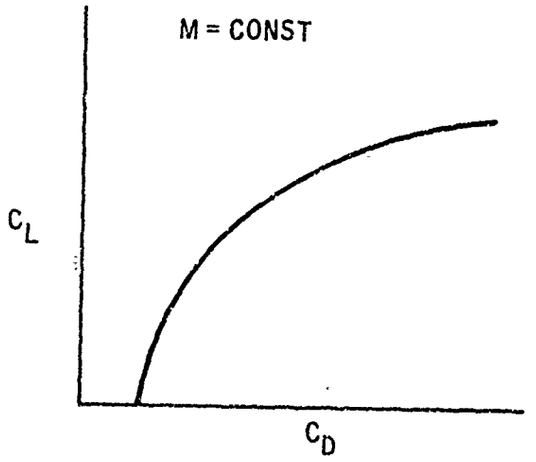

Figure 12. Drag Polar

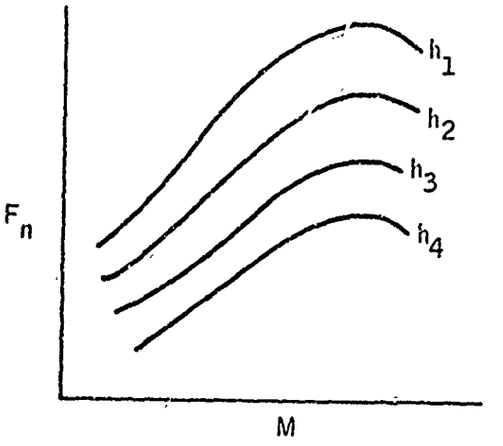

Figure 13. Drag Thrust

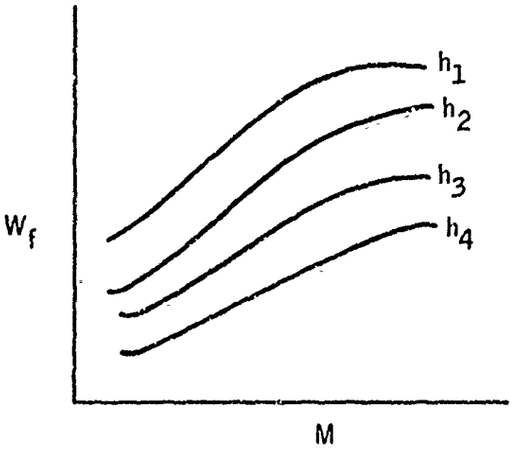

Figure 14. Total Fuel Flow

regression technique used gave fits with (generally) 1 percent or less maximum error over the ranges of interest. Cubics were used for drag polars; net thrust and fuel flow curves were fit with quartics.

Most of the performance computations were done with the aid of a time-share computer, the Honeywell Computer Network. In a number of cases, these were verified in the man-in-the-loop simulation. Figure 15 shows excess power contours for the nominal aircraft described earlier.

The maneuver slats installed on the test F-4J have a distinct effect on the drag of the aircraft throughout the flight envelope. A comparison of the slatted and unslatted drag polars for a relatively low mach number is shown in Figure 16.

As might be expected, the slatted vehicle high-lift drag coefficients are lower; i.e., the aircraft will be able to maneuver more efficiently. However, at lower lift coefficients in the subsonic speeds the fixed-slat vehicle drag is higher. As a part of the analysis, the unslatted F-4J excess power contours were also computed and plotted. The results are given in Figure 17.

Optimal Flight Paths

In Figure 18, the minimum time energy climbs for slatted and unslatted F-4Js are compared.

To determine maximum performance benefits from a minimum time energy climb, a comparison was made between this type of climb and a NATOPS-type subsonic climb and level acceleration. The latter was composed of a climb at mach 0.95 to a somewhat arbitrary 40,000-ft altitude and a level acceleration to a final energy of 91,000 ft. The results for several aircraft weights are given in Table I.

The optimal path figures include a 15-sec transition dive time. A similar comparison was made for the unslatted aircraft, as shown in Table II.

The final energy level was 100,000 ft in this case, and the initial conditions were somewhat different as indicated. Since the comparisons are between an optimal and a nominal climb in each case, the variation in initial and final conditions is unimportant. The difference in energy changes arises from the difference in optimal climb paths for the two configurations.

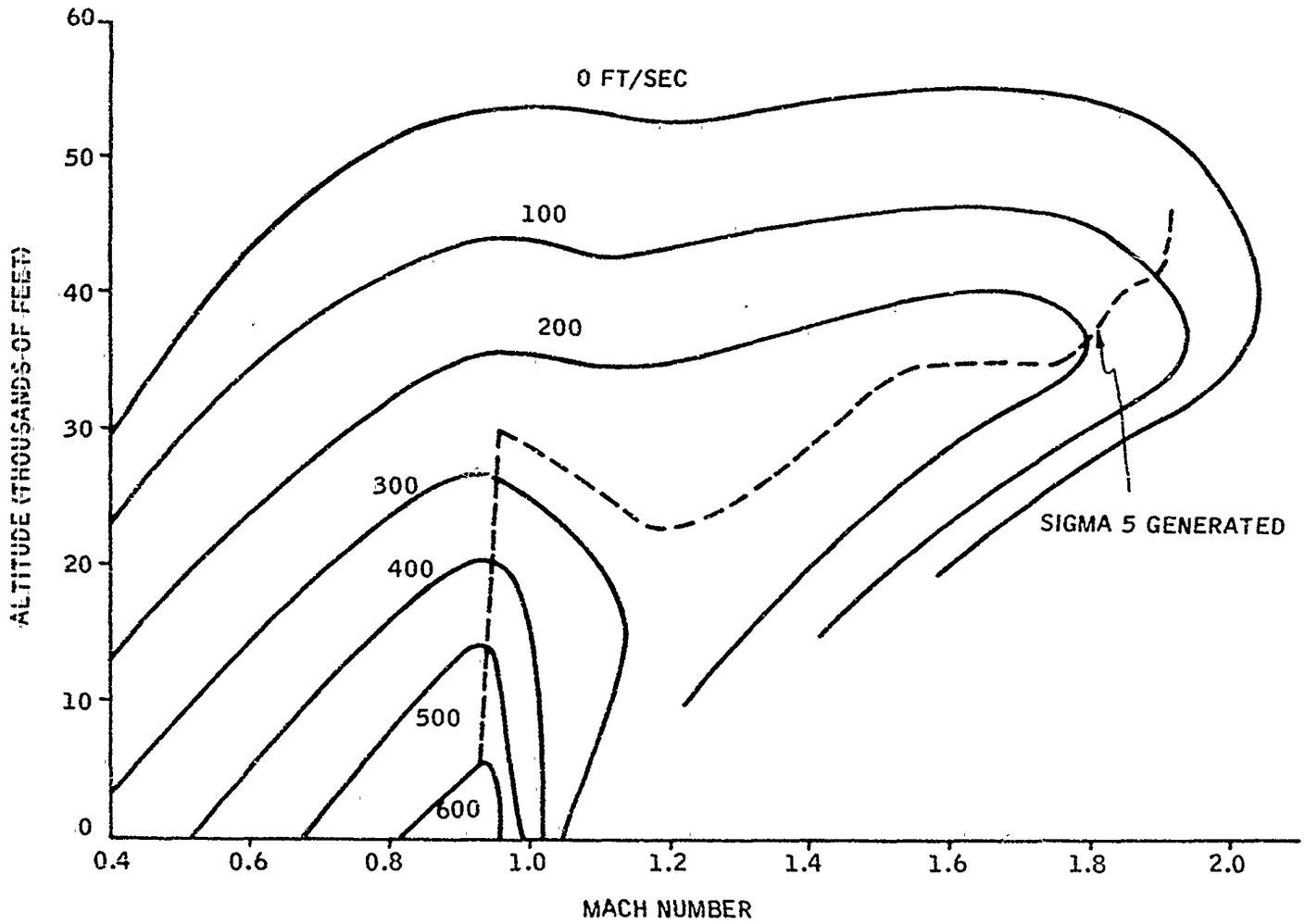

Figure 15. Excess Power Contours, Slatted Aircraft

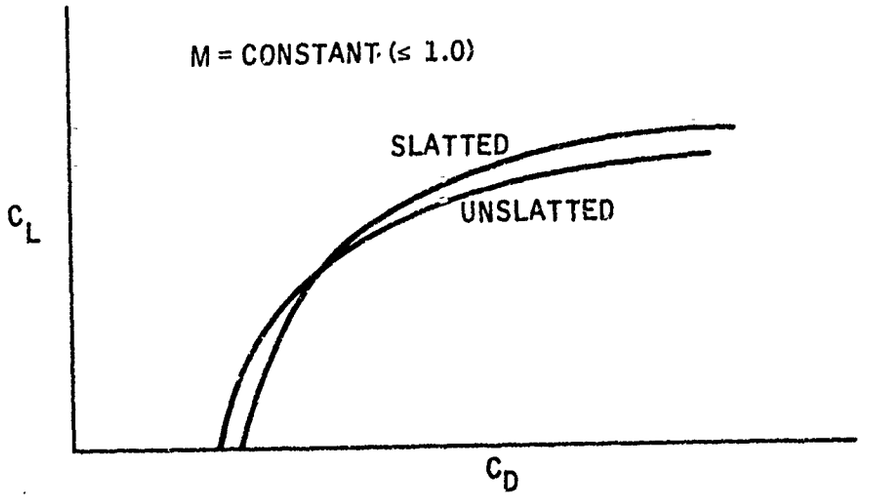

Figure 16. Slatted versus Unslatted Drag Polars

Table I. Slatted Aircraft Performance Comparison

Aircraft Weight (lbs)	Optimal Path (sec)	Climb Plus Level Acceleration At 40,000 Ft (sec)	Time Saved (sec)
35,000	190	233	43
40,000	225	285	60
45,000	260	340	80
50,000	305	435	120
55,000	360	540	180

Table II. Unslatted Aircraft Performance Comparison

Aircraft Weight (lbs)	Optimal Path (sec)	Climb Plus Level Acceleration at 40,000 ft (sec)	Time Saved (sec)
35,000	176	228	52
40,000	204	271	67
45,000	232	329	97

Initial Conditions
H = 22,800 ft; E = 37,500 ft

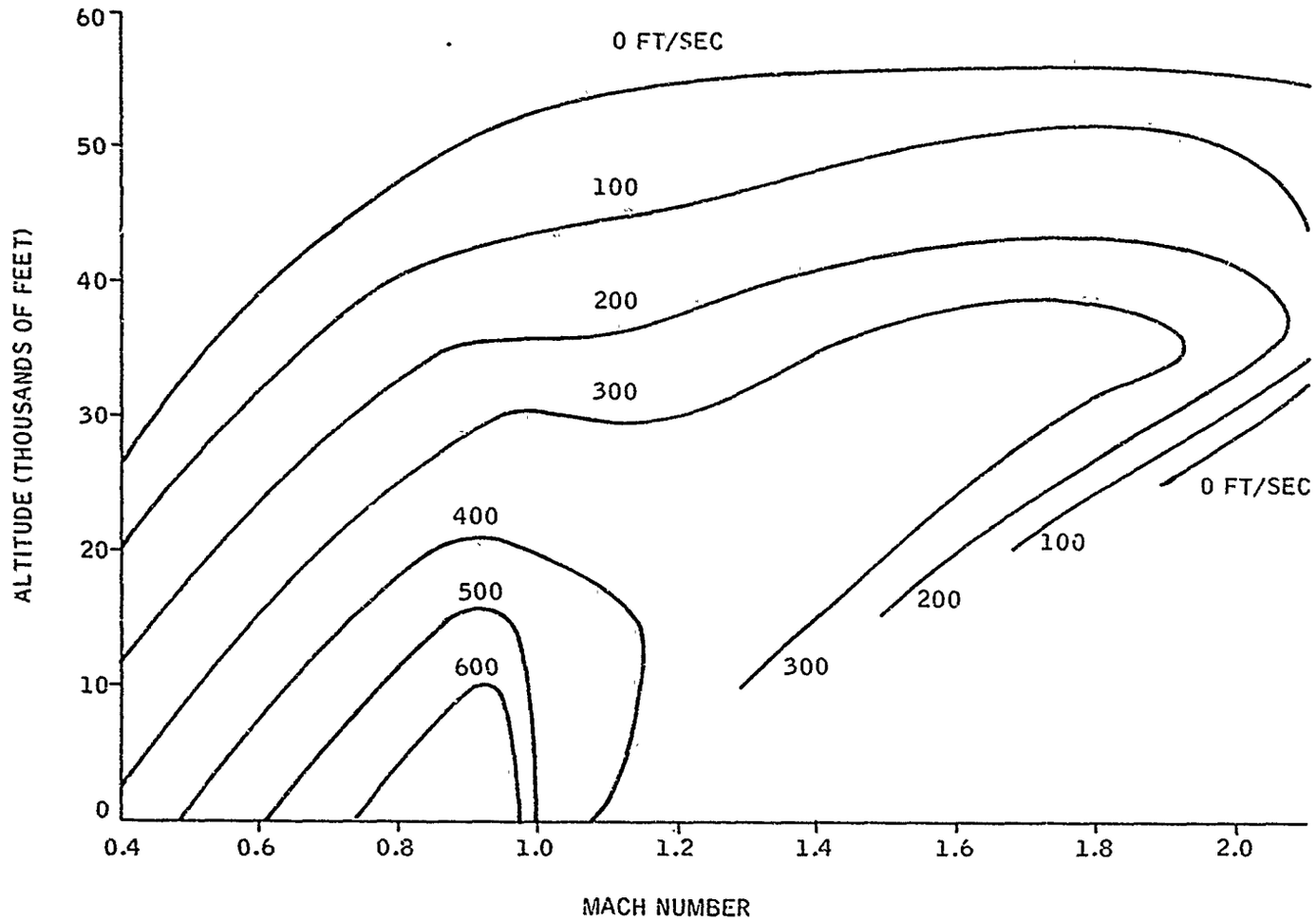

Figure 17. Excess Power Contours, Unslatted Aircraft

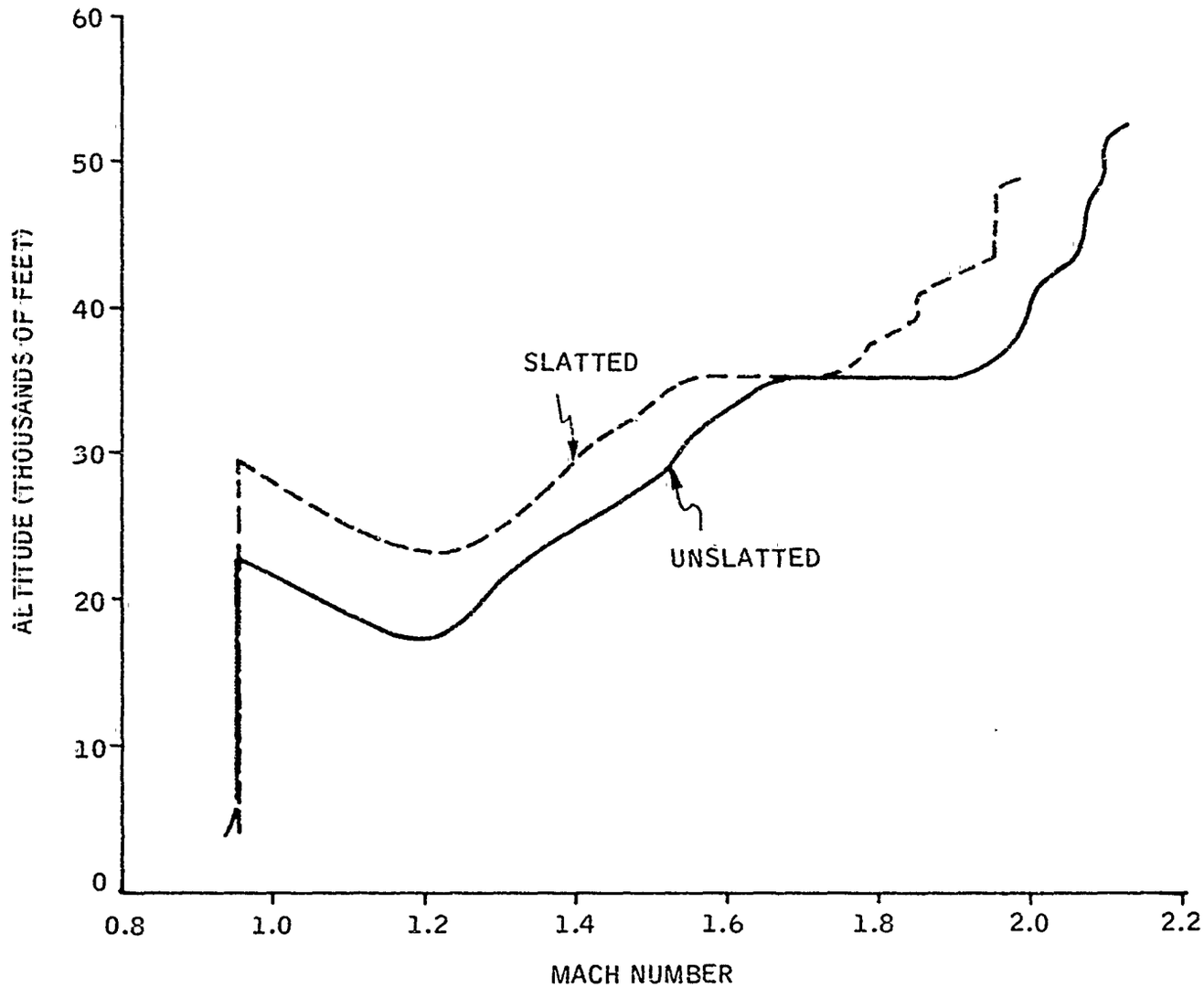

Figure 18. Minimum Time Energy Climbs

A Time-Share computer program was modified to accommodate a variable weight aircraft; i.e., to incorporate provisions to burn fuel. A level acceleration from mach 0.838 to mach 1.9 took 198 sec; the NATOPS Flight Manual for the F-4J shows 180 sec. This is believed to be good correlation, in view of the fact that the Flight Manual performance figures are reportedly optimistic.

Sensitivity Studies

Four sensitivity studies are reported here: (1) variation of excess power contours and optimal paths with non-standard atmospheric temperature, (2) optimal path variation with vehicle gross weight, (3) energy rate shift with drag data differences, and (4) fuel losses incurred by flying off the optimal path by a given mach number error. A question of energy rate sensitivity to control stick or normal acceleration disturbances arose in the man-in-the-loop simulation study on aircraft calibration applications of the meter. Results of a study of this question are given in the last part of this section under Aircraft Calibration.

Temperature Sensitivity -- The practical treatment of nonstandard day conditions in flight test remains as one of the major energy management problems. As an aid in further understanding of the problem, the nonstandard day excess power contours of Figures 19 to 22 were made. Reduction of NATC F-4J thrust data for hot, cold, intermediate hot, and intermediate cold days was again done with the aid of the Time Share Computer.

Use of the relationship

$$q = \gamma p M^2/2$$

in the thrust and drag equations

$$L = C_L qS$$

$$D = C_D qS$$

together with the use of pressure altitude, simplified the task by eliminating the need for developing a nonstandard day atmospheric density model.

Minimum time energy climb paths for these nonstandard days are given in Figure 23. Except for the cold day, these are smoother than the standard day path.

At the time this temperature sensitivity study was conducted, the intent was to fly an essentially constant calibrated airspeed climb in the supersonic region and use a calibrated airspeed overlay to trim the airspeed in such a

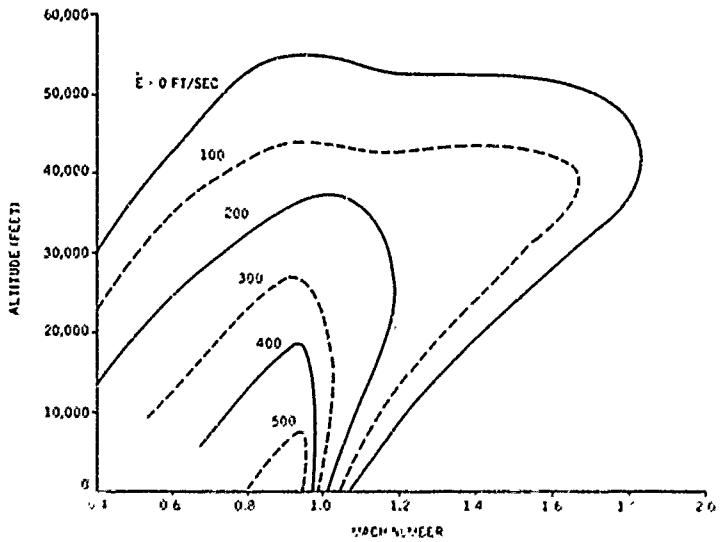

Figure 19. Slatted F-4E Excess Power Contours -- Hot Day

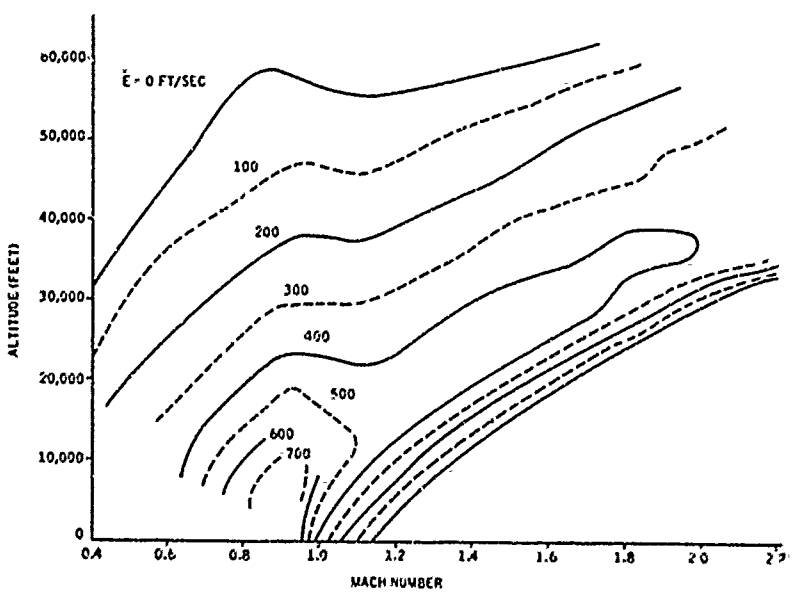

Figure 20. Slatted F-4E Excess Power Contours -- Cold Day

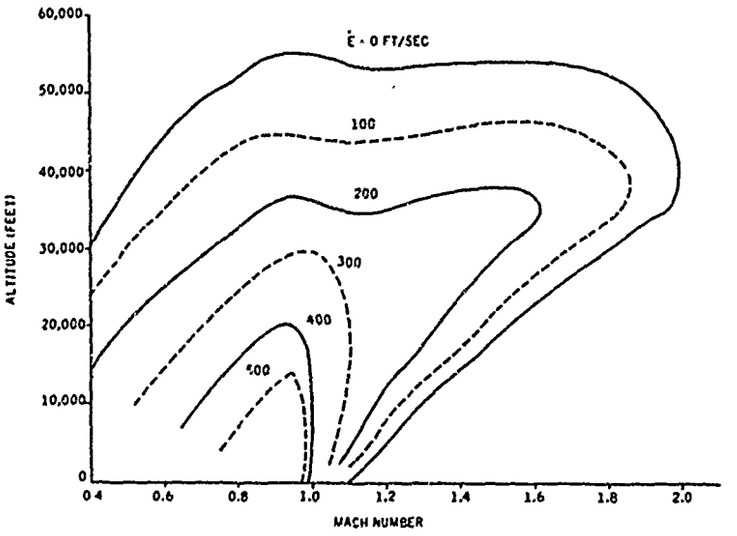

Figure 21. Slatted F-4E Excess Power Contours -- Intermediate Hot Day

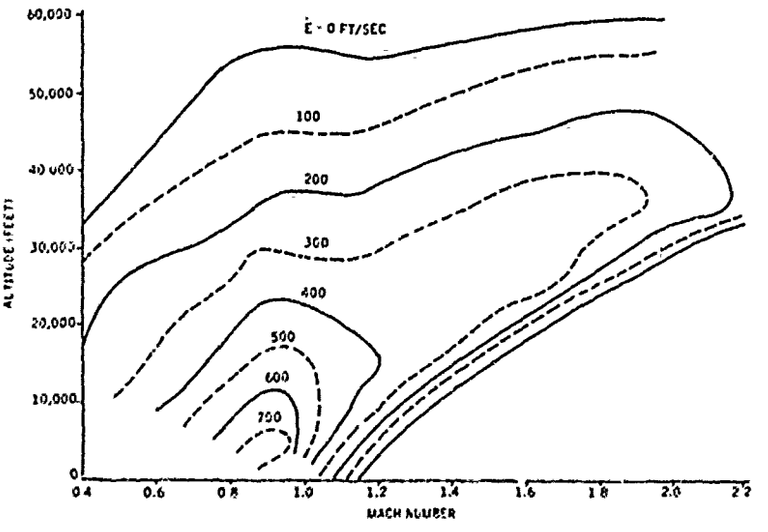

Figure 22. Slatted F-4E Excess Power Contours -- Intermediate Cold Day

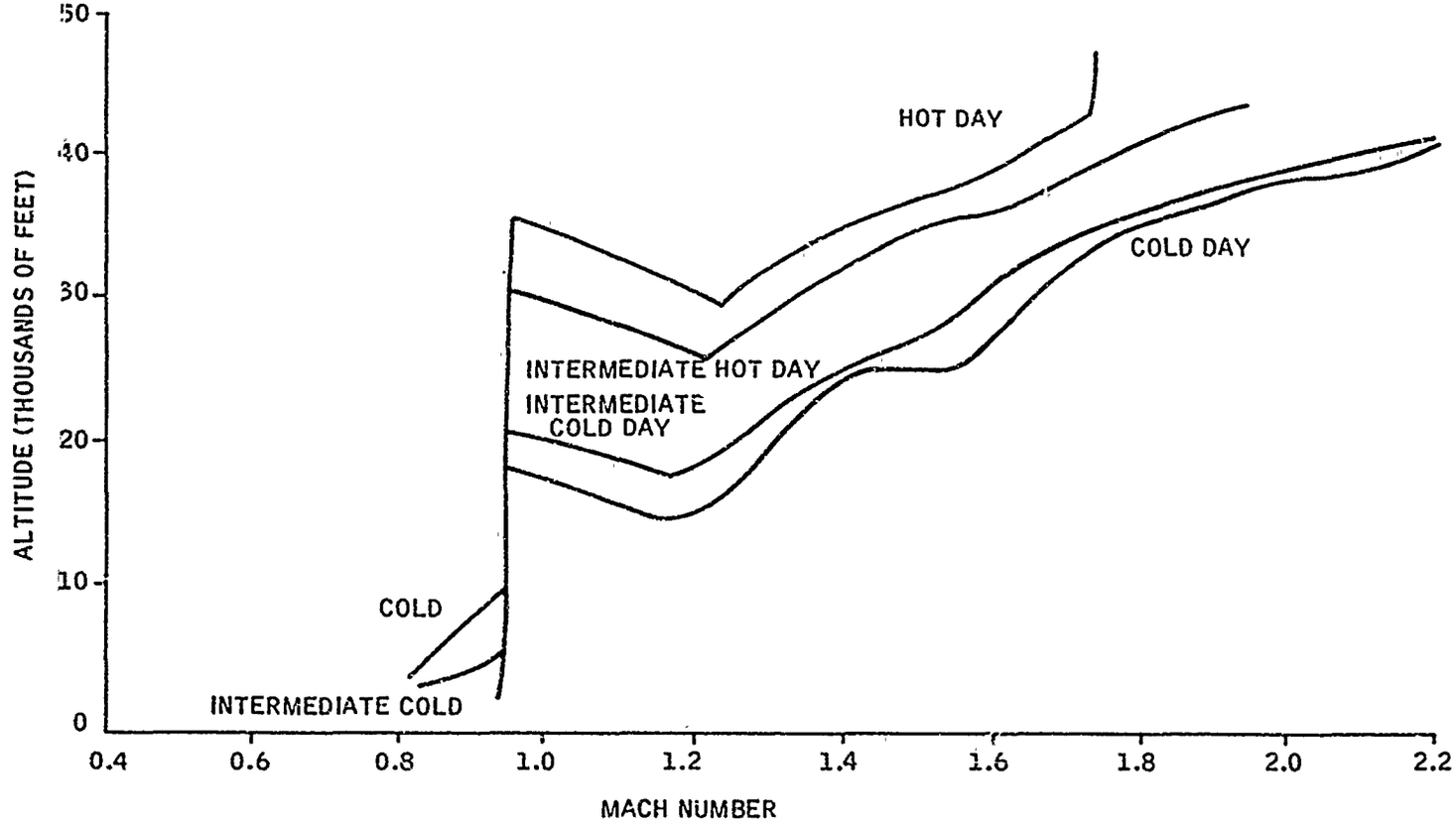

Figure 23. Non-standard Day Minimum Time Energy Climb Paths

way as to obtain optimal performance. Figure 24 illustrates a calibrated airspeed overlay. This was subsequently de-emphasized, but it still may have merit, particularly in that it offers the potential of simplifying the treatment of the temperature problem.

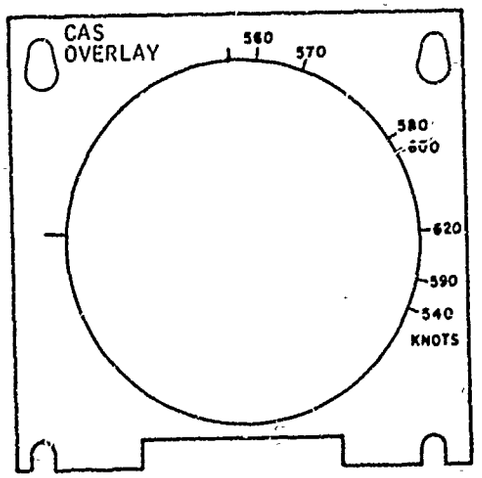

Figure 24. Calibrated Airspeed Overlay for Energy Meter

Table III was made with the aid of a plot of constant calibrated airspeed, together with Figure 23.

Table III. Effect of Temperature on Calibrated Airspeed

Day	Approximate CAS Range (kts.)	Approximate Median
Hot	500 - 550	525
Intermediate hot	525 - 575	550
Standard	590 - 650	620
Intermediate cold	600 - 675	640
Cold	640 - 700	670

Figure 25 gives a suggested correction to the nominal optimal climb speed as a function of atmospheric temperature increment. This is an admittedly crude approximation for these reasons:

- The effect of nonstandard temperatures on the optimal path is not a simple shift in airspeed over the whole climb.

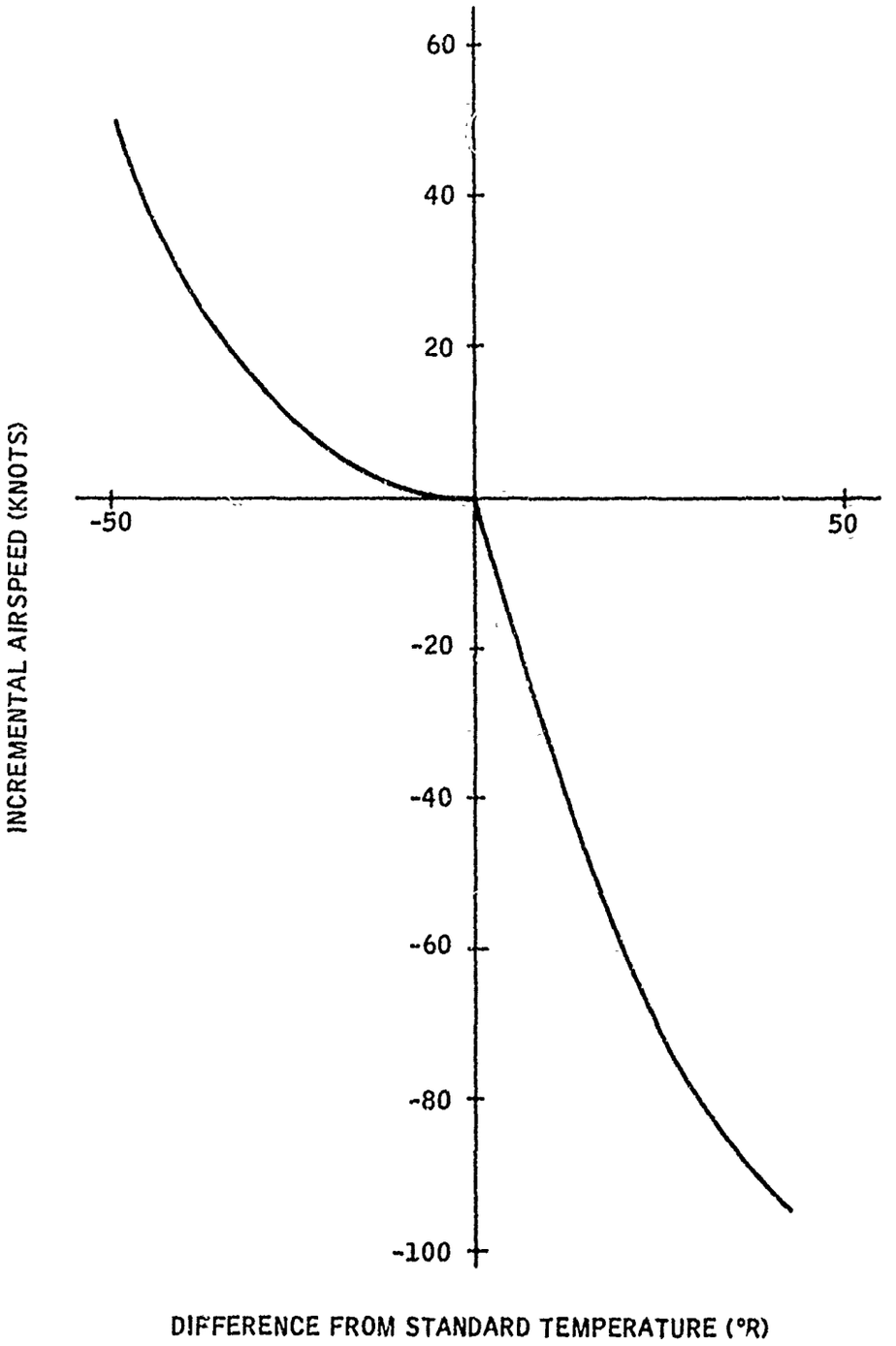

Figure 25. Approximate Corrections to Constant Calibrated Airspeed Climb

- MIL-STD-210A nonstandard day temperatures do not shift uniformly from nominal at all altitudes.

These corrections should provide a base for possible further refinements, should they be desired at a future date.

Weight Sensitivity -- Most of the analyses in this study were done with a constant-weight vehicle. In previous studies, the sensitivity of the optimal path under consideration to weight variation has been relatively small. As a check on this, several minimum-time energy climb paths were computed with different aircraft weights. The results are given in Figure 26, where paths for slatted F-4Js weighing 30,000, 40,000, and 50,000 lb are plotted. These curves verify the initial conclusion that this particular path, the one of primary interest in this study, is reasonably insensitive to weight variations. For example, if one flies a 50,000-lb aircraft on a 40,000-lb optimal path at an energy level of 60,000 lb (altitude 29,200 ft, mach 1.412), he will be off the optimal path by only 0.003 in mach number and 180 ft in altitude.

Drag Coefficient Sensitivity -- Excess power contours developed in different places, supposedly for the same aircraft, often look quite different. One of the significant reasons is the difference in drag data. To examine the drag coefficient increments of plus and minus 10 counts ($\Delta C_D = \pm 0.0010$). These paths are shown in Figure 27. The paths themselves do not show the sensitivity. For the point cited in the discussion of weight sensitivity (approximately 29,000 ft altitude, mach 1.4), a 10-count drag coefficient (about a 2 percent change in the region) causes a 7 percent change in energy rate.

Fuel Sensitivity -- For the scope of the analysis and flight test originally envisioned for this study, only a military-thrust-type, minimum-fuel climb was feasible. A computer program was written to determine the optimal path, fuel consumption on that path, and performance at any arbitraty mach number increment off the optimal path.

Total fuel expended in ± 0.1 mach off-nominal minimum fuel climbs (starting at 20,000 energy ft, up to 47,000 energy ft) increased by 7.4 percent for the slow climb and by 12 percent for the fast climb. Although these are significant percentages, the absolute values of fuel involved are relatively small. Consequently, it was believed that little emphasis should be given to minimum-fuel-type operation.

Nevertheless, a few minutes of flight time devoted to determining the minimum-fuel climb could be worthwhile. It may be used to verify or modify the type of curve shown in Figure 28, a smoothed minimum-fuel climb path, which is compared with NATOPS climb.

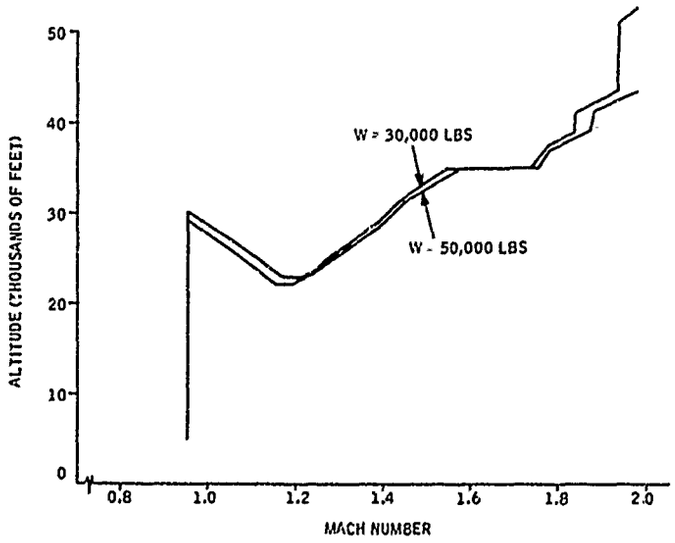

Figure 26. Minimum Time Energy Climb as a Function of Weight

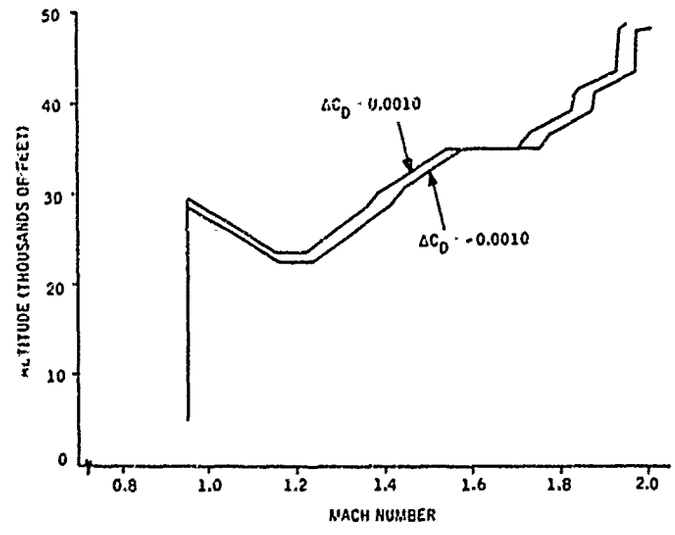

Figure 27. Minimum Time Energy Climb Drag Sensitivity

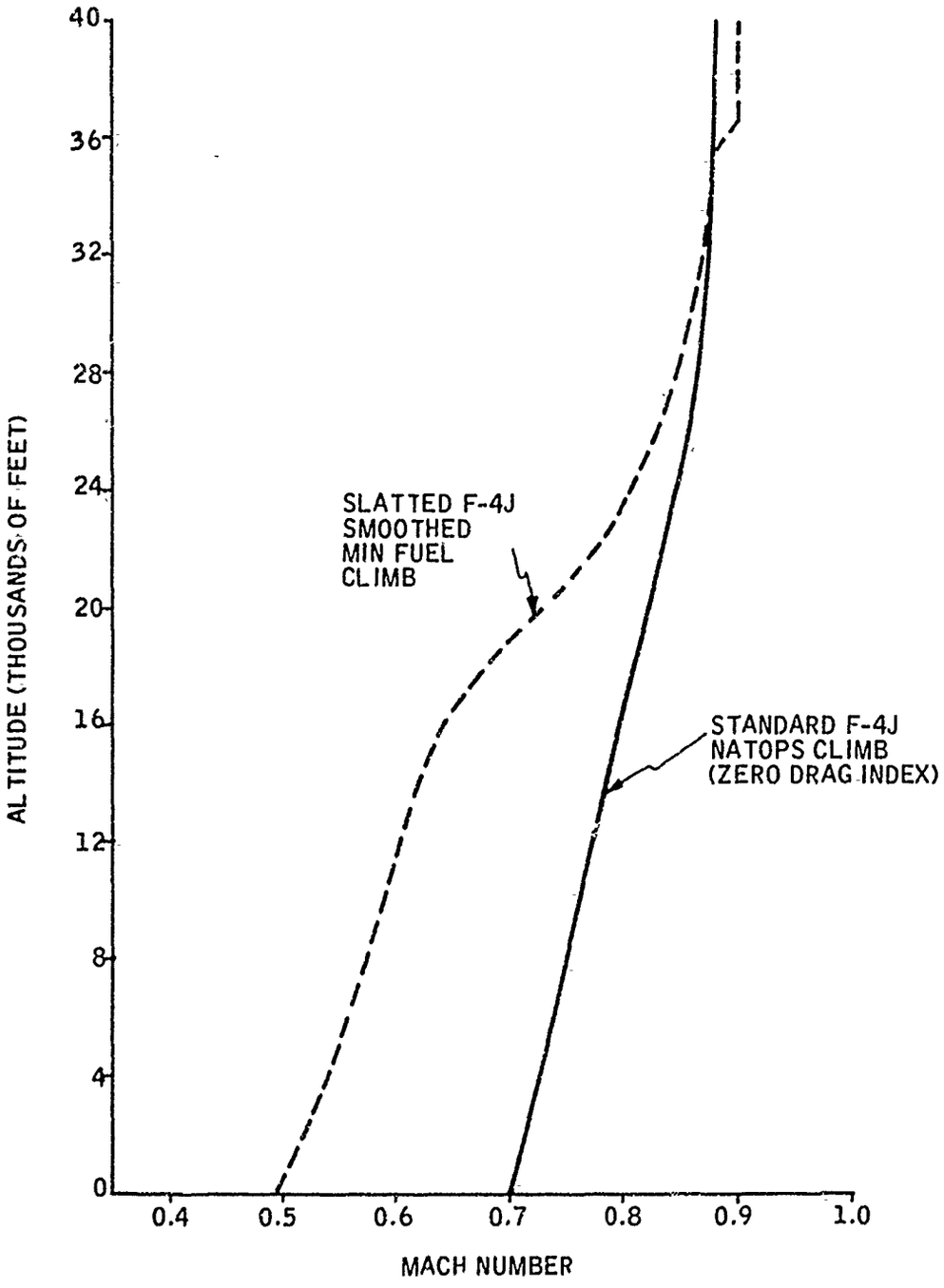

Figure 28. Climb Comparison

SIMULATION

An existing hybrid simulation with man-in-the-loop capabilities was modified extensively for use in establishing the meter format, determining meter utilization procedures and testing the actual meter by means of a hardware tie-in.

Description of the Simulator Facility

The simulation used an XDS Sigma 5 digital computer, an EAI PACE analog computer, an Adage 770 link, a DD40 alphanumeric and vector graphic display oscilloscope, and a Honeywell-constructed fighter control station. Figure 29 illustrates the interconnection of these elements. A simplified flow chart of the simulation is given in Figure 30.

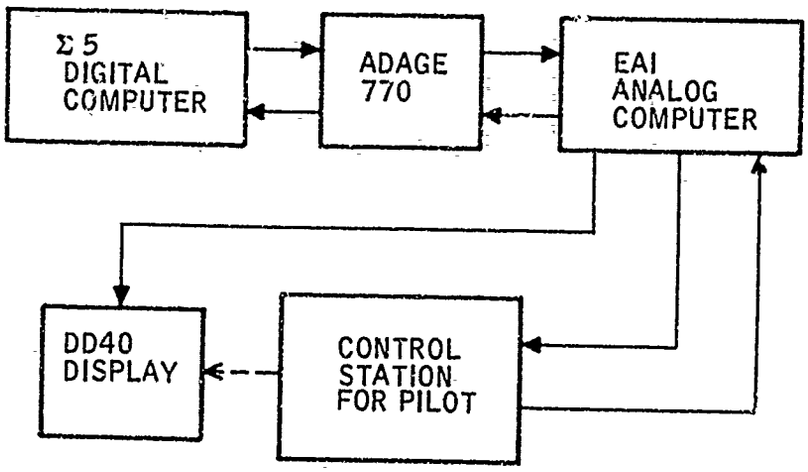

Figure 29. Man-in-the-Loop Simulation

In addition, a partial cockpit shell was constructed and fitted with the essential cockpit displays (attitude indicator, altimeter, airspeed indicator, machmeter, g-meter, angle of attack indicator, and rate of climb indicator). This was used in the meter hardware checkout.

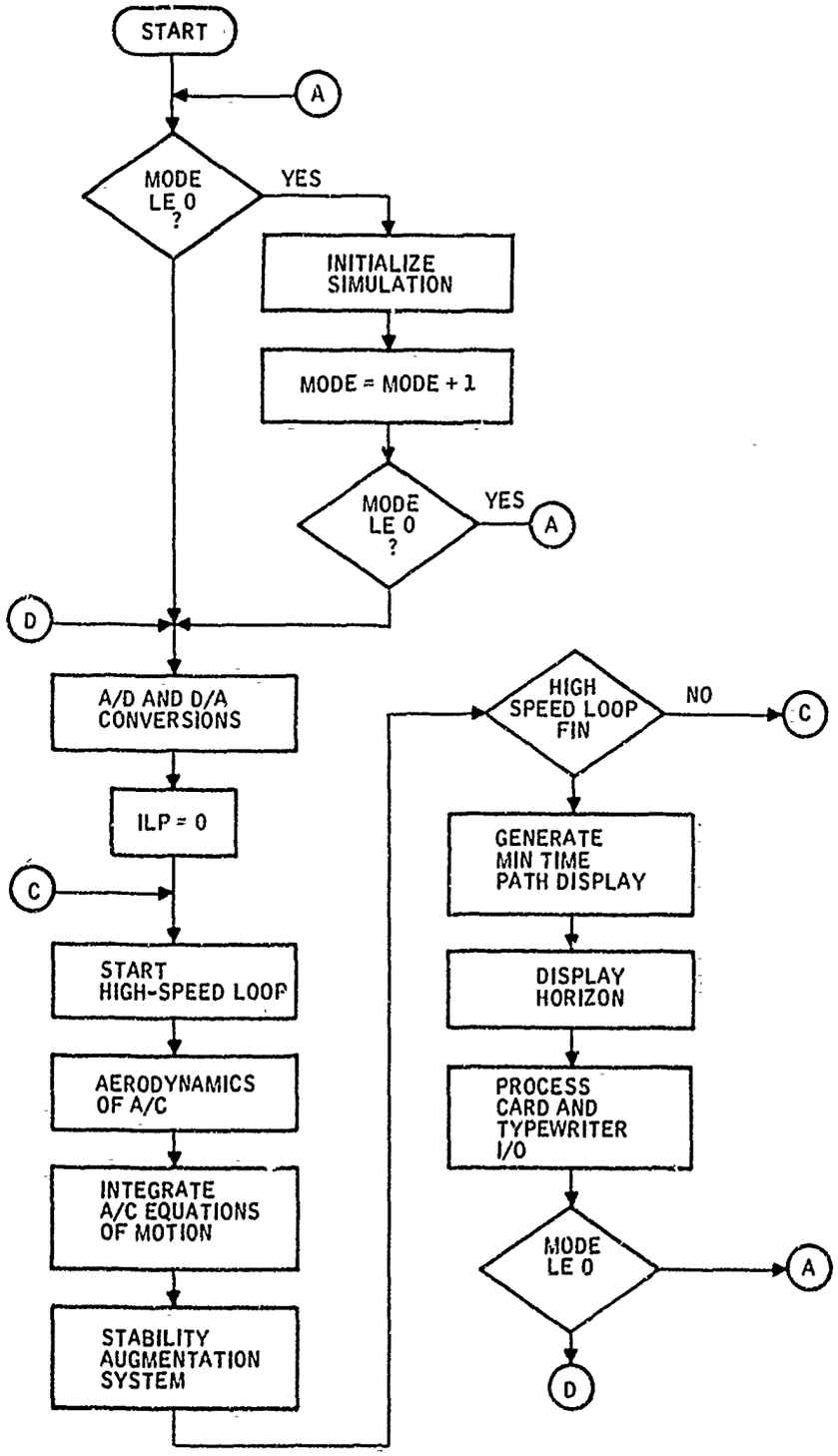

Figure 30. Simulation Flow Chart

The principal tool in the design of the meter format was the DD40 oscilloscope. Figure 31 shows essentially the final form of the display. Below the center horizontal line, arranged in as nearly the order found in the F-4J as possible in this type of display are an altimeter, a rate of climb indicator, a g-meter, an altitude indicator, and a machmeter. In a final modification, an airspeed indicator was incorporated in the machmeter display to simulate the F-4J airspeed/machmeter. The altimeter pointer makes one revolution per 1000 ft, and the altitude is given digitally to ± 20 ft. Climb rate is conventionally in thousands of feet per minute. The greatest shortcoming in the display was in the attitude indicator, which appeared unfamiliar to pilots. However, it did not materially affect the evaluations.

The display at top center, labelled H-M, was used as a training aid. Shown on it is the F-4J minimum-time energy climb path in altitude-mach number coordinates. The circle represents the aircraft position; extending through the circle is a constant energy line segment and a "predictor". The latter shows the instantaneous direction of motion of the aircraft in the h-M plane.

The E meter is shown in the upper right corner, though its position could be changed (within limits of the space available) by a command on a teletype terminal. Energy and energy rate scales are the same as those in the hardware version of the meter. The outermost scale represents a minimum-time energy climb path overlay. The overlay is used in conjunction with the machmeter, though if for some reason it is preferred, an altitude overlay can be made. This is a command mach number; i.e., the mach number indicated by the energy needle is that which the aircraft should be flying at that energy level if the pilot wants to be on the minimum-time energy climb path.

Man-In-The-Loop Studies

Meter Format -- One of the primary functions of the man-in-the-loop studies was to evaluate and develop the meter display format. The change in scale factor at -300 ft/sec on the energy rate scale was incorporated and found to be unobjectionable in simulation flying. This was done to allow a greater range of negative energy rates to be displayed. A velocity limit was added to the E needle to simulate a practical rate limit existing in the drive mechanism to be used in the hardware design. A response time of 1 second for travel of the needle from zero to full scale, an achievable hardware goal, was judged to be fully adequate as a result of trials with a number of responses.

The first attempts at following a specified path by use of an E meter overlay were made with command mach numbers at even energy levels; e.g., 60, 70, and 80 thousand energy ft, etc. Interpolation between these levels was found to be somewhat difficult because command mach numbers at successive

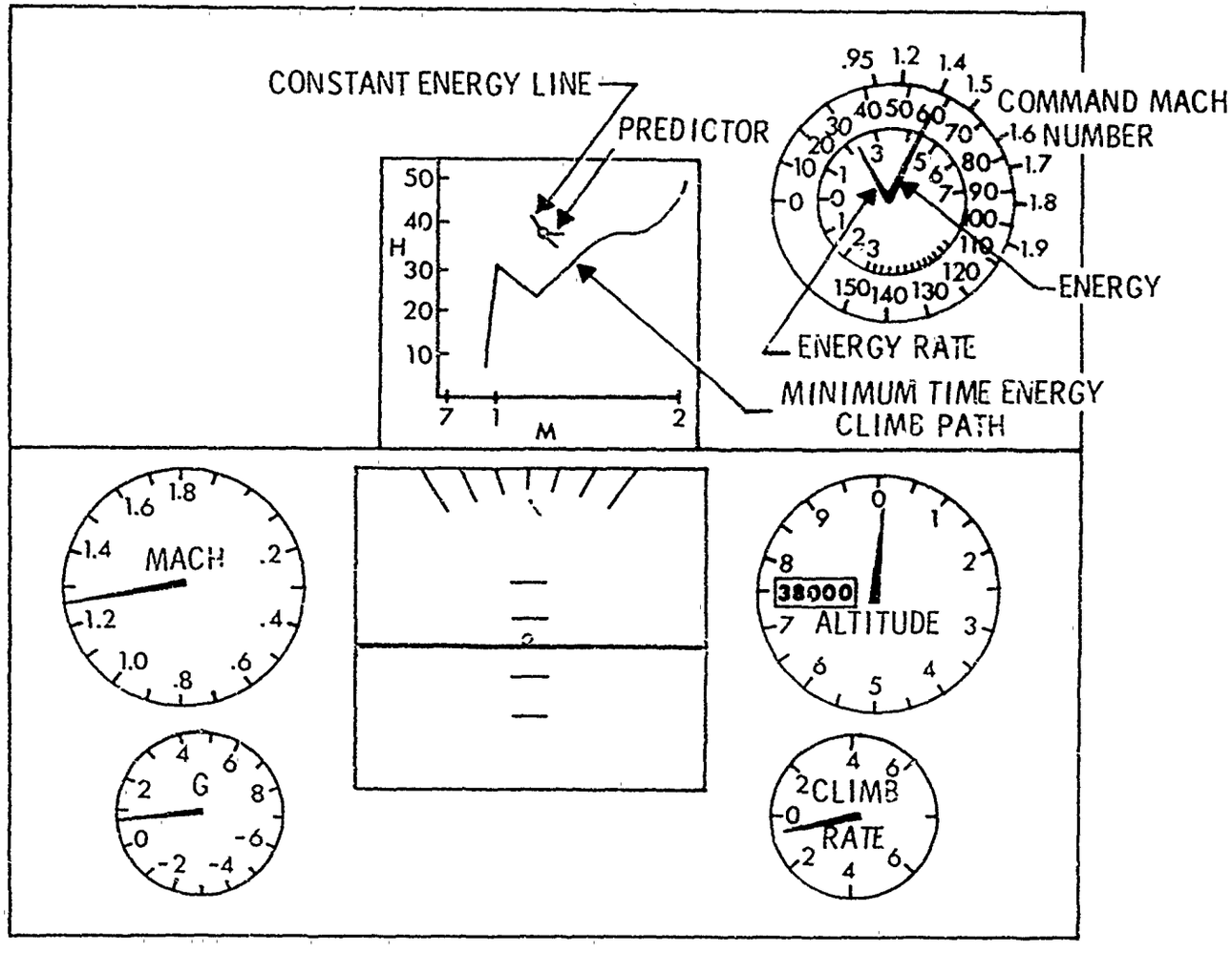

Figure 31. Energy Management Display

energy levels are 1.22, 1.45, 1.61, etc. The program was modified to place command mach numbers at intervals of Mach 0.1; this considerably eased the task of interpolation and, consequently, made following the schedule simpler.

Altitude Overlay -- The question arose as to whether a command altitude could be followed in a minimum-time energy climb in lieu of a command mach number. Another program modification was made to write command altitudes (with even increments) on the overlay scale. Although only a limited effort was made to evaluate this type of overlay, it was found to be feasible. The value of an altitude overlay may be significantly enhanced when the meter is mounted appreciably closer to the altimeter than to the machmeter.

Path Acquisition Rule of Thumb -- The E meter with a command path overlay offers a simple means of determining, at a glance, the desired mach number. Acquiring the desired path, however, must be done efficiently to avoid needless energy losses. This applies particularly to acquisitions from above the desired path. A rule of thumb for path acquisition was developed to ensure efficient convergence. Within the flight envelope, dives without a throttle reduction will generally be made at energy rates significantly above the zero level often referred to in discussions of the energy state approximation. Thus, a constant attitude dive was found to be a good substitute. The rule is as follows:

1) Note the command mach number
2) Push over to a pitch attitude of -10 to -15 deg
3) When actual mach number is 0.1 greater than the command mach number noted in 1, begin a 1.5 to 2 g pullout
3) Ease off the stick as the actual and command mach numbers converge.

In trials of this technique on the simulator, the energy rate was maintained well above zero in the pullout.

Comparison of Performance with h-M and E Meter -- The h-M display discussed earlier is one of the oldest and therefore most familiar displays used in energy management simulation work at Honeywell. A comparison between performance using it and performance using another display thus is akin to comparison of performance against a standard. No sustained effort was made at this type of comparison and no comparison was made at the end of the study. However, results of an early test are given in Table IV.

Table IV. Time to Climb versus Display Comparison

Trial	Display	E_{final} (Ft)	Time (Sec)	Corrected Time* (Sec)	Difference (Sec)	(%)
1	h-M	82920	184.4	186.4	---	---
2	E meter	83370	196.7	194.6	8.2	4.4
3	E meter	83260	190.2	187.9	3.1	1.7
4	h-M	82820	184.8	184.8	---	---

*Time for E meter runs changed to estimated values at final energy levels for h-M runs; e.g., in run 2, the time at which energy level of 82920 ft was passed is estimated to be 194.6 sec, based on the final level of $\dot{E}$ in run 2. The final two columns compare trials 1 and 2 and 3 and 4, respectively. This is because these runs were made in separate sessions on the computer, and initial conditions were not identical.

Initial conditions were 25,000 ft altitude and Mach 0.9 (0.89 for runs 1 and 2). A preliminary subjective evaluation was that climbing at 600 KCAS is of the same order of difficulty as an optimal climb using the E meter in the present configurations. This was the judgment of a nonpilot subject, however.

As might be expected, performance is somewhat better with the h-M display. The disadvantage is the complexity of the system required to generate it. In addition, despite its simplicity, the E meter provides energy and energy rate indications which are not available in the h-M display as configured.

Times to climb obtained on the Time Share computer were verified on the hybrid simulation within the limits of the human operator control capability. Another example of the type of saving that can be realized was demonstrated repeatedly. The initial condition was mach 0.9 at 40,000 ft altitude. In one case a dive was made to a minimum time energy climb path, followed by a climbing acceleration on the path back to 40,000 ft, at about mach 1.8. This This path saved 25 percent of the time required to perform a level acceleration between the same initial and final conditions.

Aircraft Calibration --

Minimum Time -- One of the significant potential uses of the E meter is in aircraft calibration. Given sufficient fuel and time, the pilot could cover a large part of the flight envelope and generate excess power contours, using little more than the E meter, the altimeter, a knee pad, and a pencil.

For the purpose of the flight test, the plan was to gather data for computation of the minimum time energy climb, since much less flight time is required for this task.

The method is to fly level acceleration at a series of altitudes through preselected energy ranges. If data recording capability is not present, the pilot may elect to use the altitude hold mode and record energy rates at selected energy levels himself, or he may want to fly the aircraft himself and relay the readings for the observer to record. Both of these methods have been simulated, and the results given here represent the latter type.

One man flew the aircraft and read the energy rates; a second man recorded them. Peak energy rates representing points on the optimal path were determined from the type of plot sketched in Figure 32. It should be noted that the peak energy rate at a given altitude will not, in general, correspond to the peak energy rate at the energy level represented by that point. This is shown pictorially in Figure 33.

At altitude h_1, the peak energy rate occurs at Point A. Constant energy line E_1 is drawn through this point, and it is seen that in this hypothetical case the peak energy rate for that energy occurs at point B at a lower altitude and higher mach number at altitude h_1, as suggested by point C.

If there were enough data, plotting would be unnecessary; the peaks could be determined by a scan of the data, and, in fact, several of the peaks were obtained by inspection of the tabular data. However, gathering of sufficient data to make this possible for all points would necessitate flying level accelerations at more altitudes. If the aircraft performance were well enough known, this could be partially countered by further reducing the range of energies covered. In short, given sufficiently knowledgeable engineers, sufficiently capable pilots, and a sufficiently large flight test range, the test could be conducted in such a way as to eliminate plotting. However, these are not expected to exist in combination; furthermore, the energy meter is being built because we are not now able to plan well enough to do just that. Except at the high end, the energy rate at the calibrated point was within 2 ft/sec of the optimal value. A direct comparison was not readily available above 37,000 ft because of a difference in atmospheric model in this range. A change to bring them into agreement was made after this test was run.

The results showed the feasibility of using this calibration technique as part of the flight test. The disadvantage is the time required. Judicious choice of energy range (e.g., 50,000 to 85,000 ft) would help.

Minimum Fuel -- The value of minimum fuel calibration and climbs in the flight test were also investigated. The clear advantage of this operation in flight test is the significantly longer flight time allowed with the much lower fuel consumption than in afterburner operation. In the following investigation military throttle setting was considered. A calibration technique similar to that described earlier for determination of minimum time climb was explored.

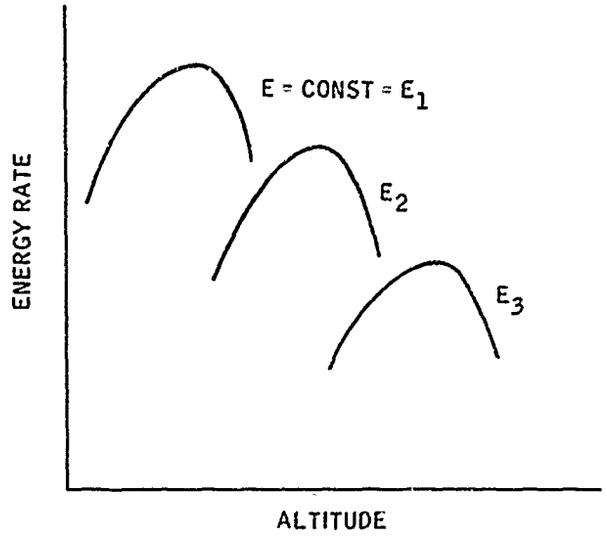

Figure 32. Peak Energy Rate Determination

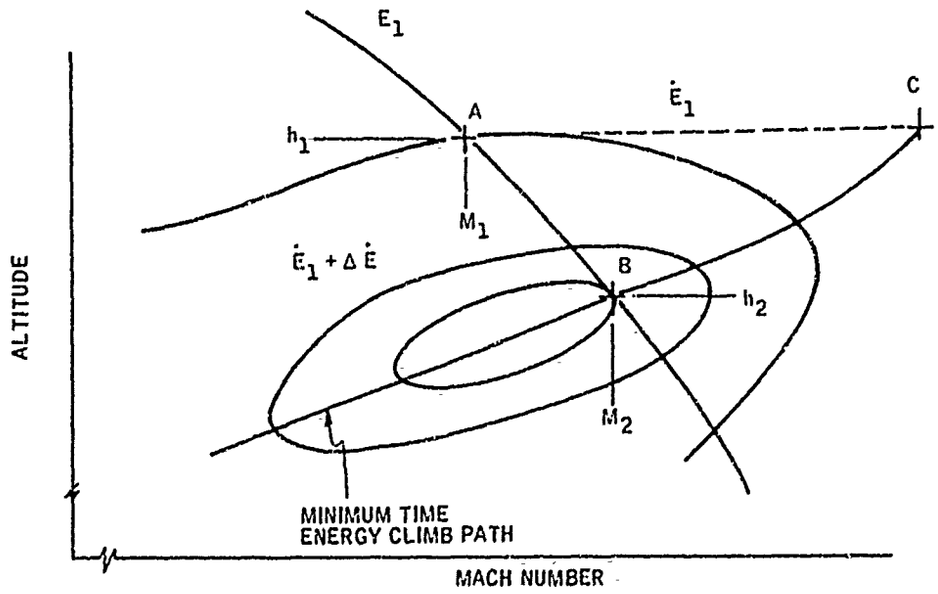

Figure 33. Graphical Determination of Minimum Time Energy Climb Path

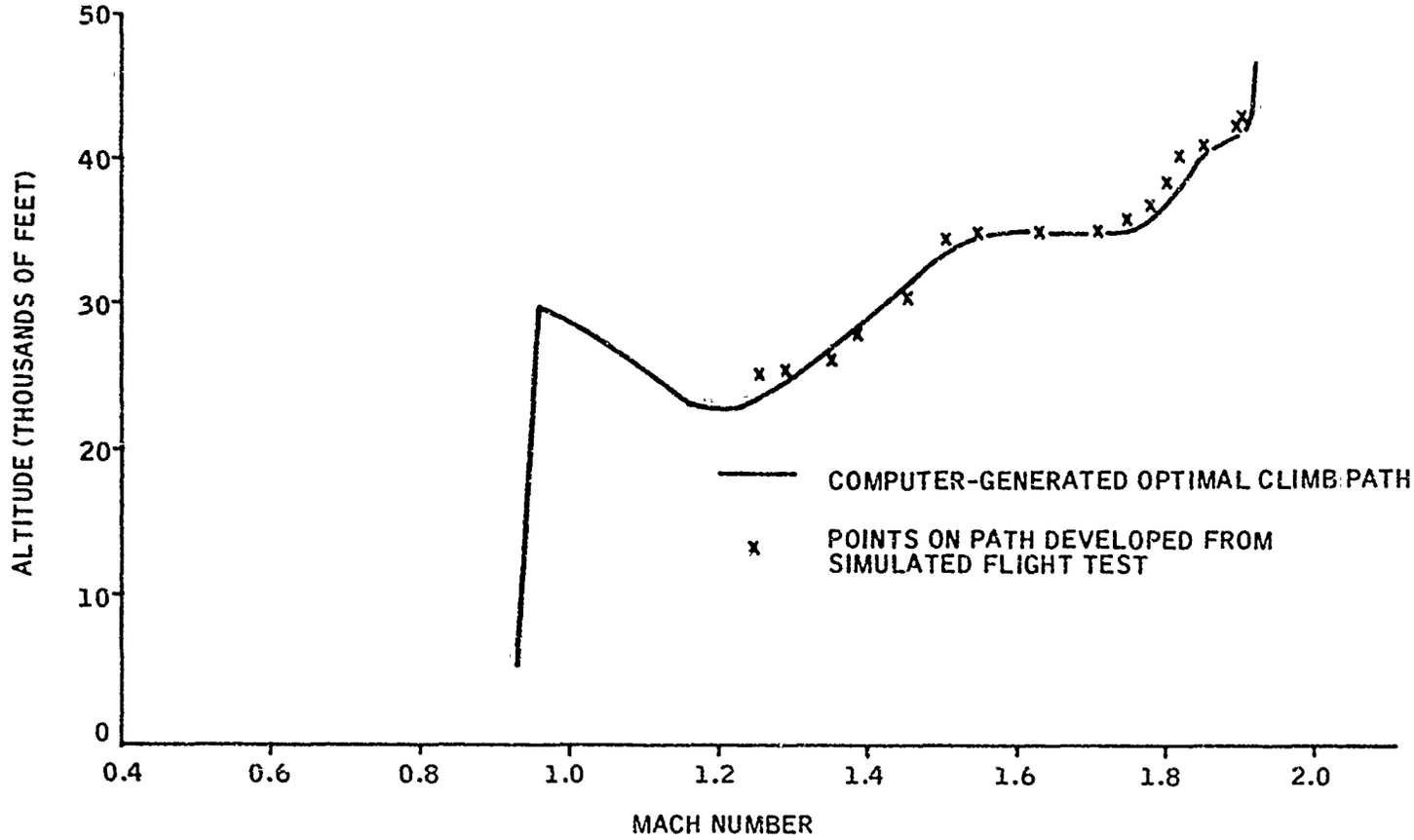

Figure 34. Minimum Time Climb Path -- Slatted F-4J

In the subsonic region the problem illustrated in Figure 35 appears.

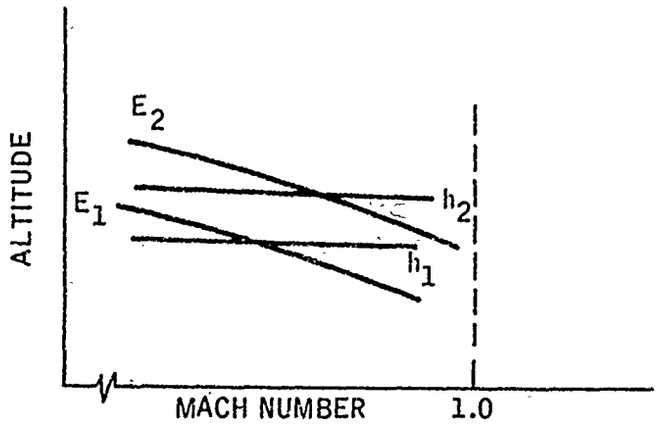

Figure 35. Energy Contours in Subsonic Region

Because the lines of constant energy are realitively shallow, a larger number of closely spaced (in altitude) accelerations are required. However, an alternative method is possible. It has been found that the minimum time climb path can be determined to the nearest 0.001 mach number by noting the peak $\dot{E}$ at a given altitude. The reason is that the shape of the $\dot{E}$ contour is such as to make the points of constant E and constant h tangencies practically coincident, as shown in Figure 36.

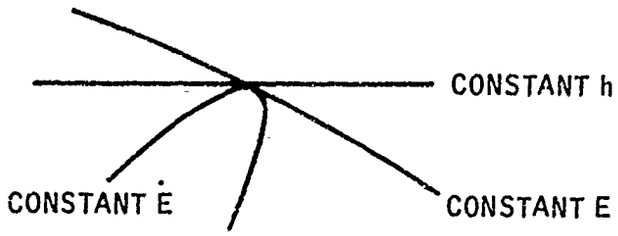

Figure 36. Altitude Coincidence at Energy/ Energy Rate Tangency

This investigation was made in part to determine whether a similar result would be obtained with $\dot{E}/W_f$ contours.

An interesting phenomenon was noted when the minimum fuel climb was computed on the HCN. Figure 37 shows an S curve in this path. There are a actually 2 dives in this subsonic climb. Because this is an unusual result, two other paths were computed, as shown. The first is a minimum-fuel climb without the drag increment for military thrust; the second is a minimum-time climb (for military thrust). Since removal of the drag increment removed the irregularity and since the former is a well-behaved function of mach number, the plot of Figure 38 was made. The points on these curves were taken from level acceleration runs.

The bulges on these curves can be seen to be responsible for the idiosyncracies. The constant energy lines were initially tangent at the right side of the $\dot{E}/W_f$ curve. At a certain energy level (27,000 ft in this case) the point of tangency shifted to the left (a lower altitude and thus, for a given energy level, a higher mach number). A shift back and forth between peaks produced the S curve. Figure 39 shows similar results for the aircraft without the military thrust drag increment. The right-hand bulge is less prominent, and thus one might expect a smoother climb path.

The significance of this for the present purpose is that where the point of tangency occurs at the right-side bulge, the optimal mach number is quite different from that determined by taking the tangency with a constant altitude. Three factors may minimize the problem noticed here.

1) The actual aircraft drag probably is somewhat different, and these bulges may not appear.

2) The resulting values of $\dot{E}/W_f$ are quite similar at a given altitude if either "bulge" is chosen,

3) If flight path acceleration is small, the path will be essentially an altitude climb, and an altitude tangency makes good sense.

A sensitivity investigation (described in the following subsection) showed that potential benefits did not warrant emphasis on this type of effort, though an exploratory investigation could be useful.

Effects of Normal Acceleration in Calibration Runs -- "Flight" in the simulator, of course, lacks the cues available in actual flight. Further, without a force-feel type control stick, an operator in a fixed-base simulator is much more apt to put in control stick disturbances than if flight loads were present to hinder his motions. In a simulator run in which an attempt to hold constant airspeed was made, the sensitivity of energy rate to stick disturbances (or normal acceleration) was especially noted. Because of the

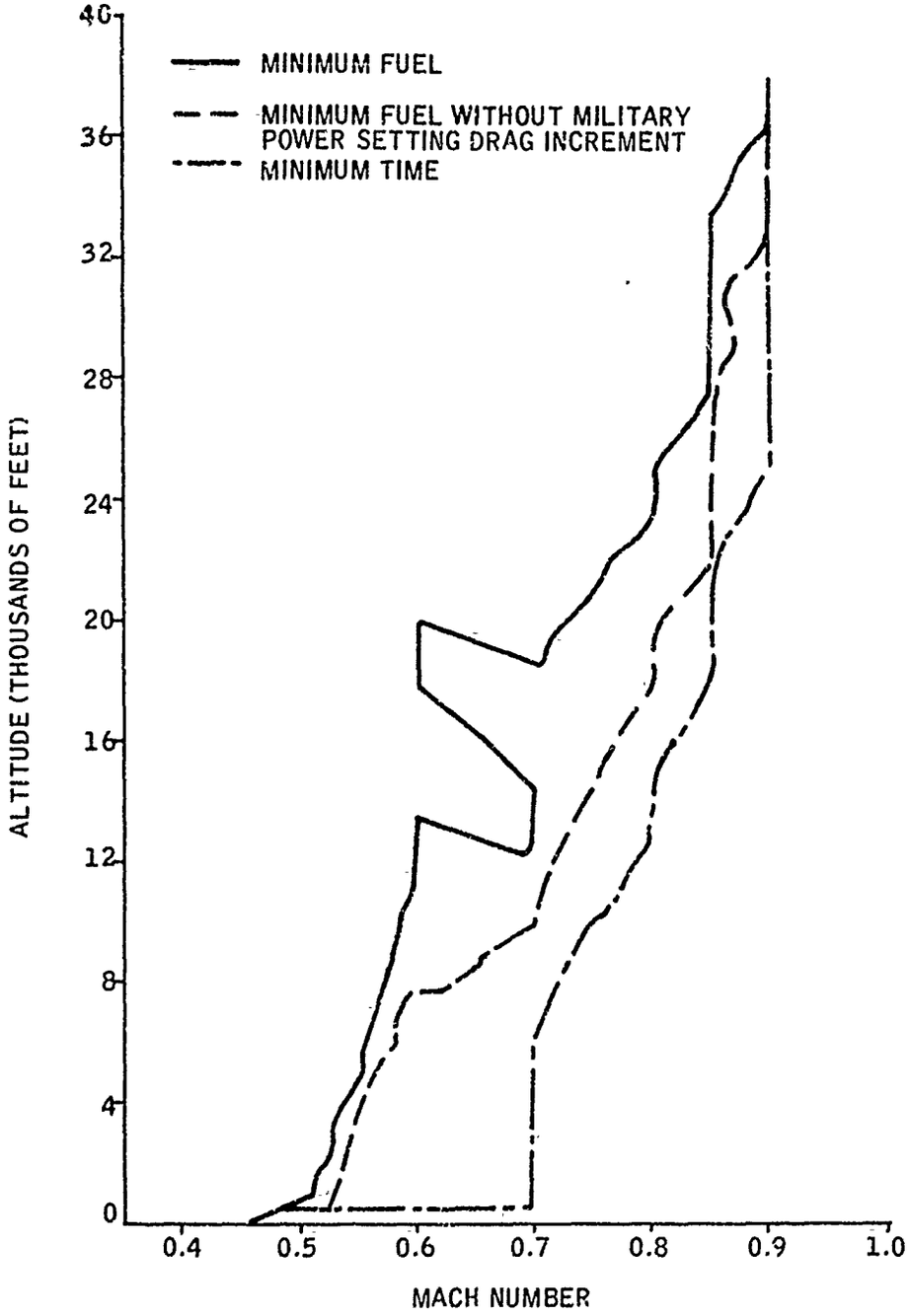

Figure 37. Military Thrust Climbs -- Slatted F-4J

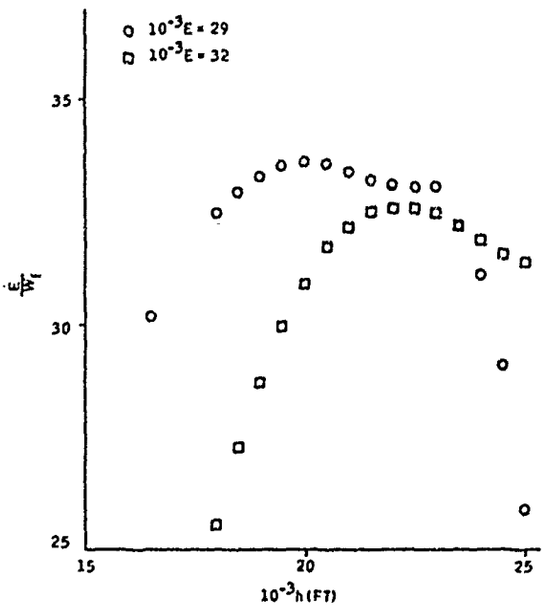

Figure 38. Minimum Fuel Climb Calibration Curves -- Slatted F-4J with Military Thrust Drag Increment

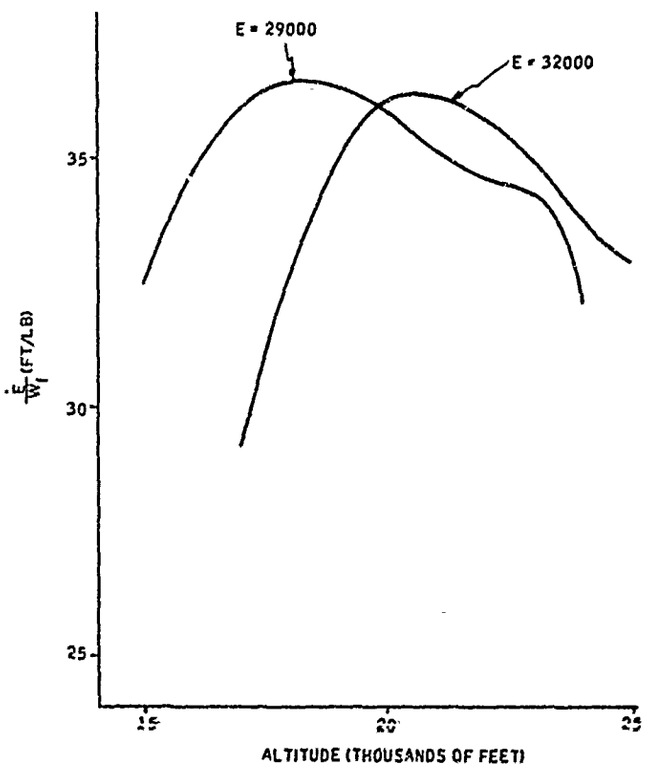

Figure 39. Minimum Fuel Climb Calibration Curves -- Slatted F-4J without Military Thrust Drag Increment

importance of this phenomenon in calibration runs, this sensitivity was investigated.

The sensitivity of $\dot{E}$ to normal acceleration was found to be

$$\frac{d\dot{E}}{d_{a_n}} = V\left[C_1 + \left(2C_2 + \frac{2}{C_{L_\alpha}}\right) a_n \frac{W}{qS} + 3\,C_3 \left(\frac{W}{qS}\right)^2\right]$$

where C_1, C_2, C_3 are drag equation coefficients (cubic C_D versus M polynomial) and the other symbols are defined in the Nomenclature.

Sensitivity was evaluated at the following flight condition:

$h = 30,000$ ft

$M = 1.5$

For a 40,000-lb airplane operating in the vicinity of 1-g flight,

$$\frac{d\dot{E}}{d_{a_n}} = -126 \frac{\text{ft/sec}}{g}$$

This number was approximately verified on the $\Sigma 5$ simulation, though it appeared somewhat smaller in magnitude there.

A similar calibration was done with constant calibrated airspeed (V_C) runs rather than constant altitude. This led to a consideration of the effect of varying V_C. Variation of $\dot{E}$ with calibrated airspeed at 30,000-ft altitude was estimated at speeds of 550, 600, and 650 knots with the following results:

V_C, kts	$\frac{\Delta E}{\Delta V_C}$ $(\frac{\text{ft/sec}}{\text{kt}})$
550	0
600	-0.5
650	-1.3

Altitude sensitivity is also of interest, but its magnitude is smaller, as may be seen as follows for $M = 1.5$:

h (ft)	$\dot{E}$ (ft/sec)
28,000	232
28,500	235
29,000	237
29,500	238
30,000	240
30,500	242
31,000	244
31,500	245
32,000	246

Thus, at 30,000 ft altitude

$$\frac{\Delta \dot{E}}{\Delta h} = 4 \text{ ft/sec/1000 ft}$$

The results, specifically the sensitivity of $\dot{E}$ to normal acceleration, show the importance of maintaining 1-g flight when reading $\dot{E}$. The high-g loadings on the stick at high speeds in actual flight should make the problem less severe there than it appears in the simulator.

Throttle Command Mode -- Although a minimum-fuel climb with military throttle appears to offer little in the way of checkout of meter potential, a combination military and afterburner climb can be used to save both time and fuel. Figure 40 shows results of three climbs (controlled with a unity autopilot). As shown, initial and final energy levels are 9,700 and 50,000 ft, respectively. One climb is full military throttle all the way. Another uses partial afterburner, and the third is a combination of the two. Table V gives a statement of the results of the first and third.

Table V. Partial Throttle Command

Type of Climb	Fuel (lb)	Time (sec)
Military	1400	412
Military plus Partial Afterburner	1275	225

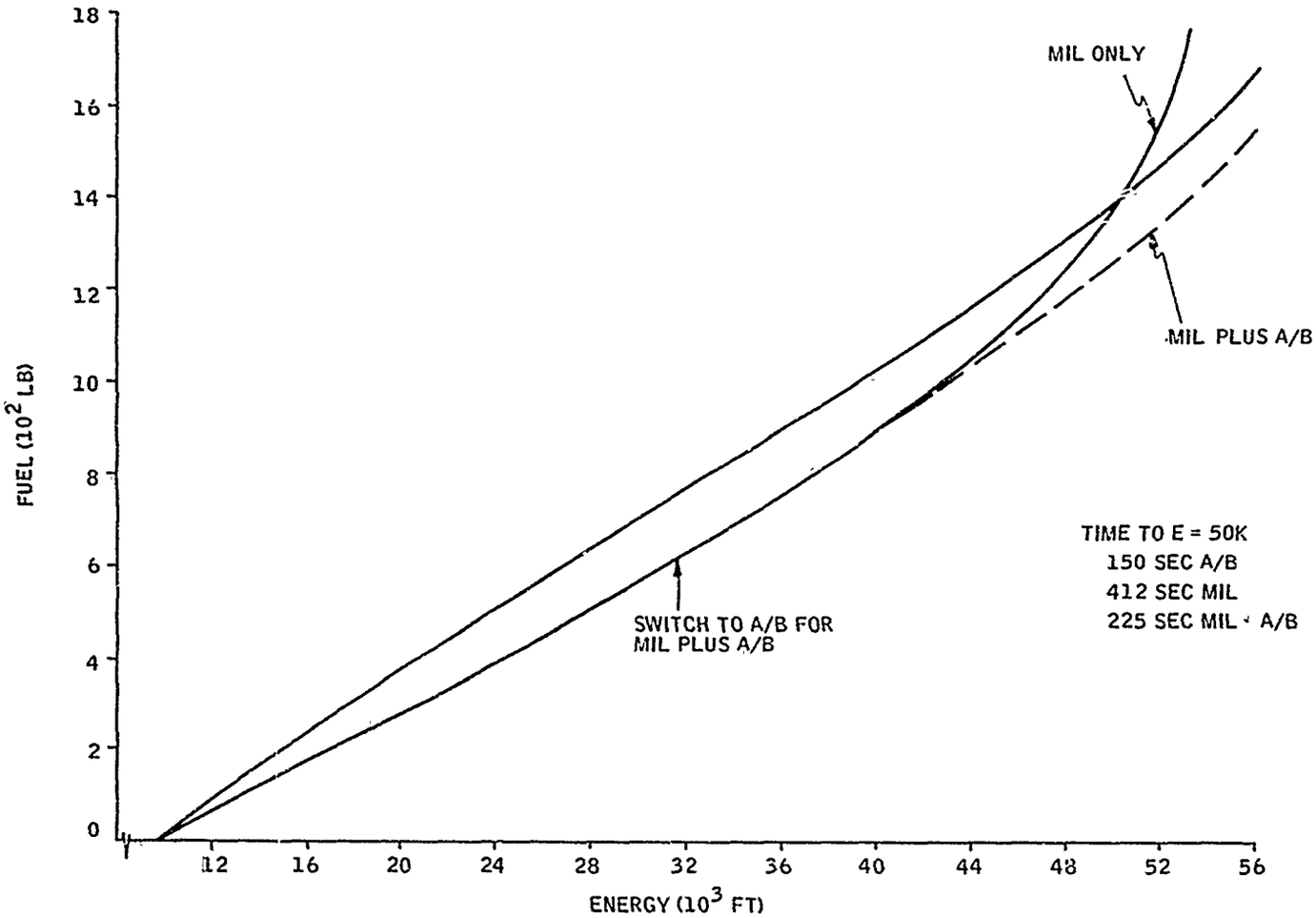

Figure 40. Comparison of Minimum Fuel Climbs

The somewhat surprising conclusion is that judicious use of the afterburner in conjunction with military throttle can save fuel as well as time.

The feasibility of using the E meter to facilitate this type of a climb was checked out in principle on the hybrid simulation. An energy rate-energy schedule was made up in the form of an E meter overlay. This schedule was maintained by means of throttle modulation, while the stick was used to hold mach number constant. The results are summarized in Figure 41. The fairly good agreement between command and actual performance following a short training period shows that use of the E meter in a throttle command mode has good potential.

Pilot Evaluations

Two NATC test pilots evaluated the E meter with the aid of the simulation. Both the simulated E meter (oscilloscope display) and the actual hardware were used.

Test Plan Formulation -- The first evaluation provided insights which helped in formulating the test plan. The second evaluation, though not a step-by-step simulation of the actual flight test, included all the elements of the proposed flight test plan:

- Full afterburner level acceleration runs for performance calibration
- Multiple-g turns
- Minimum-time energy climb path interception and following
- Schedule following with military thrust
- Minimum-fuel climb calibration.

The first evaluation, of an exploratory nature, did not include all of these elements. As a result of this evaluation the simulated rate-of-climb instrument was changed to conform more closely to that used in the aircraft. A calibrated airspeed indicator was also added to the machmeter, and this has proved to be a useful tool.

Pilot Experience -- The first pilot has been through the Air Force Research Pilot School and in Vietnam. He was well acquainted with energy management principles and carefully thought through his techniques and approach to the problem at hand. As he described his technique, it was obvious that it

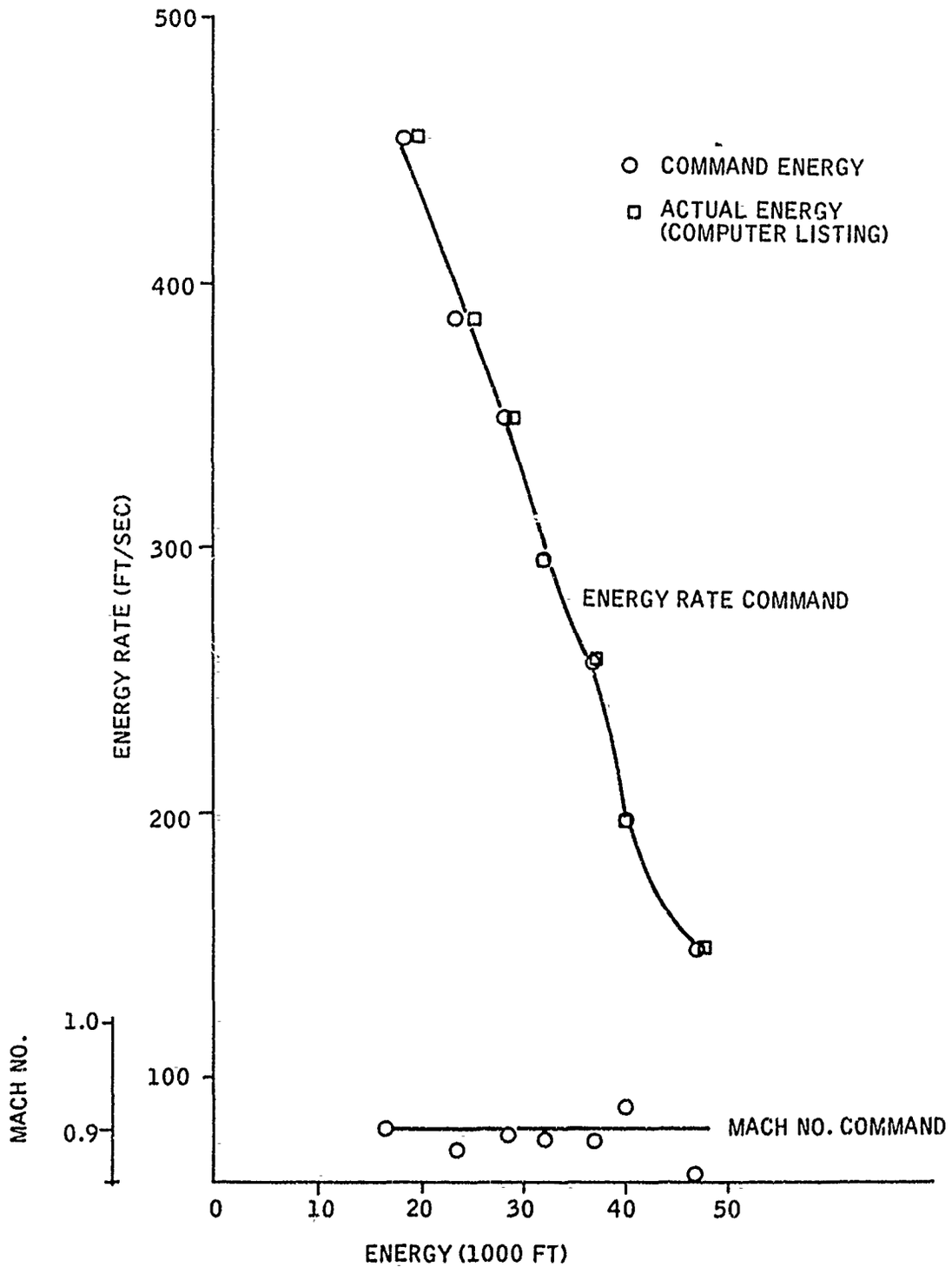

Figure 41. Man-in-the-Loop Energy Rate Command Following -- Energy Meter Overlay

would be impossible to pass these on effectively to the average operational pilot. He stated that he was confident that additional uses could be found for the meter.

The second pilot flew the F-8 well in an energy management flight test in 1971. He has also been in Vietnam and has attended the Air Force Research Pilot School. He is also a competent and knowledgeable pilot and was continually thinking of how the meter could be applied, particularly in aircraft other than fighters.

Pilot Comments and Suggestions --

1) For the calibration runs, a tape recorder strapped to the pilot's leg could replace the kneepad and pencil. This could also be used for general comments. (This must be correlated with time for the calibration runs.)

2) The proximity of energy and energy rate index marks with their different scale factors caused some difficulty. Color coding was suggested (and subsequently adopted) as a corrective measure.

3) The meter has good potential for setting up test points in flight test (i.e., a particular altitude and mach No.). These sometimes take 45 sec in an F-104. On the simulator, without engine lags, it can be done almost instantaneously.

4) Both pilots found it difficult to use the simulated attitude indicator (a problem associated with cathode ray tube representations of real world instruments).

5) The work load in the simulator is higher than it would be under VFR in the aircraft. This is because the simulator, by its nature, is an IFR-type device.

6) There is a scan problem with the E meter mounted above the glare shield. (Subsequently, NATC rearranged equipment, making a panel mount possible.)

7) The A-7 may be a good candidate for an E meter. Under heavily loaded conditions, climb to final altitude can take the whole outbound mission. If a better climb can be determined and displayed, significant benefits can result. On this mission, the pilot has adequate time to devote to a schedule-following task.

SECTION VI
METER DESIGN

INTRODUCTION

The energy/energy rate meter designed, fabricated, and delivered under this contract was shown in Figure 1. This unit, sized for easy readability, yet conserving valuable cockpit panel space, uses a standard 3.25-in.-square bezel, with an overall length of about 7.68 in., including the connector at the rear. The unit contains computing and drive electronics in addition to the servomechanism pointer-positioning components.

Mechanization Approach

The form of the expressions for energy and energy rate which are mechanized in this device was developed to use signal sources generally available in contemporary aircraft. The defining equation for energy, E, is given in Equation (1), repeated for convenience here from the first equation in Section IV.

$$E = h + \frac{V^2}{2g} \tag{1}$$

where

h = altitude, ft

V = true airspeed, ft/sec

g = acceleration due to gravity

This expression for specific energy is the sum of the aircraft kinetic and potential energies divided by the weight of the vehicle. As stated in the introduction to Section IV of this report, specific energy and specific energy rate are referred to as energy and energy rate, respectively. Specific energy rate is the time rate of change of specific energy, and may be defined several ways. First, the time derivative of Equation (1) yields

$$\dot{E} = \dot{h} + \frac{V\dot{V}}{g} \tag{2}$$

The first term is generally available as rate of climb, but rate of change of true airspeed, V, is not common.

Alternatively, $\dot{E}$ as the product of flight path acceleration force and velocity, normalized by weight for specific energy rate, gives

$$\dot{E} = m a_p \frac{V}{W} = a_p \frac{V}{g} \tag{3}$$

where

a_p = aircraft flight path acceleration

m = aircraft mass

W = aircraft weight

The acceleration force may be written in terms of excess thrust, the developed thrust less drag force, as

$$\dot{E} = (F_n - D) \frac{V}{W} \tag{4}$$

Or, since inflight measures of thrust, drag, or flight path acceleration are generally not available, one may compute a_p from its components, using body axis accelerometers and an angle-of-attack signal. This form was selected for the energy rate computation

$$\dot{E} = (a_\ell \cos \alpha - a_n \sin \alpha) \frac{V}{g} \tag{5}$$

where

a_ℓ = aircraft longitudinal acceleration

a_n = aircraft normal acceleration

α = aircraft angle of attack

Equation (1) is employed as the control equation in the servomechanism which positions the energy pointer on the meter. Since common servomechanism practice uses rate feedback for stabilization, the question has been asked as to why such a feedback in the energy pointer positioning control system is not employed as a source for energy rate, rather than Equation (5). Consideration of the dynamic ranges of the E and $\dot{E}$ variables displayed on the scales of the meter shown in Figure 1 answers the question. The dynamic range of these scales was selected by analysis and simulation of the aerodynamics of the F-4J vehicle. If noisy altitude and/or airspeed inputs combined to yield an energy error equivalent to 500 ft (1/4 minor division) in 1 sec, the energy rate pointer would rotate by 130 deg. Since the design goal on the energy indicator accuracy was 1/4 minor division, the

ratios between the dynamic ranges of these two scales ruled out the use of rate feedback generation of $\dot{E}$, and favored the selection of Equation (5), using accelerometer and angle-of-attack sensor signals, combined and multiplied by true airspeed from the air data computer. Sensitivity considerations gave some concern regarding signal-to-noise ratios that could be expected in the outputs of the accelerometers. The first flight test results demonstrated the appropriateness of Equations (1) and (5), and indicated that noise was not a problem calling for application of additional filtering. In planning the mechanization approach, circuit fabrication techniques were reviewed. The investigation of both thick and thin film circuit technology for application to this program indicated that time and cost savings could be effected by using the thick film method. This selection permitted use of techniques developed for other on-going hardware fabrication programs. It was soon apparent that a single package could contain the entire computing and display mechanization. The functions called for by Equations (1) and (5) are distributed over nine printed circuit boards, open to view in the photograph of Figure 42. The dial subassembly (in the upper left) is shown with three cards -- the unregulated power supply, transformer and motor mounting plate, and an interconnect card. This mates with the first card of the series of six, reading from lower left to upper right in Figure 42. Their functions are chopper supply and voltage regulators for positive and negative source requirements; true airspeed squaring circuit and instrument servo drivers; energy rate computation, including angle-of-attack sine and cosine function generation; energy rate shaping for scale factor change at -300 ft/sec, with flight recorder interface scaling amplifiers on energy and energy rate; angle-of-attack and altitude interfaces; and true airspeed and accelerometer interfaces.

Interface Definition

By coordination with NATC and the aircraft manufacturer, these signal source interfaces were defined and the energy meter wiring requirements established. This wiring information was transmitted to ONR for use at NATC. The data transmittal, including installation dimensions for the meter itself, is given in Appendix A.

Determination of Flight Path Acceleration Scaling

Early in the design process, the required range of inputs to the multiplier circuits had to be established. Knowing the dynamic range of all signal variables from the preceding analysis and interface definition, the one remaining question was the expected maximum value of flight path acceleration, the difference of products in Equation (5). Using a time share computer program, the maximum flight path acceleration was determined with the aid of the flight strength diagram of Figure 1-42 in Reference 6 (p. 1-139), and limitation on normal acceleration capability based on maximum lift coefficients estimated from Reference 5. As would be expected, the maximum

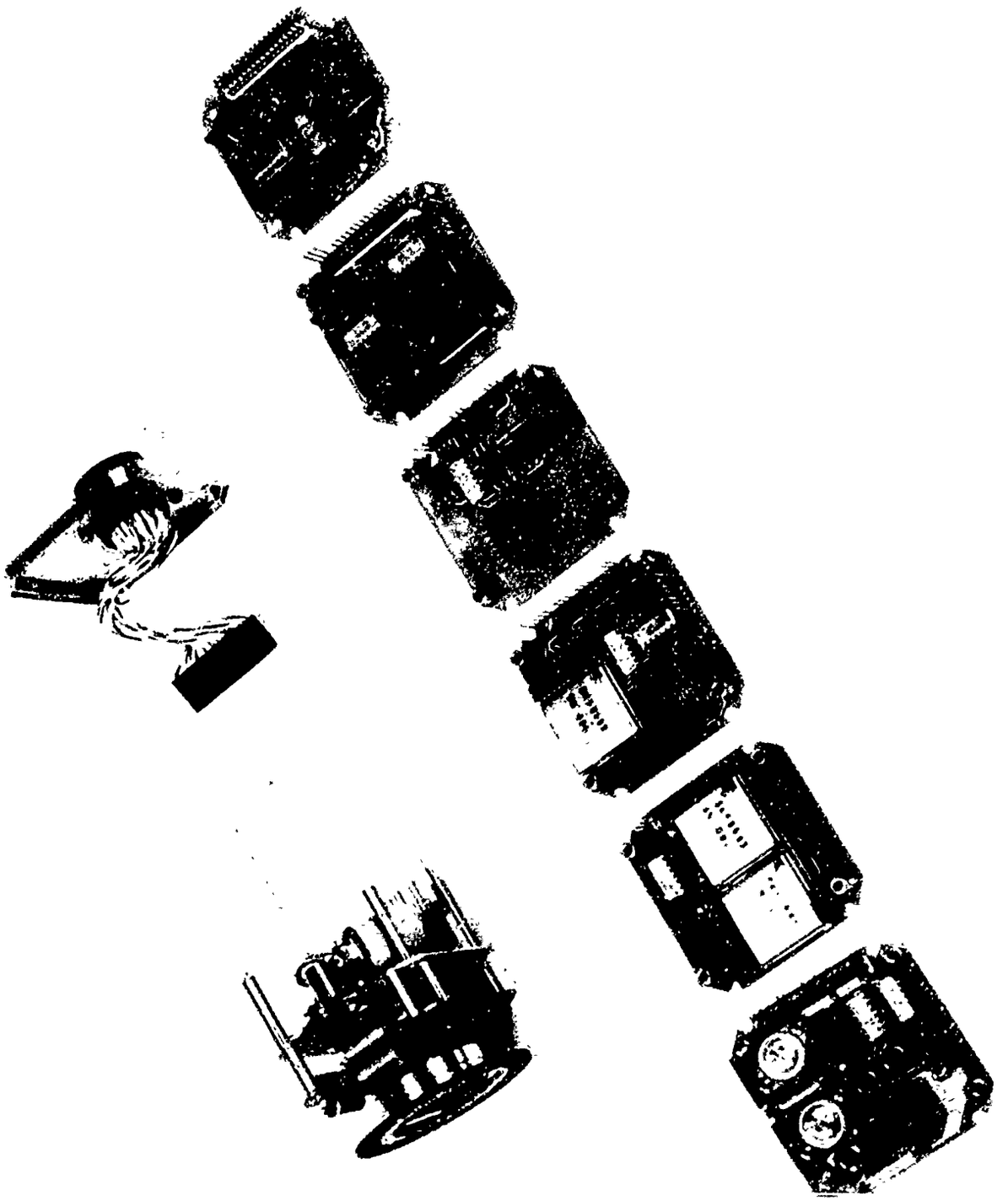

Figure 42. Subassemblies, Energy/Energy Rate Meter JG1077AA-01

positive flight path acceleration occurred at sea level, at the minimum aircraft gross weight, and was found to be 0.75 g. A maximum negative value of 1.25 was found at 35,000 ft altitude at mach 1.5. Therefore, the recommended range of input accelerations for the final $\dot{E}$ multiplier (flight path acceleration times true airspeed) was ±1.25 g. A casual consideration of this range might give the reader an impression that it was not adequate, but at an initial zero longitudinal acceleration, a 6-g pull-up would yield -1.25 g flight path acceleration only when the angle of attack reached 12 deg. The computer solution included the thrust and drag effects on longitudinal acceleration as angle of attack reached its limit for maximum lift coefficient.

Energy Rate Null Adjustment Knob for Pilots

Changes in null offset and scale factor on inputs to the energy meter can be made by resistor changes in the interface printed circuit boards. From the experience gained on this program, the desirability of giving the pilot a nulling adjustment on the energy rate reading was demonstrated. This was proposed to and authorized by the Air Force on the meters to be used in their research program with the F106 aircraft.

SECTION VII
FLIGHT TEST

INTRODUCTION

This section presents the suggested plan for flight test evaluation of the energy meters at NATC, some results of the first tests, and the rationale for the questionnaire provided for debriefing pilots participating in those tests. The flight test plan was developed for the man-in-the-loop simulation studies and was revised to respond to NATC pilot experience reported in Section V. The limited flight test data received by Honeywell was analyzed; the data indicated incorrect calibration of input signals to the energy meter. After recalibration, the meter performance was judged to be satisfactory. Flight test results obtained subsequent to the writing of this document will be given in an NATC report. The questionnaire is discussed, but pilot responses are not available at this time. The complete debriefing document is given in Appendix B.

PROPOSED ENERGY METER FLIGHT TEST PLAN

The following flight test plan was proposed for consideration in evaluation of the meter at Patuxent Naval Air Test Center.

1) Schedule following - military thrust; two flights. Climb to 30,000 ft with the following schedule (Ref. 6, Manual, pp 11-43).

Altitude (ft)	Mach No.
SL	0.55
5,000	0.59
10,000	0.63
15,000	0.67
20,000	0.70
25,000	0.74
30,000	0.76

Upon reaching 30,000 ft, begin a spiral descent at a constant $M = 0.76$ and $\dot{E} = -300$ ft/sec. Time descent to 5000 ft as a check on negative $\dot{E}$ computation. Make two climbs of this type. With the time remaining, make level accelerations at as many of the conditions listed below as possible:

Altitude (ft)	Mach No.	
	Starting	Final
30,000	0.75	0.95
25,000	0.70	0.90
20,000	0.65	0.85
15,000	0.55	0.75
10,000	0.50	0.70
5,000	0.45	0.65

Read and record $\dot{E}$ and fuel flow as frequently as possible during these runs. Ideally, the readings would be made simultaneously.

Between successive lines in the above table set up energy rates in accordance with the following:

Initial Conditions		Final Conditions		$\dot{E}$	Approximate Time (sec)
Altitude (ft)	Mach No.	Altitude (ft)	Mach No.		
30,000	0.95	25,000	0.70	-1000	11
25,000	0.90	20,000	0.65	-750	15
20,000	0.85	15,000	0.55	-500	24
15,000	0.75	10,000	0.50	-200	51

The second flight should be a repeat of the first, with an E meter overlay substituted for the altitude-mach No. schedule. It is realized that this is demanding and that probably not all of it can be done in a single flight.

2) Calibration with afterburner; three flights. Make level accelerations with maximum thrust through the following energy ranges:

Altitude (ft)	Energy (thousands of ft)	
	Initial	Final
20,000	44	56
25,000	44	66
30,000	44	78
35,000	54	93
40,000	64	93
45,000	78	93

Record $\dot{E}$ at every 2000 energy ft. Be sure that the reading is made at 1 g. Between level runs, retard the throttle and make a climb (plus turn, if necessary) at a constant $\dot{E}$ level (near -1000 ft/sec; note and record this value).

On the final flight, make level accelerations through M = 0.95 at 25,000, 30,000 and 35,000 ft altitude with afterburner. The purpose of these runs is to obtain data from which the push-over point can be determined.

3) Afterburner climb schedule following; two flights. The first of these climbs will be made with an altitude - mach number schedule; the schedule will be made from the calibration data gathered under Item 2. The second will be the same climb made with an $\dot{E}$ meter overlay to assist in schedule following. As in the military thrust climbs, criteria for comparison will be accuracy and ease for schedule following.

FLIGHT TEST RESULTS

Accurate readings of energy were obtained from the first flight. Response in the energy rate channel was satisfactory; $\dot{E}$ changes due to high-g maneuvers were adequately reflected in movements of the needle. In fact, the initial acceleration reversal typical of a stick motion was noted by one pilot in an early flight. Though this is a phenomenon familiar to analysts, it apparently is not generally noticed by pilots. Though this factor is not important in itself, it illustrates the potential that exists for the meter to aid pilots in better understanding, and thus better exploitation of the aircraft's capabilities.

The first test flight to evaluate operating characteristics of the energy meter consisted of flying a series of "steady points," (sometimes referred to as "speed power points") wherein the pilot places the aircraft in level unaccelerated flight at a number of altitudes and velocities. Table VI presents

Table VI. Pilot Recorded Data for 22 Steady Points

Point	Cockpit				
	V_i (KIAS)	Hp_i (ft)	V_T (KTAS)	E Meter (ft)	$\dot{E}$ Meter (ft/sec)
1	235	4,000	270	8,000	+30
2	362	4,800	424	14,000	+50
3	540	5,520	625	25,000	+50
4	310	31,200	495	42,000	+50
5	373	29,600	570	45,000	+60
6	310	19,400	425	28,000	+50
7	298	30,400	503	42,000	-30
8	232	30,400	412	37,500	-30
9	334	30,400	566	45,000	-30
10	372	10,050	467	---	-10
11	480	9,700	585	26,000	0
12	286	30,600	485	41,000	-40
13	540	30,500	810	62,000	-10
14	320	20,020	442	29,000	-20
15	420	19,650	576	35,000	-15
16	260	30,020	416	38,000	-25
17	344	29,920	547	44,000	-20
18	230	35,100	410	43,000	-40
19	313	34,540	550	49,000	-40
20	143	14,920	192	17,000	-20
21	140	10,060	177	11,000	-20
22	301	9,990	363	16,000	-20

pilot-recorded data for each of 22 steady points. For each point, the pilot wrote down indicated airspeed in knots, indicated pressure altitude in feet, true airspeed in knots, and the energy and energy rate indications.

Figure 43 compares the Table VI pilot knee pad recordings of the constant level of energy at steady points number 7 and 8 against digitally computed energy levels from magnetic tape recordings of altitude and true airspeed. The computer data were printed out for a 5-sec period at 2/sec. These values compare well and are well within the accuracy goal of 1/4 minor scale division.

Nonzero $\dot{E}$ readings were noted for steady-state conditions in the first flight. These were found to be due to two factors:

1) An initial misunderstanding about the relationship of accelerometer alignment and angle-of-attack reference axes.

2) Null biases in the accelerometer outputs.

The second factor was not discovered until the first had been isolated and corrected. When the first six steady points indicated a consistently high reading on energy rate, the possible causes were sought by considering the total differential of the energy rate equation, as mechanized in the meter:

$$d\dot{E} = \frac{\partial \dot{E}}{\partial a_\ell} d a_\ell + \frac{\partial \dot{E}}{\partial a_n} d a_n + \frac{\partial \dot{E}}{\partial \alpha} d\alpha + \frac{\partial \dot{E}}{\partial V} dV \qquad (6)$$

Substituting Equation (4) for $\dot{E}$, evaluating the partial derivatives, and setting $dV = 0$ (since the pilot is flying level at constant velocity), one obtains:

$$d\dot{E} = \frac{V}{g} \left[\cos \alpha \, d a_\ell - \sin \alpha \, d a_n - (a_\ell \sin \alpha + a_n \cos \alpha) \, d\alpha\right] \qquad (7)$$

Since no steady points were flown at angle of attacks greater than 8 deg, one can assume $\cos \alpha = 1$ and $\sin \alpha = \alpha$ yielding:

$$d\dot{E} = \frac{V}{g} \left[d a_\ell - \alpha \, d a_n - (a_\ell \alpha + a_n) \, d\alpha\right] \qquad (8)$$

Furthermore, one may assume for the steady points that the nominal values $a_\ell = 0$ and $a_n = 1$ g can be substituted into Equation (8):

$$d\dot{E} = \frac{V}{g} \left[d a_\ell - \alpha \, d a_n - g \, d\alpha\right] \qquad (9)$$

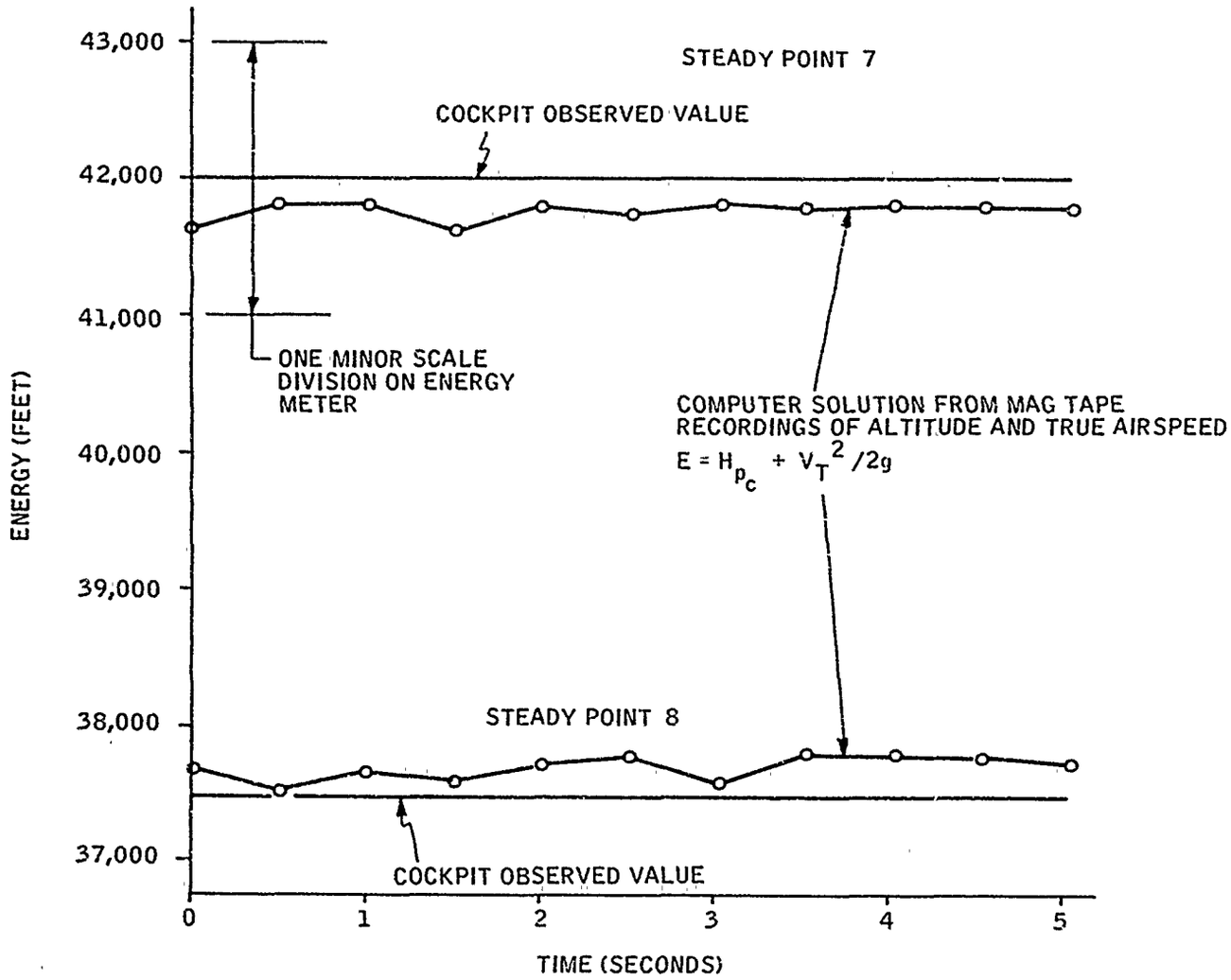

Figure 43. Energy Meter Readings versus Computed Values for Steady Points No. 7 and 8

It is convenient to associate the differentials with linearized finite increments in each variable:

$$\Delta \dot{E} = \frac{V}{g} \left(\Delta a_{\ell} - \alpha \, \Delta \, a_n - g \, \Delta \alpha \right) \tag{10}$$

One may consider each increment Δa_{ℓ}, Δa_n, and $\Delta \alpha$ as sensor errors, and then determine the corresponding error in indicated energy rate, ΔE. For example, with true airspeed of 700 ft/sec, perfect accelerometer indications, and an error of -4 deg in angle of attack, an energy rate error of 45 ft/sec would be displayed. An adjustment was made in the $\dot{E}$ computation circuits of the energy meter to compensate for the error noted in the first six steady points. This error was attributed to an incorrect initial understanding of accelerometer alignment with respect to the angle-of-attack reference axis. As may be observed from Table VI, the energy rate output was consistently low after the adjustment was made following steady point number 6. At this time, computer data reduction of the magnetic tape recordings from the first 13 steady points was available, and two discrepancies on the input data to the energy meter were found. The first was that the accelerometer outputs did not resolve to 1 g as they should have in the level, unaccelerated flight state.

The second discrepancy was the uncertainty between angle-of-attack data from the CADC and corrected nose-boom angle of attack. The presence of these discrepancies offered a real challenge to achieving consistent null outputs in the energy rate display for steady points. Attempts at choosing three points to solve for the three factors of Equation (10) proved fruitless. Consequently, a mean error was determined and corresponded to the equivalent of 18 milli-g null bias signal from the longitudinal acceleration input. This adjustment was made, and the entire meter was bench checked for calibration accuracy.

No detailed plots of data are available at this time to show the effectiveness of the second energy rate adjustment. NATC will present these data in their report, but informed Honeywell by telephone that, out of 15 steady points flown after the adjustment, 14 gave zero $\dot{E}$ readings. This indicated the meter was ready for the suggested test program as soon as the aircraft could be made available.

PILOT DEBRIEFING DOCUMENT

A debriefing document was prepared for pilots who have flown the energy meter in the slatted F-4J aircraft at Patuxent Naval Air Test Center. It was planned to incorporate these questionnaire responses in this final report, but they will have to await completion of the tests, and will be included in NATC's test report. Some of the questions originated from reviews with the ONR scientific officer, NATC personnel, and the USAF energy meter test program director at Tyndall AFB.

The rationale of the debriefing document is to offer the pilot the convenience of yes-no responses while providing the option of writing his qualifying opinions or comment. The document is presented in Appendix B.

SECTION VIII
REFERENCES

1. Hoffman, W.C., Bryson, A.E., "A Study of Techniques for Real-Time, On-Line Optimum Flight Path Control; Minimum-Time Turns to a Specified Track," ASI-TR-71-4, September 1971.

2. Rutowski, E.S., "Energy Approach to the General Aircraft Performance Problem," Journal of the Aeronautical Sciences, Vol. 21, No. 3, March 1954, pp 187-195.

3. Boyd, J.R., Christie, T.P., and Gibson, J.E., "Energy Maneuverability (U)," APGC-TR-66-4, March 1966 (Secret).

4. Bryson, A.E., Jr., Desai, N.N., and Hoffman, W.C., "Energy State Approximation in Performance Optimization of Supersonic Aircraft," Journal of Aircraft, Vol. 6, No. 6, November - December 1969, pp 481-488.

5. McDonnell Douglas Corporation Letter HI-350F4-10971, "F-4J Lift, Drag, Installed Thrust and Fuel Flow Data With and Without Fixed Leading Edge Slats," 16 December 1971 from D.H. Freeburg to N.R. Zagalsky.

6. "Naval Air Training and Operating Procedures Standardization Program: NATOPS Flight Manual F-4J Aircraft," NAVAIR 01-245 FDD-1, Change 4-15 February 1971, by McDonnell Douglas.

APPENDIX A

ENERGY/ENERGY RATE INDICATOR AIRCRAFT WIRING INFORMATION

BASIC INSTALLATION INFORMATION

The Honeywell JG1077AA01 Energy/Energy Rate (E/Ė) Indicator has been designed for installation and flight test in an F-4J airplane. Case mounting dimensions are in accordance with MS33556. Electrical connections to the device are made through an MS3112E20-41P multipin receptacle at the rear of the case.

Wiring information needed to properly connect the indicator with other equipment on the airplane is given on Honeywell drawings SK58227 and SK58228. The first drawing covers the case where the Fire Control System is not installed and hooked up on the airplane. The second drawing covers the case where the Fire Control System is present. The E/Ė Indicator is designed to accommodate both of these conditions with no change in the indicator. Different aircraft wiring is required in each case, however, as shown on the drawings.

EXISTING AIRPLANE EQUIPMENT

The design of Honeywell's JG1077AA01 Indicator assumes that the following components and systems are installed in the F-4J flight test airplane and are operative:

1. AiResearch Model 42400-113 Air Data Computer (ADC)

2. Test receptacle J314B and mating plug P314B

3. Longitudinal and normal accelerometers, type Kistler 303M121a. Range ±1 g for the longitudinal and -2 to +8 g for the normal. Output signal 0 to 5 vdc, linear over the operational range of accelerations.

Also, the indicator is designed to operate with excitation to both true angle of attack output 20B and true airspeed output 15A in the ADC supplied either by the Fire Control System or the indicator.

When the Fire Control System is used, the scale factor of the true angle of attack signal, output 20B, is 0.5 volt, 400 Hz per degree. The signal is 0 volt at 0 degrees and is phased in phase with the excitation for positive angles. This signal, which is supplied to the Fire Control System, will be shared by the E/Ė Indicator. Load impedance of the indicator will be approximately 100K ohms.

Similarily, when the Fire Control System is used, the scale factor of the true airspeed signal, output 15A, is 0.0166 v/knot with an excitation of -25 vdc. Full scale signal is -25 v at 1500 knots, and the signal is from 150 to 1500 knots. This signal also, normally supplied to the Fire Control System, will be shared by the E/Ė Indicator.

EXISTING AIRCRAFT WIRING

The intent is to tie in the E/Ė Indicator to the aircraft with a minimum of change to the present wiring. This is accomplished at J314B as the basic connection point to the ADC. The mating connector, the ADC, and the Fire Control System (when used) are unaltered. This wiring is identified by flag note [22] on SK58227 and SK58228.

REQUIRED NEW WIRING FOR ENERGY/ENERGY RATE INDICATOR

Additional wiring required by the E/Ė Indicator is shown on SK58227 and SK58228. Connections to the ADC are made through the test connector, J314B. This provides a convenient means of tying into the ADC with minimum impact on existing aircraft wiring.

Since the system operation is different when the Fire Control System is used, than when it is not used, two different wiring harnesses will be required. The differences are shown on the SK drawings.

When the shorting plug, P314B, is disconnected from the test connector, J314B, wiring must be provided in order to maintain continuity in those circuits that are not related to the E/Ė system. This wiring is identified symbolically by flag note [5] on the SK drawings.

Details of the wiring at test connector J314B were not defined by McDonnell Engineering except for the specific connections used by the E/Ė Indicator. Pin assignments for other connections must be determined by the customer.

The test connector, J314B, is a Bendix type PT00CP-20-41S multipin receptacle, and P314B is obviously a mating connector. Suitable cable connectors to mate with J314B and P314B must be furnished by the customer.

A mating connector for the receptacle on the E/Ė Indicator is furnished by Honeywell with each device. The receptacle is type MS3112E20-41P.

Connections to the Kistler accelerometers are made at a header provided on each device. Power connections to 115 V, 400 Hz single-phase power will be deter nined by the customer. The circuit should be capable of supplying 10 watts. No fusing is provided in the indicator. Case ground should be tied to airframe ground at the instrument panel.

Energy and energy rate signals are available for flight recording if desired. The load impedance of the recorder should be 1 megohm or higher to obtain 1 percent accuracy in the recorded signal. This is based on a source impedance of 10K ohms for both signals.

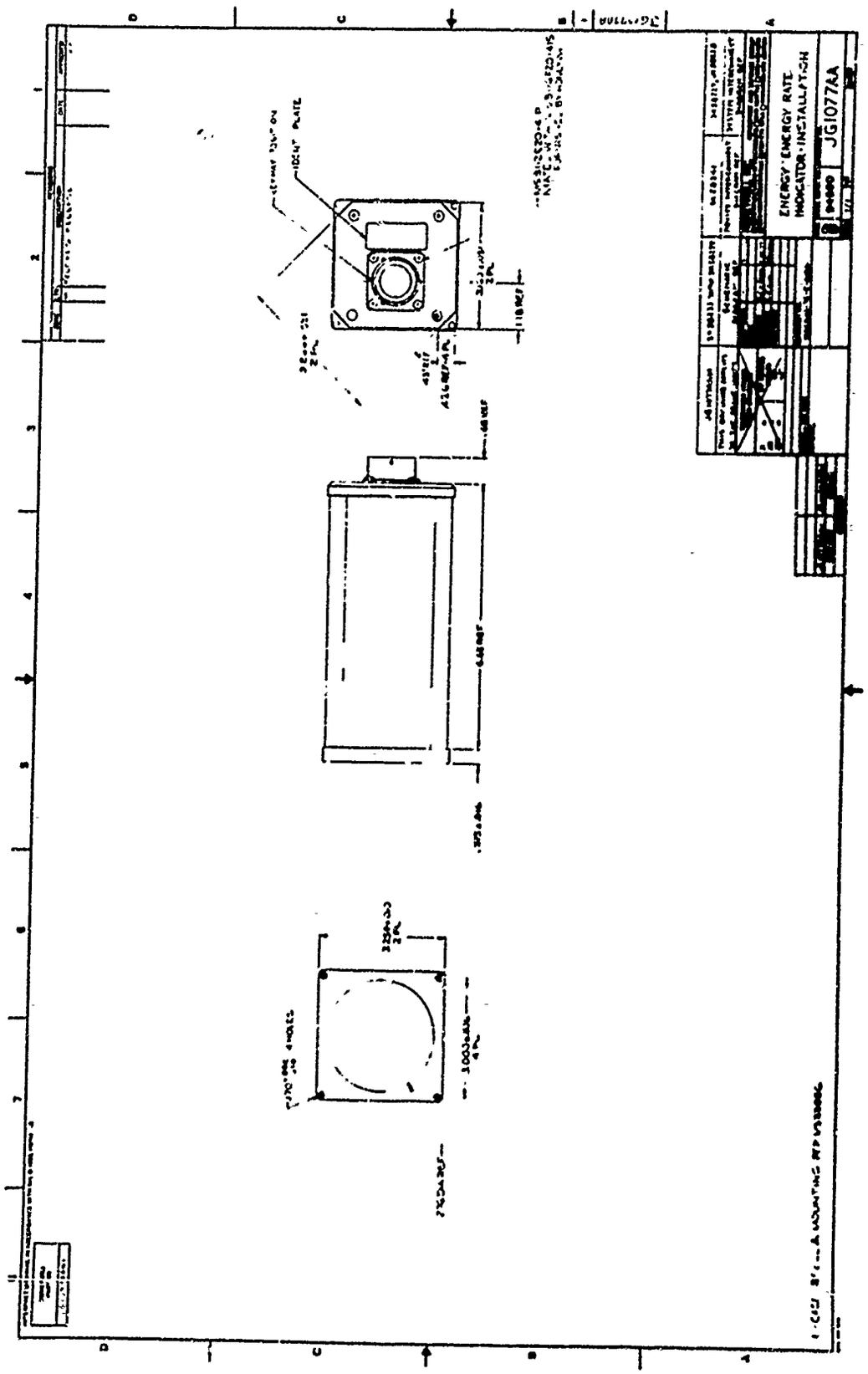

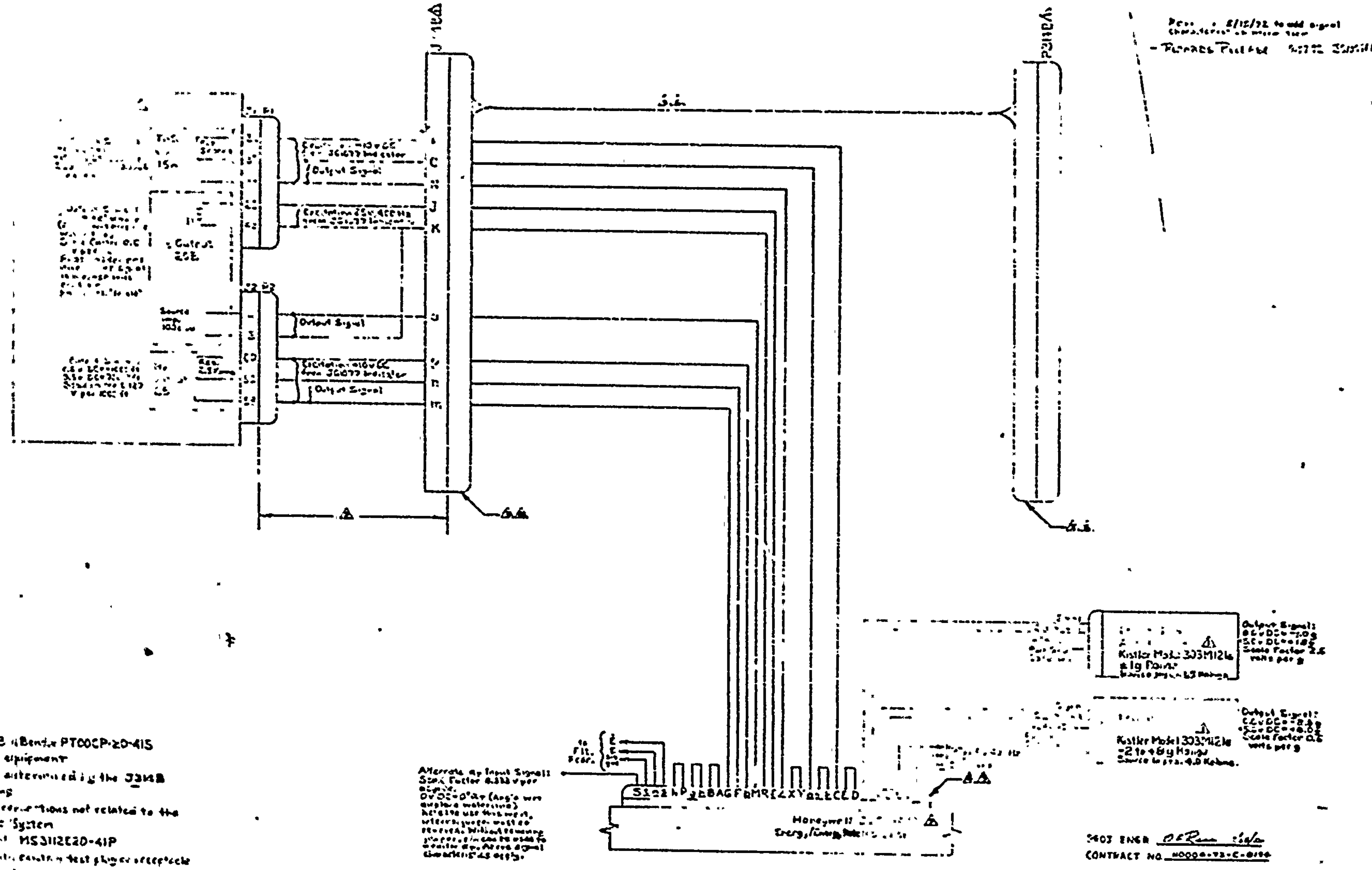

1. Test connector J314B (Bendix PT00CP-20-41S)
2. Honeywell supplied equipment
3. Pin selection to be determined by the J314B test connector wiring
4. Other required interconnections not related to the Energy/Energy Rate System
5. Connects to mate with MS3112E20-41P
6. Connects to mate with existing test plug receptacle
7. Existing wiring
8. Existing

F-4J Wiring Breakout for the Energy/Energy Rate System with Fire Control System Removed from Airplane

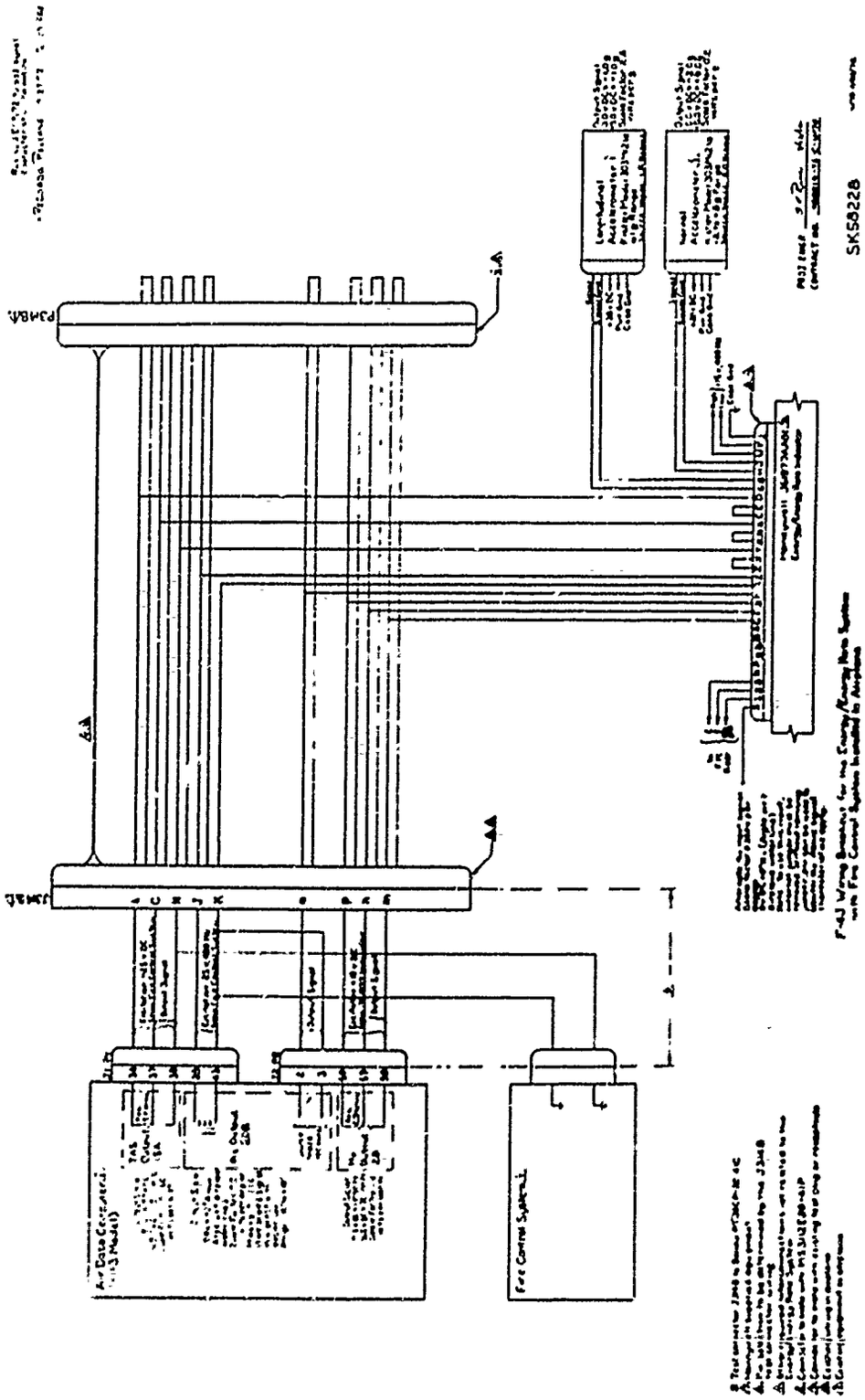

APPENDIX B
PILOT'S DEBRIEFING DOCUMENT

PILOT'S DEBRIEFING DOCUMENT

Introduction:

Review of this document prior to completion of your Energy/Energy Rate Meter flights is encouraged, since it may suggest aspects of meter utilization which could be noted prior to or following formal flight test tasks.

NAME _____

RANK _____ AFFILIATION _____

DATE _____

1. Approximate Total Flying Time _____
2. Approximate Total Instrument Time _____
3. Approximate Total Instrument Time in high performance jet aircraft _____
4. Formal training in Energy Management theory/concepts
   Yes _____ No _____
5. Time in application of energy management principles:
   in flight simulator _____;
   in actual flight _____.
6. Hours of flight experience with the E Meter _____.

Note: This sheet may be separated from attached document if desired.

PILOT'S DEBRIEFING DOCUMENT

(After flying with the Energy/Energy Rate Meter)*

1. Does the E Meter offer the potential to bridge the gap between theory given you in training sessions on energy management concepts and your flight operational realization of those concepts? Yes _____ No _____.

   Qualifying Opinion _____

   _____

   _____

2. Does the continuous availability of the energy and energy rate displays on the E Meter suggest a convenient means to develop and easily implement tactics based upon energy management theory? Yes _____ No _____.
   For example, certain tactics might be based upon achieving specific flight states (altitudes, mach numbers), consistent with your current energy level.

   Qualifying Opinion _____

   _____

   _____

3. Does the E Meter expedite setting up cruise conditions?

   Yes _____ No _____

   Qualifying Opinion _____

   _____

   _____

* Please relate your responses exclusively to your flight experience with the E Meter, not to any simulator experience.

4. Do you feel that the E Meter would be beneficial as a training aid, by providing quantitative flight energy data for the pilot to correlate with his basic flight instrument readings and knowledge of energy management theory?

Yes _____ No _____

Qualifying Opinion _____

_____

_____

For example, using the E Meter as a training aid, he could relate the feel of his aircraft in a "quickest, tightest turn" to his indicated $\dot{E}$. Thus, one can associate a given $\dot{E}$ with the maximum achievable turn rate. To gain energy at a maximum rate, he can correlate altitude and airspeed points with his current energy level. While all pilots have an intimate knowledge of the exchange option between airspeed and altitude, do you feel the E Meter affords insight as to how to best effect this exchange?

Yes _____ No _____

Qualifying Opinion _____

_____

_____

5. Note your feeling about E Meter readability

a. Energy rate readout (see Figure 1)

(1) Location of zero point.

Present position at 9 O'clock (consistent with rate-of-climb indicator), is OK _____

Prefer a 12 O'clock position _____

No preference for either of these _____

Prefer _____ O'clock

5. (Continued)

(2) Full scale range.

Present +700 to -2000 ft/sec (linear +700 to -300, compressed linear scale -300 to -2000 is OK _____.

For these flight tests, I liked the number of minor scale divisions (20 F/S increments +700 to -300, and 100 F/S increments -300 to -2000), as shown in Figure 1(b). Yes _____ No _____

If No, would prefer: _____

_____

_____

For operational use, I feel that I would like the number of minor scale divisions (50 F/S for the range +700 to -300) as shown in Figure 1(a).

Yes _____ No _____

If No, other preference: _____

_____

_____

Prefer uniform linear scale with reduced range

Yes _____ No _____

If Yes,

Would like maximum positive @ _____

Would like maximum negative @ _____

Other preference: _____

_____

_____

5. (Continued)

b. Total energy readout.

(1) Location of zero point

Present position @ 9 O'clock is OK _____

Prefer _____ O'clock

(2) Full scale range

Present linear 0 to 150,000 ft. scale is OK _____

Prefer linear scale 0 to _____ ft.

Other preference, e.g. non-linear _____

_____

_____

For these flight tests, I liked the number of minor scale divisions (2000 ft. increments).

Yes _____ No _____

If No, would prefer _____

_____

_____

For operational use, I feel that I would like the number of minor scale divisions (5000 ft. increments) shown in Figure 1(a). Yes _____ No _____

Other preference _____

_____

_____

c. Mach bezel overlay (for the slatted F-4J)

Present optimal climb overlays as shown in Figure 2 giving command Mach number for each energy level were

satisfactory _____

not satisfactory _____

Do you find the Mach-energy correlation more informative than the conventional Mach-altitude correlation of "kneepad" schedules such as those in Table 1?

Yes ____

No ____

These schedules were used in generating the overlays of Figure 2.

If you feel the overlays were "not satisfactory":
Would like to see _____

_____

_____

Have you flown any energy profiles (such as in Table 1) previously?

Yes _____

No _____

If yes, specify type, the number of each profile flown, and method used in the flight, e.g. instruments, kneepad schedule.

Minimum Time Climbout _____, Flown ____ times, Reading: Mach ___
Alt. ___
R/C ___
g's ___
Sched ___

Minimum Fuel Climbout ___ , Flown ___ times, Reading: Mach ___
Alt. ___
R/C ___
g's ___
Sched ___
Fuel Flow ___

6. Can you envisage any other uses for the meter?

Some suggestions by pilots have been received such as:

a. To enable the pilot to understand his aircraft more fully and to see directly how he is doing in managing energy. In the latter case use of the E Meter would be analogous to use of the angle-of-attack meter. Every flight that is not a combat flight is a training flight, and thus there is a continuing potential for improving performance.

b. Pre-intercept maneuvering, to get into position with the best energy and energy rate for an encounter.

c. To improve turning performance.

d. To develop rules of thumb for use during combat.

* * * * * * * *

This concludes the formal debriefing document. On the following page is an exploratory question to which your response is entirely optional.

Optional, exploratory question:

A significant advantage in aircraft control decoupling is given to a pilot by an on-line display of energy. Consider the altitude vs. velocity plot:

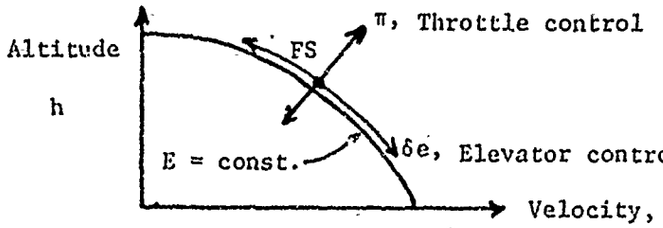

where a line of constant energy $(h + V^2/2g)$ is shown, together with a point FS representing a particular flight state. The pilot knows that from equilibrium level flight, if he holds the stick steady while advancing the throttle, he will accelerate and climb; while if he reduces throttle his vehicle will lose altitude and slow down which demonstrates strong interactions of control inputs.

Elevator control, at control throttle, will carry him along a line of constant energy as shown in the above plot, again demonstrating strong interactions or coupling. The transformation of this plot to altitude-energy coordinates uncouples these controls, so that when energy is controlled through throttle inputs and altitude is controlled through elevator deflection there should be significant decoupling of these inputs, as shown in the plot:

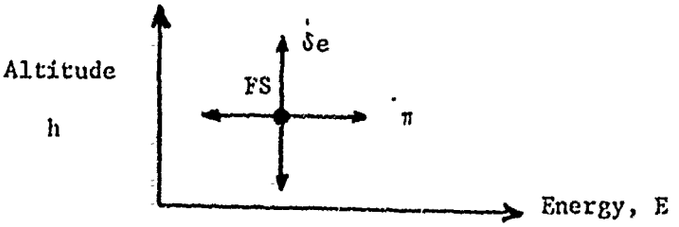

In your flight tests of the E Meter, did you find this decoupling a useful quality: Yes _____ No _____

Qualifying Opinion _____

_____

_____

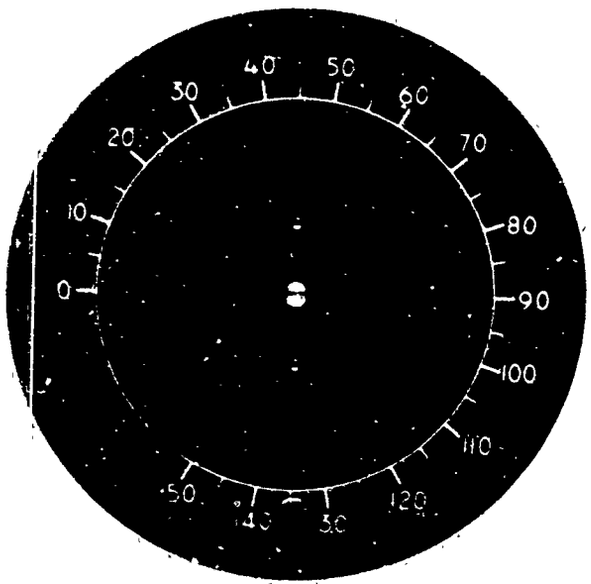

(a)
Operational
Dial

(b)
Engineering
Test
Dial

FIGURE 1 ENERGY METER SCALES

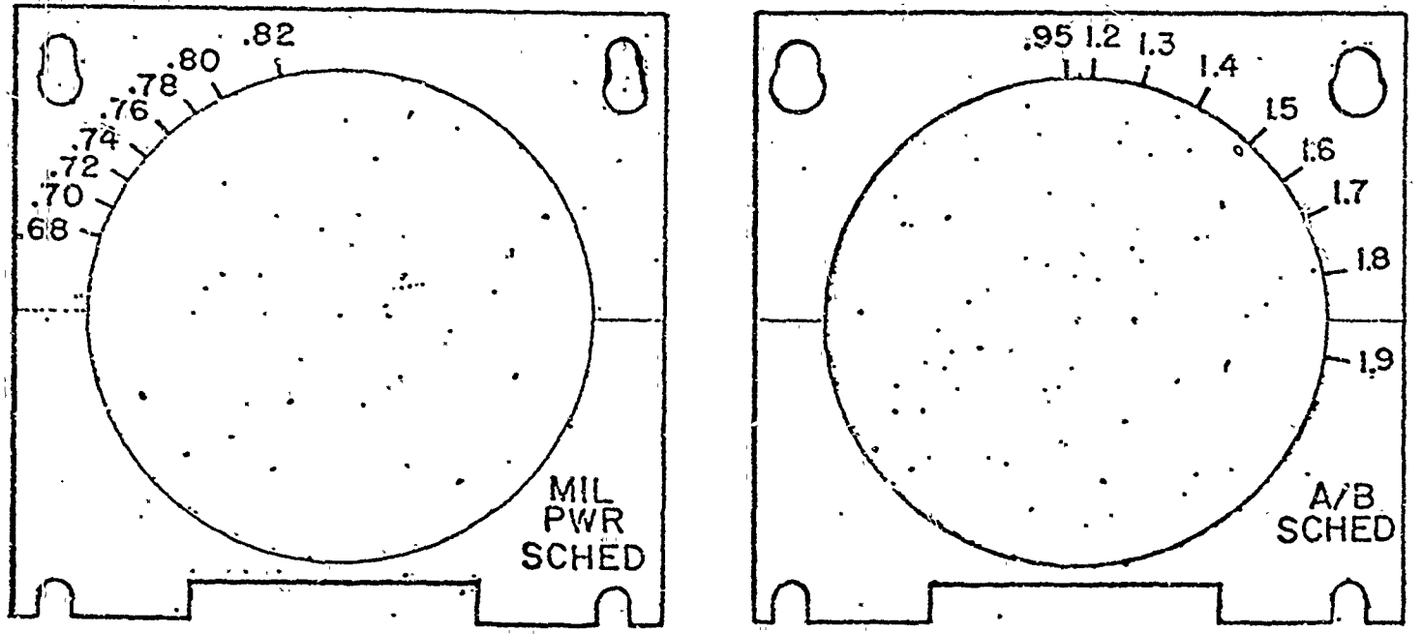

FIGURE 2 METER BEZEL OVERLAYS FOR OPTIMAL CLIMBOUT FOR SLATTED F-4J

A/B

E	M	h
46.45	1.2	23000
52.50	1.3	25570
59.25	1.4	28870
66.67	1.5	33000
72.50	1.6	34850
77.50	1.7	35100
84.70	1.8	37560
94.55	1.9	42000

h	M
23000	1.200
25000	1.283
28000	1.373
30000	1.425
32000	1.467
35000	1.580
35000	1.710
36000	1.835
38000	1.900
42000	1.900

MIL PWR

E	M	h
8.75	0.68	SL
12.50	0.70	3230
16.00	0.72	6420
19.50	0.74	9610
23.25	0.76	13090
27.00	0.78	16580
30.50	0.80	19810
37.75	0.82	27020

h	M
SL	0.680
5000	0.711
10000	0.742
15000	0.772
20000	0.801
25000	0.815

Note: Left hand schedules for pilots preferring to hold specific mach number and fly to designated altitude.
Right hand schedules for pilots preferring to hold specific altitude and fly to designated mach number.

TABLE 1 CLIMBOUT SCHEDULES
FOR SLATTED F-4J

APPENDIX C

ENERGY METER PROGRAM FOR NASA FRC

CONTRACT NUMBER: N00014-72-C-0194
MODIFICATION NUMBER: P00002

1 August 1972

ATTACHMENT NUMBER 2

The Contractor shall:

1. DEFINE INTERFACE

   Determine the compatibility of the present meter design with available signals in the NASA aircraft for which the meter is intended and define the interface.

2. DESIGN MODIFICATION

   Make minor modifications to the existing design incorporating required scale factor and null shifts to accommodate the NASA research aircraft.

3. FABRICATE METERS

4. DELIVER METERS

   Deliver two (2) energy meters and associated equipment to NASA, Flight Research Center, P.O. Box 273, Edwards, California 93523. The first shall be delivered on or before 30 September 1972, and the second on or before 30 November 1972.

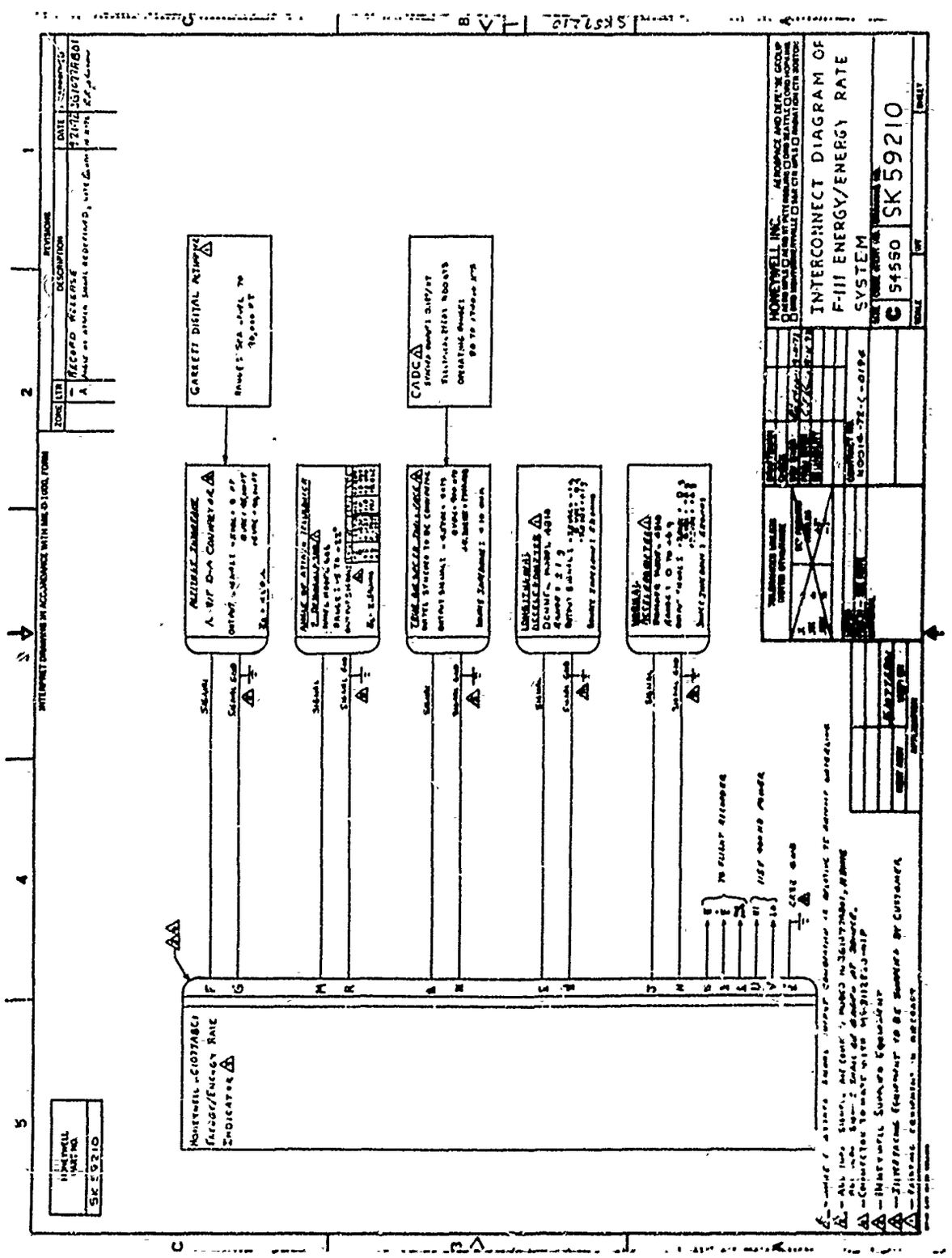

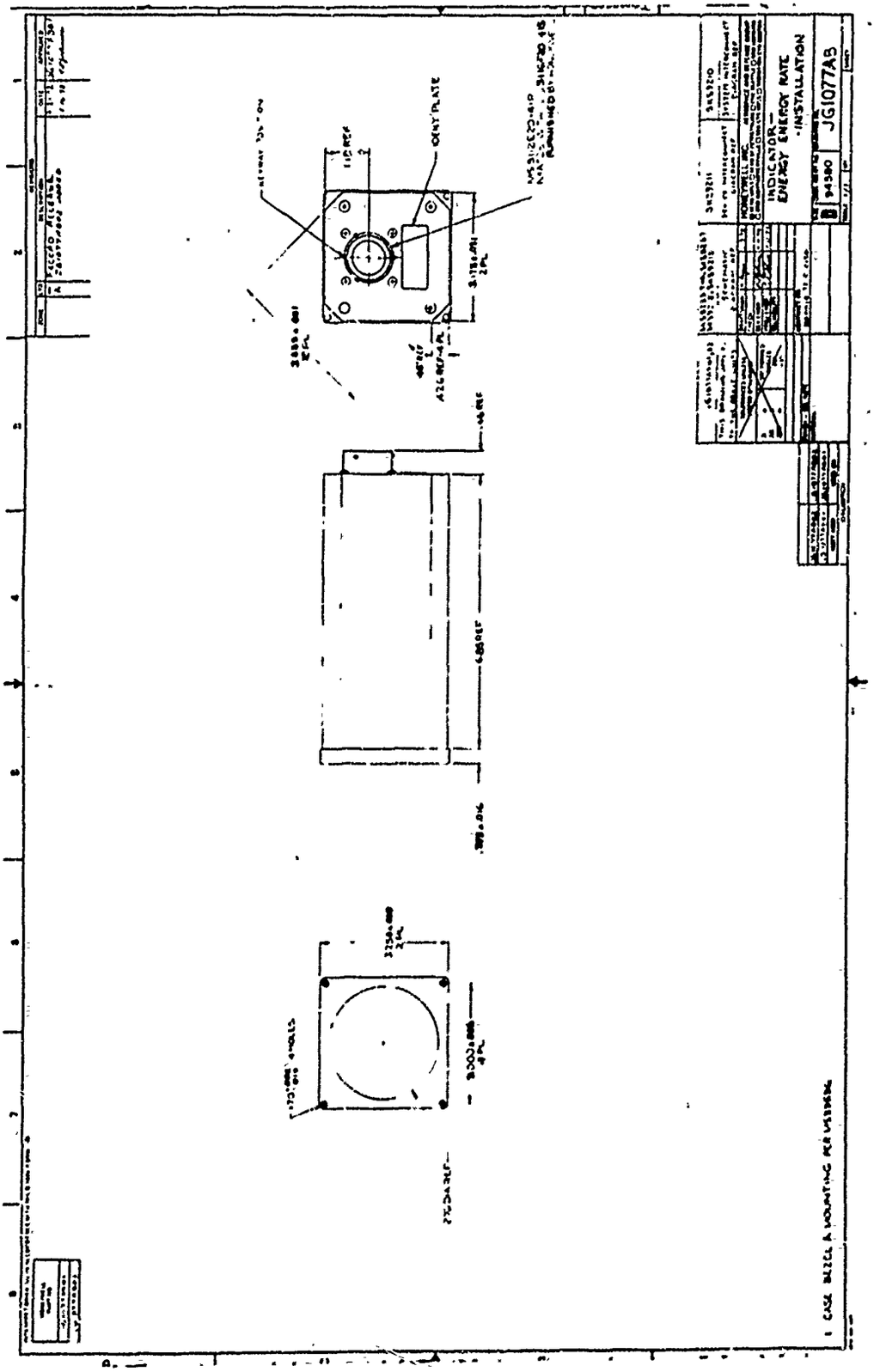

APPENDIX D

ENERGY METER PROGRAM FOR USAF

CONTRACT NUMBER: N00014-72-C-0194
MODIFICATION NUMBER: P00003

1 November 1972

ATTACHMENT NUMBER 3

The Contractor shall

1. DEFINE INTERFACE

   In conjunction with the USAF, establish the signal input and output voltage and impedance levels to determine interface compatibility between present meter design and the USAF aircraft for which the meter is intended.

2. METER DESIGN MODIFICATION, FABRICATION

   Make mirror modifications to the existing meter design incorporating required scale factor and null shifts to accommodate the USAF research aircraft. This shall include both meter input driving signals and for in-flight recording of meter output indications. Fabricate the two meters. Provide written functional description of the meters and installation drawings and interface schematics.

3. ACCELEROMETER PACKAGE DESIGN, FABRICATION

   The temperature controlled two-axis accelerometer package mounting surface shall be designed to accommodate USAF alignment provisions in the F-106 research aircraft. Fabricate the two accelerometers and their enclosing package. Provide written functional description of the package and installation drawings and interface schematics.

4. DELIVERY

   As directed by the Scientific Officer designated hereunder, deliver two Energy Meters and one two-axis accelerometer package.

HONEYWELL

ENERGY MANAGEMENT DISPLAY SYSTEM

DATA PACKAGE

Introduction

This system will be installed in USAF test aircraft F-106B, 57-2541 at Tyndall AFB under Test Plan ADC/ASD/ADWC Project 73-02, "Flight Test and Evaluation of Energy Management Display," January 1973.

Attachments

This data package consists of the following items:

(1) Functional Description, Energy Meter JG1077AF-01

(2) Functional Description, Two Axis Accelerometer Assembly GG1143AA01

(3) Dwg. SK59741-"Interconnecting Diagram of F-106 Energy/Energy Rate System"

(4) Dwg. JG 1077AF-"Indicator - Energy/Energy Rate Installation"

(5) Dwg. GG 1143AA01-"Accelerometer Assy Linear, 2 Axis Installation Dwg"

ATTACHMENT 1

Functional Description, Honeywell Energy Meter JG1077AF-01

This device is a dual pointer indicator displaying aircraft specific energy level (E) and specific energy rate of change ($\dot{E}$). It contains computing and drive electronics in addition to the pointer-positioning electromechanical components. It is designed to accept dc analog input voltages representing true airspeed, V, altitude, h, angle of attack, α, normal and longitudinal acceleration, a_n and a_ℓ. These acceleration signals are furnished by the GG1143 AA01 accelerometer assembly described in attachment 2. The indicated energy and energy rate signals are also provided in a form suitable for in-flight recording for subsequent analysis.

The formulas utilized for computation of E and $\dot{E}$ are:

$$E = h + V^2/2g$$

$$\dot{E} = \frac{V}{g} [a_\ell \cos \alpha - a_n \sin \alpha]$$

In a climb, the pilot utilizes the meter display of specific energy (kinetic plus potential) and specific excess power (rate of change of energy) to efficiently exchange airspeed (kinetic energy) for altitude (potential energy).

Pre-computed optimal trajectories for minimum time or minimum fuel climbs can be expressed in terms of a schedule of Mach numbers or altitudes corresponding to each energy level on the meter outer dial. These schedules can be printed on a template overlay which is easily snapped over the meter bezel. Pilots have shown an interest in a variety of such templates, designed for easy change in flight. This feature is a convenient and economic alternative to a more sophisticated mechanization such as a computer-based energy management system. Additional overlays could indicate flight envelope boundaries corresponding to a given energy level.

The energy rate display allows the pilot to measure how efficiently he is transitioning between flight states, and to moderate his maneuvers in such a way as to preclude the large negative energy rates associated with high "g" induced drag effects.

The meter can also be utilized to derive specific excess power contours (energy rate versus airspeed and altitude) for calibration of the actual test aircraft. It should also be useful as a training aid in quantifying tactics, such as exchanging turning rate for energy rate in high "g" turning maneuvers.

Revised
28 March 1973

ATTACHMENT 2

Functional Description, Honeywell Linear Accelerometer Assembly
GG 1143AA01

The GG1143AA01 accelerometer assembly is a two axis linear accelerometer package designed to be used in conjunction with the Honeywell JG1077AF Energy/Energy Rate Indicator.

When properly mounted on the aircraft the sensors will produce electrical analog signals (D.C.) proportional to the longitudinal (X-axis) and vertical (Z-axis) accelerations experienced by the aircraft.

The package obtains its power from the 115 V 400∿and 28 VDC aircraft power sources. The 400∿AC power is used to provide +10 and -5 VDC regulated bias voltages for the accelerometers and the 28 VDC is used to control the temperature of the two accelerometers to approximately 160°F.

The package is attached to the aircraft by means of three mounting feet, the mating surfaces of which are ground to position the input axis of the vertical accelerometer normal to the mounting surface and the input axis of the longitudinal accelerometer in a plane parallel to the mounting surface. The line connecting the centers of the two alignment pins in the base of the assembly is perpendicular to the input axis of the longitudinal accelerometer. The alignment pins then can align the azimuth angle of the longitudinal accelerometer.

The electrical termination of the package is accomplished in connector J1. A mating connector is supplied with the package as shown on the installation drawing. The electrical function of each pin in the connector J1 required for interconnection is indicated on the interconnecting diagram SK 59741.

It should be noted here that terminals L (+10 VDC), M (-5 VDC) and N (TCA OUTPUT) are used for testing purposes only. NO CONNECTIONS SHOULD BE MADE TO THESE TERMINALS. The self test terminals G and H when unergized should be floating and not connected together.

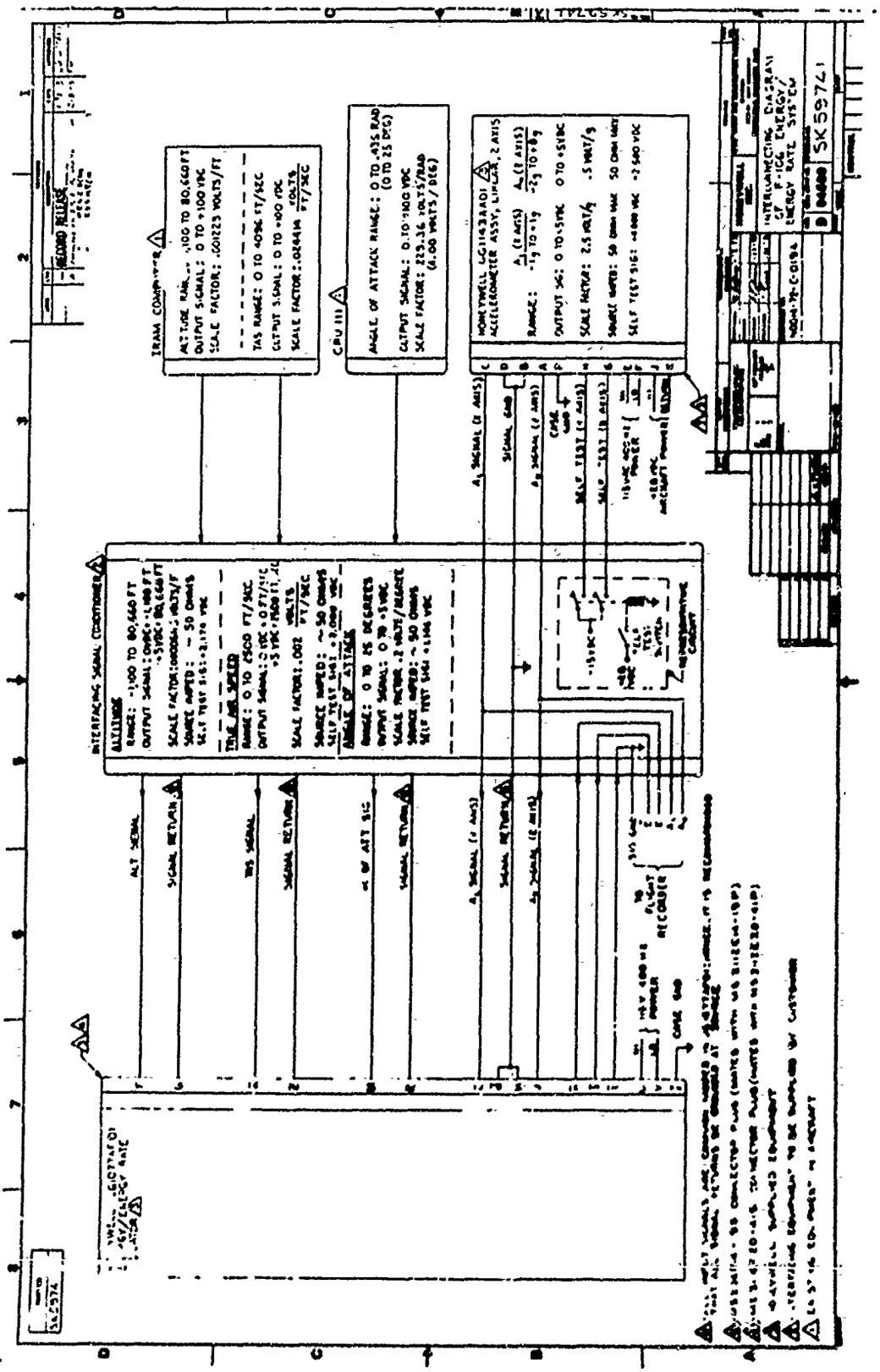

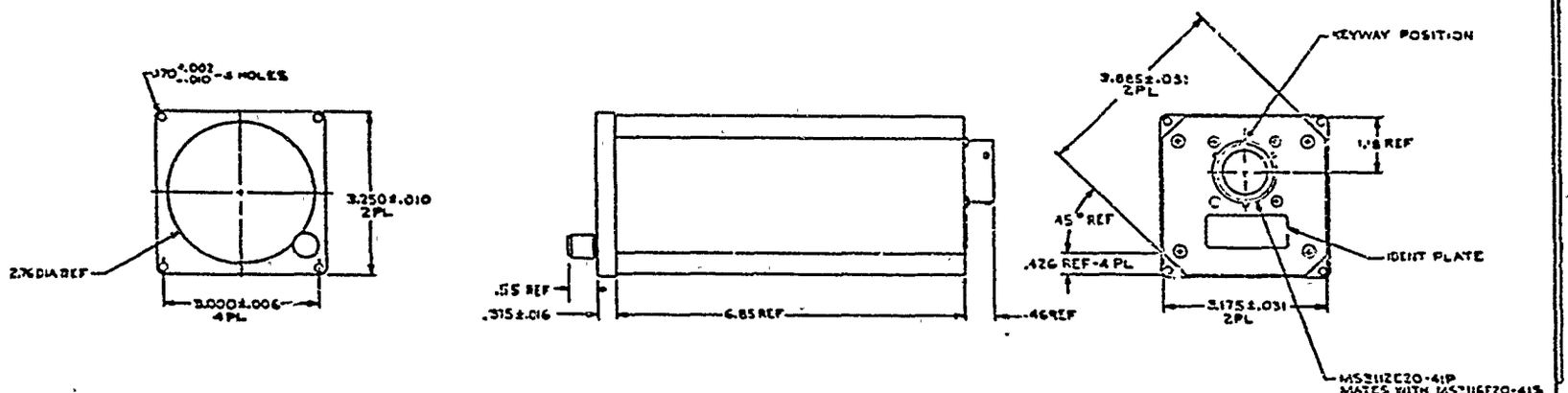

1 - CASE, BEZEL & MOUNTING PER MS33556

JG1077AF01	SK5EC233 THRU SK5E237 SK5E255	SK59740	SK59741
THIS DRAWING APPLIES TO THE ABOVE UNITS	SCHEMATIC DIAGRAM REF	REV EE INTERCONNECT DIAGRAM REF	SYSTEM INTERCONNECT DIAGRAM REF

INDICATOR, ENERGY / ENERGY RATE— INSTALLATION

D | JG1077AF

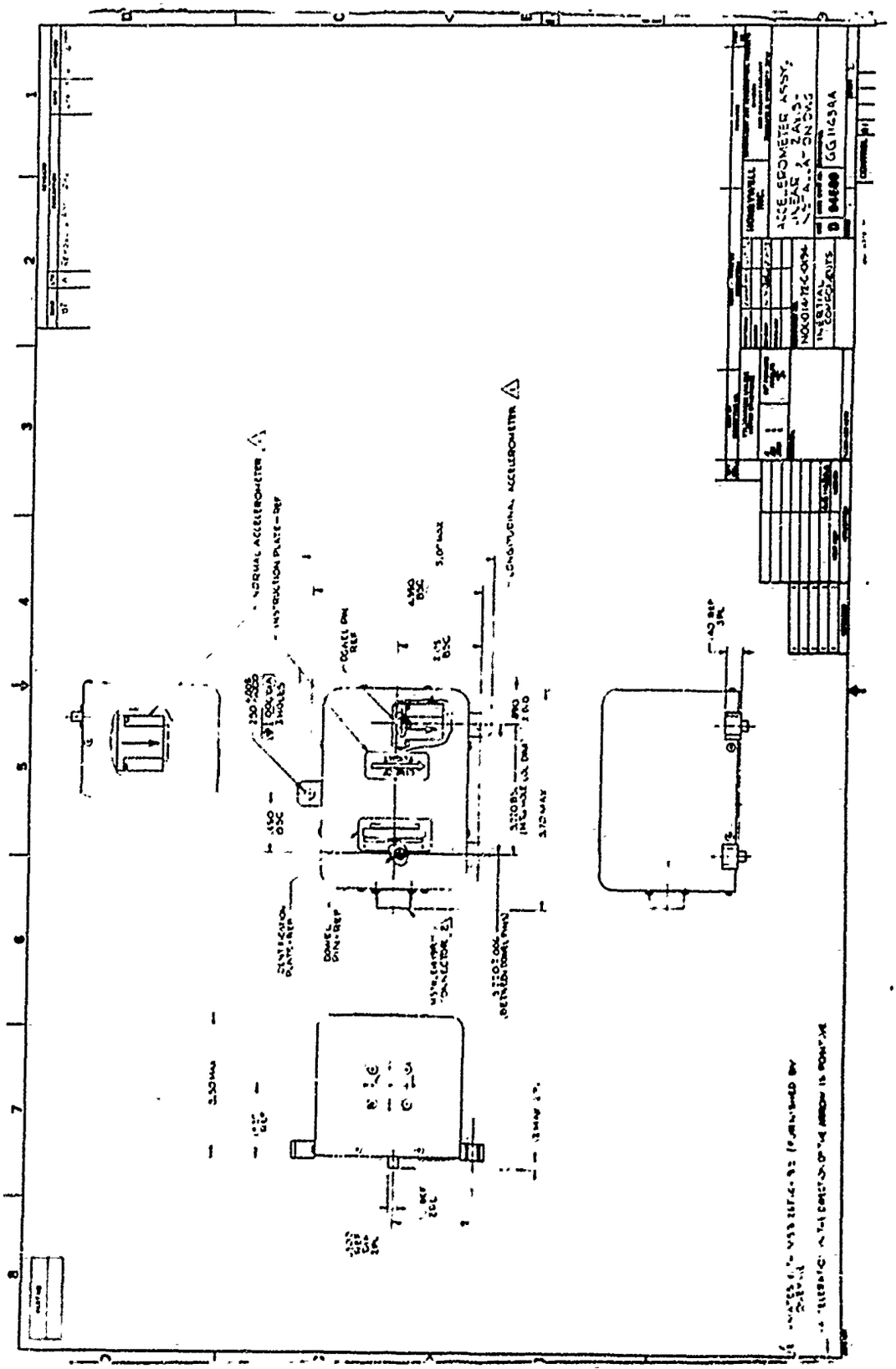

APPENDIX E

JG1077AA01 MAJOR CHARACTERISTICS

I. MECHANICAL CHARACTERISTICS

Weight - 2.2 lb
Case Configuration - Per MS33556
Dimensions

Bezel - 3.25 x 3.25 x 0.375 in.
Case - 3.16 x 3.16 x 6.85 in.
Overall Length Including Connector - 7.7 in. max.

Dial Markings

Energy Scale - lusterless white
Energy Rate Scale - lusterless yellow (No. 33538 per FED STD 595)
Dial Background - lusterless black

Connector - MS3112E20-41P

II. ELECTRICAL CHARACTERISTICS

Power Requirements - 115v, 400 Hz; 9 watts max.

Operating Temperature - -5°F to +160°F

Energy (E) Computation

Range - o to 150,000 ft
Response - 7 seconds max full scale
Accuracy* - ±(500 ft + 1% of reading)

Energy Rate ($\dot{E}$) Computation

Range - -2000 to +700 ft/sec
Response - 2 seconds max full scale
Accuracy (steady state)*:

Null (zero) point - Pilot adjustable to zero for steady state zero energy rate conditions.

Expanded Scale (1300) to +700) - ± (5 + 2% of reading)
Condensed Scale (-300 to -2000) - ± (20 + 2% of reading)

---

*Assumes no sensor errors